

**THE EVALUATION OF PRESSURE DISTRIBUTION AND BULK
DENSITY MODELS FOR INFIELD AGRICULTURE AND
FORESTRY TRAFFIC**

BAREND JAN MARX

Submitted in partial fulfilment of the requirements
for the degree of MSc Engineering

School of Bioresources Engineering and Environmental Hydrology
University of KwaZulu-Natal
Pietermaritzburg
South Africa

2006

DISCLAIMER

I wish to certify that the work reported in this dissertation is my own original and unaided work except where specific acknowledgement is made.

Signed:



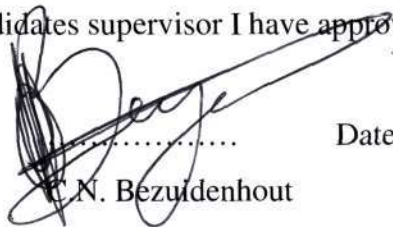
Barend J Marx

Date:

10/4/2006

As the candidates supervisor I have approved this dissertation for submission.

Signed:



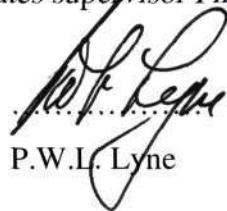
C.N. Bezuidenhout

Date:

10/4/2006

As the candidates supervisor I have approved this dissertation for submission.

Signed:



P.W.L. Lyne

Date:

10/4/06

ACKNOWLEDGEMENTS

The author wishes to express his sincere appreciation for the assistance given by the following, without whom this research would not have been made possible:

- Dr CN Bezuidenhout, School of Bioresources Engineering and Environmental Hydrology, University of KwaZulu-Natal, for supervision and endless assistance and encouragement throughout the project.
- Prof PWL Lyne, South African Sugarcane Research Institute (SASRI), for supervising this project and providing advice, encouragement and support throughout.
- Dr CW Smith, Institute for Commercial Forestry Research (ICFR) for his advice and assistance throughout the project.
- Dr S Lorentz, School of Bioresources Engineering and Environmental Hydrology, University of KwaZulu-Natal, for his help and advice during the project.
- Dr JJH van den Akker, Wageningen University, The Netherlands, for advice, assistance and for allowing the use of the SOCOMO model.
- Mr JL Eweg, School of Bioresources Engineering and Environmental Hydrology, University of KwaZulu-Natal, for providing the data to evaluate the decision support system and for advice and encouragement.
- Dr R van Antwerpen and Mr E Meyer, South African Sugarcane Research Institute, for their advice and assistance during the project.
- Prof D Schreiner, School of Civil Engineering, University of KwaZulu-Natal, for his expert advice with the project.
- Mr M Holder, School of Civil Engineering, University of KwaZulu-Natal, for assisting with triaxial tests.
- SASRI, ICFR and UKZN for the use of their laboratories for testing.
- Mr S Thornton-Dibb, School of Bioresources Engineering and Environmental Hydrology, University of KwaZulu-Natal, for his assistance with programming.
- Ms D Rietz, Institute of Commercial Forestry Research for her assistance with troxler and core sample readings.
- The Department of Transport, South African Sugarcane Research Institute and the National Research Foundation for funding the project.
- The University of KwaZulu-Natal for post graduate scholarship and financial support.
- Mr P Odell for the use of his farm and equipment for testing.
- To my family, friends and the members of 18 Shores Rd digs for their encouragement and support during this time.

ABSTRACT

There is evidence that soil compaction, through the use of mechanised equipment, causes detrimental effects to soil quality and reduces long-term productivity of soils. For economic reasons, farmers need to purchase larger, heavier machinery in order to cultivate larger areas under crops, resulting in larger forces on the soil. The severity of soil compaction is governed by various soil and vehicle properties and normally causes an increase in the soil's bulk density and a decrease in the air filled porosity. These changes in soil properties have negative effects on crop production and environmental sustainability. The aim of this study was to investigate and develop a model based decision support system for soil compaction management and research.

Soil compaction occurs during the transfer of stresses from the tyre interface into the soil. Numerically, it has been modelled using both mechanistic and empirical models, which attempt to simulate the stress propagation and also sometimes the consequent damage to the soil. The SOCOMO soil compaction model is described and this model computes the stress at a point in the soil for any given horizontal and vertical stress distribution at the soil / tyre interface. It has been successfully used in the Netherlands and in Sweden to map the impact on the soil.

The SOCOMO model was tested and verified at a forestry site in Richmond, KwaZulu-Natal. Relationships to determine bulk density were also tested and verified. The SOCOMO model performs satisfactory (RMSE = 47.9 kPa), although it tends to overestimate the pressures within the soil. This could be as a result of the high organic carbon content in the particular soil. Models predicting bulk density also performed satisfactory (RMSE = 69.9 kg.m⁻³), but resultant densities in the soil are generally underestimated. Future research is needed to find better relationships to estimate changes in dry bulk density and to test the model on a wider range of soils. If the model performs satisfactory it could provide a useful tool to determine the impact of soil compaction on crop yield.

TABLE OF CONTENTS

DISCLAIMER	i
ACKNOWLEDGEMENTS	ii
ABSTRACT	iii
LIST OF TABLES	vii
LIST OF FIGURES	ix
1. INTRODUCTION	1
1.1 Introduction and Rationale	1
1.2 Problem Statement	1
1.3 Aims and Objectives	3
2. AN OVERVIEW ON THE EFFECTS OF SOIL COMPACTION ON CROP PRODUCTION	4
2.1 Introduction	4
2.2 Maize	4
2.3 Silage Maize	6
2.4 Soyabeans	6
2.5 Forestry	7
2.6 Sugarcane	8
2.7 Other Cereals	9
2.8 Grasses	10
2.9 Other Crops	11
2.10 Conclusion	12
3. AN OVERVIEW OF PROCESSES OCCURRING DURING SOIL COMPACTION	14
3.1 Introduction	14
3.2 Determinants of the Severity of Soil Compaction	15
3.3 Effects of Soil Compaction on Soil Properties (Macro Scale)	15
3.3.1 Soil strength	15
3.3.2 Bulk density	16
3.3.3 Soil aeration	16
3.3.4 Hydraulic properties	18
3.4 The Soil Compaction Process (Micro Scale)	21

3.4.1	Compression of solid particles	21
3.4.2	Compression of fluids within pore spaces	22
3.4.3	Re-arrangement of soil particles	22
3.4.4	Change in fluid contents	23
3.4.5	Relationships between applied loads and resulting compaction	24
3.5	Conclusion	27
4.	A REVIEW OF SOIL COMPACTION MODELLING	29
4.1	Introduction	29
4.2	Pseudo-Analytical Models	30
4.2.1	Modelling the stress propagation through the soil	30
4.2.2	Modelling the stress – strain behaviour	33
4.2.3	An overview of some of the pseudo-analytical soil compaction models that have been developed	36
4.3	Finite Element Method (FEM) Soil Compaction Models	40
4.3.1	Modelling the propagation of displacement through the soil	40
4.3.2	Modelling the stress – strain behaviour	41
4.3.3	An overview of some FEM soil compaction models	45
4.4	The Soil Compaction Model (SOCOMO)	47
4.4.1	Theoretical basis and description of SOCOMO	47
4.4.2	Model sensitivity	50
4.4.3	Experiences of other users with SOCOMO	53
4.5	Discussion and Conclusion	55
5.	DERIVATION OF DEFAULT GEOTECHNICAL SOIL INPUT VALUES FOR THE SOCOMO MODEL	57
5.1	Introduction	57
5.2	Methodology	58
5.2.1	Determination of pre-consolidated soil strength (<i>SS</i>)	58
5.2.2	Establishing mean / median geotechnical inputs for each soil texture	60
5.2.3	Correcting geotechnical inputs with respect to bulk density	62
5.3	Results and Discussion	63
5.4	Conclusion	66
6.	A DESCRIPTION OF THE SOCOMO DECISION SUPPORT SYSTEM (DSS)	67

6.1	Introduction	67
6.2	The DSS User – Interface	69
6.3	Soil Inputs	70
6.4	Vehicle Inputs	71
6.4.1	Tyre selection	71
6.4.2	Contact area scenarios	71
6.4.3	Loading scenarios	73
6.5	DSS Outputs	76
6.5.1	Pressure distribution	76
6.5.2	Compacted dry density	77
6.6	Conclusions	78
7.	EVALUATION OF THE SOCOMO DECISION SUPPORT SYSTEM	79
7.1	Introduction	79
7.2	Methods	79
7.2.1	Site description	79
7.2.2	Vehicle description	80
7.2.3	Soil pressure measurements	81
7.2.4	SOCOMO DSS simulation runs	82
7.3	Results and Discussion	83
7.3.1	Observed data	83
7.3.2	Model evaluation	85
7.4	Conclusions	88
8.	DISCUSSION, CONCLUSIONS AND RECOMMENDATIONS	90
8.1	Discussion and Conclusions	90
8.2	Future Recommendations	92
9.	REFERENCES	94

LIST OF TABLES

Table 2.1 Research carried out by various authors on the effects of soil compaction (SC) on maize yield	5
Table 2.2 Experimental trials to determine the effects of soil compaction (SC) on silage maize yield	6
Table 2.3 Research conducted to determine the effects of soil compaction (SC) on soyabean yield	7
Table 2.4 An overview of research conducted on the effects of soil compaction (SC) in forestry	8
Table 2.5 Effects of soil compaction (SC) on sugarcane production	9
Table 2.6 Experiments showing the effects of soil compaction (SC) on cereal crops	10
Table 2.7 Experiments carried out to determine the effects of soil compaction (SC) on grasslands	11
Table 2.8 Experiments to determine the effects of soil compaction (SC) on other crops	12
Table 4.1 Classification of soil compaction models (after Defossez and Richard, 2002)	29
Table 4.2 Summary of pseudo-analytical soil compaction models	37
Table 4.3 Summary of the tests conducted by Gupta <i>et al.</i> (1985) and O'Sullivan <i>et al.</i> (1999) (after Defossez and Richard, 2002)	37
Table 4.4 Evaluation of the models developed by Gupta <i>et al.</i> (1985) and O'Sullivan <i>et al.</i> (1999) (after Defossez and Richard, 2002)	39
Table 4.5 Summary of some FEM compaction models (after Defossez and Richard, 2002)	45
Table 4.6 Summary of tests conducted by Raper and Erbach (1990), Kirby (1994) and Gysi <i>et al.</i> (2000) (after Defossez and Richard, 2002)	46
Table 4.7 Evaluation of the FEM models at different depths (z) developed by Raper and Erbach (1990), Kirby (1994) and Gysi <i>et al.</i> (2000) (after Defossez and Richard, 2002)	46
Table 4.8 Authors that have used SOCOMO with success	47

Table 5.1	Angle of internal friction (θ), cohesion (C) and structural strength (SS) of the major subsoils in the Netherlands (after van den Akker, 1999)	57
Table 5.2	A summary of soils and their properties obtained from Francis (1988). Properties include texture (see Table 5.3), dry density (DD), internal angle of friction (θ) and cohesion (C)	59
Table 5.3	Description of soil textures	61
Table 5.4	Summary of the default geotechnical properties assigned to soil texture. N/A denotes insufficient data	63
Table 5.5	The slopes (ζ) and intercepts (ξ) used to correct θ and C for changing dry densities	65
Table 6.1	Coefficients for Equation 6.1 for estimating contact area from tyre width, diameter, inflation pressure and load for rigid and soft surfaces (after O'Sullivan <i>et al.</i>, 1999)	72
Table 7.1	Description of Richmond soil properties	80
Table 7.2	Description of the SOCOMO simulations carried out for the Richmond trial. The different references and concepts are explained in Section 6.3 and 6.4	83
Table 7.3	Peak pressures recorded in each soil pressure sensor (from Eweg, 2005)	84
Table 7.4	Dry bulk densities (kg.m^{-3}) before and after the compaction event	84
Table 7.5	Test statistics comparing the SOCOMO DSS against measured data. The best situation is highlighted for each test statistic	85

LIST OF FIGURES

Figure 3.1 The effect of soil particle movement on porosity (Dejong-Hughes <i>et al.</i> , 2001)	17
Figure 3.2 Graph showing flattening of soil water retention curves for increasing bulk densities (Smith <i>et al.</i> , 2001)	19
Figure 3.3 Graphs showing the effects of changes in bulk density on porosity (dotted line) and AWC (solid line) (after Smith <i>et al.</i> , 2001)	20
Figure 3.4 Stress components of the stress tensor necessary to completely describe the forces acting on a cubical element of soil, where σ_x , σ_y and σ_z are normal stresses acting on the soil element and τ_{zy} , τ_{zx} , τ_{yz} , τ_{yx} , τ_{xz} and τ_{xy} are shear stresses acting on the soil element (Harris, 1971)	25
Figure 4.1 Stresses on a volume element caused by a point load P , where P (kPa) is the applied load, r (m) is the distance under the loading point P , θ (radians) is the angle between the radius and the vertical and σ_r (kPa) is the major principle stress acting on the soil element (Defossez and Richard, 2002)	32
Figure 4.2 Curves of equal pressure under a load point of 8 kN at three concentration factors (after Defossez and Richard, 2002)	32
Figure 4.3 Pressure distributions in the contact area between the soil and tyre for different concentration factors Söhne (1958)	33
Figure 4.4 Isotropic compression diagram, where κ and λ are compression parameters, v (dimensionless) is the specific volume, P (kPa) is the applied load and p_c (kPa) is the pre-consolidation pressure (Defossez and Richard, 2002)	35
Figure 4.5 Comparison of simulated and measured observations for the model developed by Gupta <i>et al.</i> (1985). These results are from Plot 1 (see Table 4.3)	38
Figure 4.6 Comparison of simulated and measured observations for the model developed by O'Sullivan <i>et al.</i> (1999). These results are from Plot 1 (see Table 4.3)	39

Figure 4.7 Technique used to approximate non-linear stress – strain behaviour used in pseudo-elastic models. The tangent modulus is $E_T = dq / d\varepsilon_l$, Poisson's ratio is $\mu = \varepsilon_l / \varepsilon_2$ and q is the deviator stress (Defosseze and Richard, 2002)	42
Figure 4.8 Yield surfaces in the modified Cam Clay critical state model (Kirby, 1994)	43
Figure 4.9 Composition of stresses acting on a volume element owing to a point load on a semi-infinite solid where: σ_z , σ_h , and σ_t are the vertical, horizontal and tangential stresses, respectively; τ_z and τ_h are the vertical and horizontal shear stress; P is the vertical point load; r and θ are polar co-ordinates	49
Figure 4.10 Area of soil under the tyre affected by plastic deformation (■), structural failure (■) and combined failure (■) as a result of a vehicle passing over the soil	51
Figure 4.11 Scenario one sensitivity analysis: Area of soil under the tyre affected by plastic deformation (■), structural failure (■) and combined failure (■) as a result of a vehicle passing over the soil	52
Figure 4.12 Scenario two sensitivity analysis: Area of soil under the tyre affected by plastic deformation (■), structural failure (■) and combined failure (■) as a result of a vehicle passing over the soil	53
Figure 5.1 Technique of Casegrande (1936) being applied to a Karoo dolerite (from Francis, 1988)	60
Figure 5.2 A soil triangle plot showing the texture distribution of the soils used by Francis (1988)	61
Figure 5.3 Graphs illustrating how C and θ vary with dry density	62
Figure 5.4 Box and whisker plots for θ and C	64
Figure 5.5 Box and whisker plots for SS	64
Figure 6.1 Flow chart showing some keyboard inputs required by the SOCOMO model	68
Figure 6.2 The user – interface of the SOCOMO DSS	69

Figure 6.3 Graph illustrating the load distribution over the soil surface ($r = 0.8$, $n = 3$ and $m = 16$). This distribution represents a dry soil	74
Figure 6.4 Graph illustrating the load distribution over the soil surface ($r = 0.8$, $n = 3$ and $m = 4$). This distribution represents a medium wet soil	75
Figure 6.5 Graph illustrating the load distribution over the soil surface ($r = 0.8$, $n = 3$ and $m = 2$). This distribution represents a wet soil	75
Figure 6.6 Typical DSS outputs of pressure distribution obtained from SOCOMO	76
Figure 6.7 Typical DSS outputs of compacted dry density calculated using Larson <i>et al.</i> (1980)	78
Figure 7.1 Self-loading trailer used to apply the compaction	80
Figure 7.2 Diagram of the fluid filled pressure sensor made out of latex (Eweg, 2005)	81
Figure 7.3 Diagram illustrating (A) the “T” piece, (B) the Motorola MPX 5700DP pressure transducer and (C) the tap used to pre-pressurise the bulb (from Eweg, 2005)	81
Figure 7.4 Diagram showing sensor orientation in the soil.	82
Figure 7.5 Graphs illustrating dry density (A) before the compaction event and (B) after the compaction event	84
Figure 7.6 Graphs illustrating the difference between the pressure (kPa) data collected by Eweg (2005) and a SOCOMO simulation	86
Figure 7.7 Residual plot comparing the measured pressures (kPa) against simulated pressures (BI1)	87
Figure 7.8 Graph illustrating measured pressures (kPa) against the pressures simulated in Test BI1. The shaded points are directly under the centre of the tyre at different depths	87
Figure 7.9 Graph illustrating the simulated dry densities for Test BI1 (colour shadings) against the measured dry densities in the soil profile (labelled dots in Mg.m^{-3})	88

1. INTRODUCTION

1.1 Introduction and Rationale

Currently there are 430 thousand and 1.5 million hectares under sugarcane and timber production on the eastern shores of South Africa, respectively (Bezuidenhout, 2005). The timber industry is often situated on steep slopes with relatively high rainfall. Each year about 20 million tonnes of biomass is extracted by each of these industries and sent to their respective mills using heavy vehicles that travel infield to collect their payloads. As a result of this, the soil is being compacted to a certain degree. Soil compaction problems are increasing in modern agriculture due to increased mechanization. Mechanization is on the increase as a result of farmers needing to cultivate more land in order to maintain their profit margins (in other words, the bigger your fields are, the larger the vehicle you require). Larger and heavier vehicles traveling over the soil are causing a decline in the long term productivity of various soils (Smith *et al.*, 1997).

There is widespread evidence that soil compaction (SC) affects crop production. Soil compaction is considered to be a problem in which various factors, such as machine, crop, soil and climatic conditions play an important role. These factors may have significant economic and environmental consequences in agriculture (Soane and van Ouwerkerk, 1994).

1.2 Problem Statement

Both the Institute for Commercial Forestry Research (ICFR, Pietermaritzburg, South Africa) and the South African Sugarcane Research Institute (SASRI, Mt Edgecombe, South Africa) have identified SC as a potential problem and as a result have well developed soil sustainability research programs. For a number of years, researchers at ICFR have been determining the impacts of harvesting methods and soil tillage on forest productivity (Smith, 2004). Researchers from SASRI have found that little is known of the long term effects of sugarcane monocropping on changes in chemical, physical and biological soil properties (Meyer, 2004). They have found in some areas that soils are losing their productive potential because of soil degradation. Soil

compaction as a result of harvesting and tillage methods was identified as one of the causes of soil degradation. Researchers from SASRI and ICFR have conducted extensive trials in their respective industries to determine the impacts of infield transport on productivity (Swinford and Boevey, 1984; Smith and Johnston, 2001). Conclusive evidence from these trials confirmed that SC results in changes in soil properties that affect crop growth rates and ultimately production (Swinford and Boevey, 1984; Smith and Johnston, 2001). It was also noted by these researchers that most of the effects of SC could have been prevented had effective management practices been in place in these industries (Torres and Rodriguez, 1995; Grigal, 2000).

The Forestry Stewardship Council (FSC) is an international network that promotes the responsible management of the world's forests (FSC, 2003). The purpose of the FSC is to bring people together to find solutions to the problems created by bad forestry practices and to reward good forestry management. The FSC is a stakeholder owned system that promotes good management of the world's forests. The FSC sets standards for responsible forestry management, it accredits organisations that can certify forest managers and producers to FSC standards, it provides a trademark that provides international recognition to organizations that support the growth of responsible forest management, it's product label allows consumers to recognize products and organizations that support responsible forest management. Fifty million hectares in more than 60 countries have been certified according to FSC standards in the past 10 years (FSC, 2003). In order to be accredited by FSC, the timber industry in South Africa needs to prove that it has good management practices. Since this timber is extracted by vehicles, infield SC can be a problem, as it decreases soil health and environmental sustainability. Management practices need to be put in place to minimize the effects of SC.

1.3 Aims and Objectives

The aim of the project was to investigate and develop a model based decision support system for SC management and research. The specific objectives of this project were:

1. To review the effects of SC on crop production (see Chapter 2).
2. To gain an in depth understanding of the SC process (see Chapter 3).
3. To review existing SC models with the aim of selecting one for evaluation within a decision support context (see Chapter 4).
4. To ensure that models can be widely applied by ensuring that input variables can be obtained with relative ease (see Chapter 5).
5. To develop and evaluate a decision support system that can be used for SC management and future research (see Chapters 6 and 7).

It is known that SC is caused by external forces such as the passage of vehicles (infield transport), water droplets, tillage, livestock movement etc. The work conducted in this dissertation will concentrate on the effects of the passage of vehicles.

2. AN OVERVIEW ON THE EFFECTS OF SOIL COMPACTION ON CROP PRODUCTION

2.1 Introduction

Worldwide literature has clearly documented the fact that soil compaction (SC) caused by wheel traffic has a negative effect on crop responses and on future site productivity (Warkotsch *et al.*, 1994). This chapter provides an overview of various research studies on crop responses to SC. The crops reviewed include maize, silage maize, soyabeans, forestry, sugarcane, cereals, grasses and various other crops (e.g. sugarbeet and cotton). In most cases, SC was found to significantly decrease crop yield, crop growth rates, root proliferation, nutrient and plant efficiencies, and effect seedling emergence. This Chapter does not look at the effects of SC on soil properties, which will be described in Chapter 3.

2.2 Maize

Research studies have been conducted by various authors in many countries to determine the effects of SC on maize yield. Some of the results from these experiments are summarized in Table 2.1. In the eight cases mentioned in Table 2.1, SC caused major reductions in maize yield. This was recorded on a wide range of soils, from clay soils in the United States to sandy loams in Syria. The most dramatic reduction in maize yield as a result of SC was measured by Gaultney *et al.* (1982), where yield reductions of 54% were measured in the first year and 22% in the second year, after the compaction event. Other authors in Table 2.1 found yield reductions of between 5% and 40% as a result of medium and heavy axle loads. As a result of the compaction event, there was a marked decrease in plant height and leaf area and root elongation.

Table 2.1 Research carried out by various authors on the effects of soil compaction (SC) on maize yield

Author and Country – Soil. Treatments. Results.
<p>Phillips and Kirkham (1962), USA – Clay</p> <p>Treatments: Heavy and moderate compaction treatments were applied by a Ford tractor (rear tyre contact pressure 130 kPa, front tyre contact pressure 82 kPa) making up to 20 passes.</p> <p>Results: 15 – 35% decrease in maize yields.</p>
<p>Gaultney <i>et al.</i> (1982), USA – Silty Loam</p> <p>Treatments: Compaction was applied by a Case 1175 tractor systematically driven lengthwise across plots.</p> <p>Results: In the first year maize yield decreased by 54% whilst in the second year the yield decline was about 22%.</p>
<p>Voorhees <i>et al.</i> (1989), USA – Clay Loam</p> <p>Treatments: 9 Mg and 18 Mg axle treatments were applied with and without inter-row compaction.</p> <p>Results: During the first year, grain yields decreased by 9% and 30% as a result of 9 Mg and 18 Mg axle treatments on the Webster soil, respectively. There was little effect on a Ves soil as only a 6% decrease was noted after 18 Mg axle loading. In the second year grain yields decreased by 12% as a result of 18 Mg axle treatments.</p>
<p>Lowery and Schuler (1991), USA – Kewaunee and Rosetta soils</p> <p>Treatments: 8 Mg and 12 Mg axle treatments were applied using a combine harvester (front wheel inflation pressure of 220 kPa) and a liquid manure tank (150 kPa inflation pressure) towed by a tractor (rear wheel inflation pressure of 100 kPa).</p> <p>Results: Plant height decreased with increasing compaction. Maize yields decreased by 14% and 43% as a result of 8 Mg and 12 Mg compaction treatments on the Kewaunee soil and by 4% and 14% on Rosetta soils, respectively.</p>
<p>Lal (1996), USA – Clay</p> <p>Treatments: 10 Mg axle load created by an empty single axle grain cart and a 20 Mg axle load from the same full grain cart.</p> <p>Results: Maize yields during the 3 year rotation decreased by 16% for the 10 Mg axle loads and 25% for the 20 Mg axle loads.</p>
<p>Lal and Ahmadi (2000), USA – Silty Loam</p> <p>Treatments: Three axle treatments for the Wooster site and three treatments for the Crosby site. Wooster site: Regular machine traffic, 7.5 Mg axle loads on controlled traffic lanes and 7.5 Mg axle loads on the entire plot. Crosby site: A control, 10 Mg axle loads and 20 Mg axle loads.</p> <p>Results: Wooster site: regular traffic decreased maize yield by 5% and the 7.5 Mg axle loads decreased yield by 15%. Crosby site: Axle load was found to have no significant effect on maize yield.</p>
<p>Tubeileh <i>et al.</i> (2003), Syria – Sandy Loam</p> <p>Treatments: Maize was grown in a compacted soil (1.45 Mg.m^{-3}) and in an un-compacted soil (1.3 Mg.m^{-3}).</p> <p>Results: SC greatly hampered root elongation and delayed the leaf appearance rate, thus decreasing plant height, shoot and root dry weights and leaf area. The increase in bulk density decreased the carbon assimilation rate, especially in the early growth stages.</p>
<p>Abu-Hamdeh (2003), Jordan – Clay Loam</p> <p>Treatments: 8 Mg and 19 Mg compaction treatments were applied using a 4 wheel drive truck with tyres inflated to 300 kPa. The treatments were applied before planting.</p> <p>Results: Maize yield decreased by 27% and 15% in the first and second years, respectively. SC appeared to decrease plant height and root distributions.</p>

2.3 Silage Maize

Silage maize, used as feed for livestock in the winter, is an important crop in Europe. In The Netherlands approximately 200 000 ha is grown as a continuous crop (Alblas *et al.*, 1994). Most of the crop is grown on sandy soils that are susceptible to SC. Thus, there is a growing concern regarding the impact of SC on silage maize. Table 2.2 summarizes research done to determine some of these impacts. As a result of a single SC event, silage maize yields were reduced by 15% and 38% for medium and heavy axle loads. Changes in soil properties as a result of wheeled traffic reduced the nitrogen uptake of the plants.

Table 2.2 Experimental trials to determine the effects of soil compaction (SC) on silage maize yield

Author and Country – Soil.
Treatments.
Results.
Alblas <i>et al.</i> (1994), The Netherlands – Sand
Treatments: Compaction treatments were applied by vehicles with 5 Mg and 10 Mg axle loads.
Results: The heavy axle loads reduced yields by up to 38%. Average yield reductions were 15% and 4% for axle loads of 10 Mg and 5 Mg, respectively.
Nevens and Reheul (2003), Belgium – Sandy Loam
Treatments: The trial site was compacted using a 5 Mg tractor (inflation pressure of 130 kPa).
Results: SC decreased the dry matter yield by 13% and the nitrogen uptake by 23% compared to the normally tilled plots

2.4 Soyabeans

Soyabeans are an important crop as they are the richest source of protein, compared to and equivalent amount of cheese, milk, egg or fish. Similarly to maize, soyabean is an important crop in developing countries (Voorhees *et al.*, 1976) and crop yield is frequently reduced as a result of SC. Table 2.3 summarizes various experiments conducted to determine the effects of SC on soyabean production.

Significant effects of SC were witnessed in all the experiments summarized in Table 2.3. Infield traffic caused yield reductions of up to 27% in a single year. Axle load had an effect on the severity of these reductions (the greater the axle load, the greater the reduction). The compaction event had effects on root nodulation and plant height.

Table 2.3 Research conducted to determine the effects of soil compaction (SC) on soyabean yield

Author and Country – Soil.	Treatments.	Results.
Voorhees <i>et al.</i> (1976) and Fausey and Dylla (1984), USA – Clay loam	Treatments: Various traffic treatments were applied.	Results: The total number of nodules per plant decreased by about 25 to 42% as a result of the wheel traffic in two consecutive seasons.
Johnson <i>et al.</i> (1990), USA – Clay	Treatments: The experiment consisted of two compaction treatments, namely 9 Mg axle loads and 18 Mg axle loads.	Results: The compaction treatments decreased plant height and decreased soyabean yields by 27% in a single year.
Lal (1996), USA – Clay	Treatments: 10 Mg axle load created by an empty single axle grain cart and a 20 Mg axle load from the same full grain cart.	Results: Soyabean yields during the 3 year rotation decreased by 8% for 10 Mg axle loads and 20% for 20 Mg axle loads as a result of SC.
Flowers and Lal (1998), USA – Clay	Treatments: 10 Mg axle load created by an empty single axle grain cart and a 20 Mg axle load from the same full grain cart.	Results: The yield for the control plot was 2.5 Mg.ha ⁻¹ . Soyabean yields decreased by 9% and 19% as a result of compaction by 10 Mg and 20Mg axle loads, respectively.

2.5 Forestry

Commercial forestry is an important part of many countries' economies. The effects of SC on forests can be severe, decreasing soil productivity and overall yield. These effects can be minimised if correct management practices are followed (Grigal, 2000). Table 2.4 provides an overview of the SC research conducted in different timber industries.

Of the nine cases mentioned in Table 2.4, all but one showed negative effects on yield and growth as a result of compaction. With the exception of Brais (2001), who conducted the experiment over a short time period whilst the plantation was developing, the other authors found negative consequences of SC on plant heights, growth rates and root densities.

Table 2.4 An overview of research conducted on the effects of soil compaction (SC) in forestry

Author, Tree species.	Description and Results.
Sands and Bowen (1978), Radiata pine	Description and results: The experiments were done on a sandy soil (bulk density range 1.35 to 1.6 Mg.m ⁻³ , air filled porosity at 1.6 Mg.m ⁻³ was 21%) to determine the effects of SC on root configuration and tree growth rates. It was found that SC caused an 87% decrease in dry root weight of the seedlings.
Froehlick (1979), Douglas fir trees and Ponderosa pine	Description and results: Soil compaction caused growth losses for Douglas fir trees of 14% and 30% due to moderate compaction and heavy compaction, respectively. The effects on Ponderosa pine trees were similar. A 6% and 12% reduction in growth rate was observed as a result of moderate compaction and heavy compaction, respectively.
Wronski and Murphy (1994), Ponderosa pine	Description and results: It was found that seedling height is negatively correlated with increasing bulk density. An 80% reduction in the height of seedlings was observed between bulk densities of 0.92 and 1.12 Mg.m ⁻³ .
Woodward (1996), Cedrelinga cateniformis, Caryodendron orinocense and Virola elongate	Description and results: In general, SC caused a decrease in plant height, tree diameter and tree growth rate.
Jansson and Wasterlund (1999), Picea abies	Description and results: Experiments were conducted to determine the effects of lightweight machinery (5 – 9 Mg) on young stands of Picea abies trees. The growth response as a result of the compaction was not statistically significant.
Brais (2001), Picea glauca	Description and results: After 5 years she found that tree height on a fine textured soil was 25% higher in wheel tracked area compared to the undisturbed areas. This suggests that compaction is beneficial in the early establishment period. This is because compaction can increase moisture availability in loose soils. The long term effects are unknown.
Smith and Johnston (2001), Eucalyptus grandis and Pine	Description and results: Trials were conducted on sandy soils in Zululand South Africa. It was found that SC resulted in a decrease in growth rate of 27% for Eucalyptus grandis and a 47% decrease for Pine trees. These results depend on the site and age of the trees.
Gomez <i>et al.</i> (2002a) and Gomez <i>et al.</i> (2002b), Ponderosa pine	Description and results: It was noted that SC has a negative effect on N uptake of pine trees and is affecting root growth, which is in turn decreasing tree growth rates. This is as a result of increased bulk density in the soil.
Clemente <i>et al.</i> (2005), Eucalyptus grandis	Description and results: Experiments showed that the effects of SC were greater around the base of the trees, resulting in a decrease in root elongation.

2.6 Sugarcane

The extent of SC problems in worldwide sugar industries have been discussed by Swinford and Boevey (1984). As a result of SC, sub optimal yields are being achieved and soil health is declining. Some of the results from these trials are summarized in Table 2.5.

The experiments in Table 2.5 show that SC / vehicle traffic negatively affected sugarcane production in a number of ways. Torres and Rodriguez (1995) noted that most of yield decline in sugarcane was due to stool damage.

Table 2.5 Effects of soil compaction (SC) on sugarcane production

Author and Country.	
Description and Results.	
Georges (1980), USA	Description and results: Experiments showed that as a result of SC, sugarcane re-growth was 20% shorter than the control treatment four months after the mechanical harvesting.
Swinford and Boevey (1984), RSA	Description and results: Experiments showed that yields were negatively correlated with increased bulk density. The reduction in yield for the worst treatment (compaction on row and interrow) was 32% in the first ratoon and 48% in the second ratoon. When only interrow compaction was applied, the yield reduction was 27% in the first ratoon and 35% in the second ratoon.
Torres <i>et al.</i> (1990), Columbia	Description and results: Stool damage resulted in a 7% and a 53% yield reduction for the grab loader and tractor trailer combination, respectively. Interrow compaction from the tractor and trailer reduced the yield by 9%. It was concluded that stool damage was more important than compaction, and should be avoided.

2.7 Other Cereals

The two main uses of cereals are that of human consumption (wheat, oats and rye) and alcohol production (barley, sorghum and wheat). For this reason, it is important to determine the effects of SC on cereal production (Mamman and Ohu, 1997). Table 2.6 summarizes some of the research carried out to determine the effects of SC on cereal production.

Changes to soil properties as a result of SC have caused a 38% decrease in wheat yield, a 22% decrease in sorghum yield, a 19% decrease in oat yield and a 22% decrease in barley yield (see Table 6.2). Compaction of the soil by vehicles resulted in reduced seedling emergence, reduced nutrient uptake and reduced water use efficiency of some plants.

Table 2.6 Experiments showing the effects of soil compaction (SC) on cereal crops

Author and Country – Soil – Crop.	Treatments.	Results.
Lal (1996), USA – Clay – Oats	Treatments: 10 Mg axle load created by an empty single axle grain cart and a 20 Mg axle load from the same full grain cart.	Results: Oat yields during the three year rotation decreased by 19% and 30% for 10 Mg and 20 Mg axle loads, respectively.
Abu-Hamdeh and Al-Widyan (2000), Jordan – Clay Loam – Barley	Treatments: Compaction treatments consisted of two inflation pressures (200 kPa and 400 kPa) and two axle loads (5 Mg per axle and 15 Mg per axle).	Results: Grain yields in the trafficked plots were lower than the un-trafficked plots.
Radford <i>et al.</i> (2000), Australia – Vertisol – Wheat	Treatments: Compaction was applied by traveling over a wet soil with a Ford New Holland 8060 harvester (front axle load 10Mg, inflation pressure 235kPa, rear axle load 2Mg, inflation pressure 205kPa). Lugs on the front wheel accounted for 16% of the contact area.	Results: Seedling emergence was reduced by 23%. It was noted that under less optimal growing conditions, these differences would have been exaggerated. There was no significant effect on grain yield.
Radford <i>et al.</i> (2001), Australia – Vertisol – Wheat and sorghum	Treatments: Compaction was applied by traveling over a wet soil with a Ford New Holland 8060 harvester (front axle load 10Mg, inflation pressure 235kPa, rear axle load 2Mg, inflation pressure 205kPa). Lugs on the front wheel accounted for 16% of the contact area.	Results: Soil compaction was found to reduce grain yields by reducing the soil water storage and the water use efficiency of the plant. There was a reduction in seedling emergence. Over 5 crops (3 wheat, 1 sorghum and 1 maize) yields decreased by 23% for a 10 Mg axle load on wet soil, 13% for a 6 Mg axle load on a wet soil and 1% for a 6 Mg axle load on a dry soil. Water use efficiency decreased from 14.3 to 9.7 kg.ha ⁻¹ mm ⁻¹ .
Ishaq <i>et al.</i> (2001a; 2001b; 2003), Pakistan – Sandy Clay – Wheat and sorghum	Treatments: Compaction was applied by a mechanical compactor that increased the soil bulk density from 1.65 Mg.m ⁻³ to 1.92 Mg.m ⁻³ .	Results: Wheat yield decreased by 38% in the first year and by 8% in the second year. Soil compaction reduced both the water and nutrient use efficiencies of sorghum by 22% in the first year and by 14% in the second year. The reductions in nutrient uptake by wheat due to SC ranged from 12 to 35% for N, 17 to 27% for P and up to 24% for K. For sorghum these decreases were 23% for N, 16% for P and 12% for K.
Czyż (2004), Poland – Mixture of soils – Barley	Treatments: Four compaction treatments were applied by an Ursus C360 tractor (rear axle load 1.69Mg, inflation pressure 150kPa, front axle load 0.94Mg, inflation pressure 250kPa). The treatments consisted of one pass, two passes and four passes over the trial plot.	Results: The reduction in spring barley yield depended on the number of tractor passes. The yield decreased by 2 to 19% in the loam, by 4 to 30% in the sandy loam and by 2.4 to 18% in the sandy soil.

2.8 Grasses

Grasslands are an important part of a farm enterprise as the grassland provides livestock with sustenance during summer. Excess grass is baled so that it can be fed to livestock during winter. Table 2.7 summarizes experiments conducted by various authors to

determine the effects of traffic on grassland yield. All three authors mentioned in Table 2.7 concluded that SC alters soil properties and had significant effects on the yield of grasslands. Dry yield decreased on average by 20% as a result of a compaction event.

Table 2.7 Experiments carried out to determine the effects of soil compaction (SC) on grasslands

Author and Country – Soil – Crop. Treatments. Results.
<p>Meek <i>et al.</i> (1988), USA – Sandy Loam – Alfalfa</p> <p>Treatments: Compaction treatments were applied using a John Deere 4020 tractor (rear axle load 2.02 Mg, inflation pressure 150 kPa) over 100% of the area and controlled lane traffic.</p> <p>Results: Dry yield was reduced by 10% for control lane traffic and by 17% for 100% traffic over the area.</p>
<p>Douglas and Crawford (1991), Scotland – Clay Loam – Ryegrass</p> <p>Treatments: Two compaction treatments consisting of a light pass (4.1 Mg, rear wheel inflation pressure 30 kPa, front wheel inflation pressure 40 kPa) and a heavy pass (6.2 Mg, rear wheel inflation pressure 110 kPa, front wheel inflation pressure 230 kPa)</p> <p>Results: In both years, the first and second cut yield was adversely affected by the compaction events. The most severe result was after 7 heavy passes where after 21 months, the yield decreased by 32%.</p>
<p>Jorajuria <i>et al.</i> (1997), Argentina – Sandy Loam - Lolium / Trifolium grasslands</p> <p>Treatments: Light and heavy compaction treatments were applied by 2 tractors. Light vehicle: 37 kW tractor (rear axle load 1.6 Mg, inflation pressure 114 kPa, front axle load 0.7 Mg, inflation pressure 180 kPa). Heavy vehicle: 76 kW tractor (rear axle load 2.8 Mg, inflation pressure 128 kPa, front axle load 1.4 Mg, inflation pressure 210 kPa).</p> <p>Results: Grass yield responses for all the treatments were significant, in the lane of the tractor the average decrease in dry matter production was 74%, whilst adjacent to the tyre imprints, the reduction was by 18%.</p>

2.9 Other Crops

Soil compaction research was also conducted on several other crops, including sugarbeet, cowpea, sunflowers, cotton and various vegetables. Experiments conducted by researchers on the effects of SC on crop yield are summarized in Table 2.8.

Table 2.8 shows that compaction by vehicles causes significant decreases in crop yield, leaf area and dry root matter. Some plants experienced a decrease in water use efficiency as a result of the compaction event.

Table 2.8 Experiments to determine the effects of soil compaction (SC) on other crops

Author and Country – Soil – Crop.	Treatments.	Results.
Onofioke (1989), Nigeria – Sandy Clay Loam – Cowpea	Treatments: Pot trials were compacted to 1.7 Mg.m ⁻³ , 1.4 Mg.m ⁻³ and 1.2 Mg.m ⁻³ .	Results: Leaf area, root dry matter and crop water use efficiency were significantly reduced by the high compaction treatment relative to the others.
Wolfe <i>et al.</i> (1995), USA – Silt Loam – Cabbage, cucumber, snap bean and sweet corn	Treatments: The soil was artificially compacted to a 0.1 m depth.	Results: The maturity of cabbage, snap bean, and cucumber was delayed, and the average reduction in total marketable yield in compacted plots were 73%, 49%, 41%, and 34% for cabbage, snap bean, cucumber and sweet corn, respectively.
Arvidsson (2001), Sweden – Sandy Loam – Sugarbeet	Treatments: Compaction treatments consisted of 4 passes with a 3 row harvester towed by a tractor (18 Mg on 4 axles, inflation pressure for tractor 100-150 kPa, 200-250 kPa for the harvester) and 4 passes by a self propelled 6 row harvester (35 Mg on 2 axles, inflation pressures 200-240 kPa).	Results: The differences in yield were found to be insignificant.
Dauda and Samari (2002), Nigeria – Sandy Loam – Cowpea	Treatments: 0, 5, 10, 15 and 20 passes were made over the field by a 2 wheel drive Massey Ferguson 165 tractor (total weight 4.4 Mg, mean contact pressure 31 kPa).	Results: The highest grain yield was found after 10 passes (1.4 Mg.ha ⁻¹) and the lowest grain yield after 20 passes (0.6 Mg.ha ⁻¹).
Bayhan <i>et al.</i> (2002), Turkey – Clay Loam – Sunflower	Treatments: Five compaction treatments were carried out using a 50 kW two wheel drive tractor (rear axle load 1.9 Mg, inflation pressure 159 kPa, front axle load 1.5 Mg, inflation pressure 124 kPa).	Results: The compaction treatments caused significant yield reductions of up to 22%.
Akinci <i>et al.</i> (2004), Turkey – Silty Clay Loam – Cotton	Treatments: Subsoiling treatments consisted of one and two passes with a Massey Ferguson 375 four wheel drive tractor with a subsoiler	Results: Cotton yields at each of the subsoiled plots increased (confirming that compaction causes yield decline)

2.10 Conclusion

This chapter provided an overview of the studies carried out by various authors to establish the effects of SC on crop growth and yield. Most of the cases reviewed showed that SC had detrimental effects on crop yield. In rare cases, SC was found to enhance crop growth rates during the early stages of crop development.

As a result of SC, there have been significant decreases in plant height, root elongation, leaf appearance rates and root mass in maize, soybeans and sugarcane. In the forestry industry, SC has caused a decrease in the dry root weight of seedlings, it has significantly decreased tree growth rates and has decreased nitrogen uptake by trees. Soil compaction is a major contributing factor to the reduction in seedling emergence in

wheat. It is responsible for reducing soil water storage, water use efficiency and nutrient use efficiency of plants. Vegetable crop maturity was delayed as a result of SC (i.e. the vegetable growth rate decreased).

It must be noted that the results summarized in this chapter are site and situation specific, i.e. under different conditions the results could have been different. However, the 41 experiments summarized in this chapter were conducted in different parts of the world and on different soils and mostly showed the same trend. It was found that over 90% of SC experiments resulted in negative effects on crop growth rates and yields.

In the light of this evidence, the author decided to investigate the process further. Chapter 3 provides an explanation and description of the SC process. It shows how the SC process affects various soil properties including bulk density and air filled porosity.

3. AN OVERVIEW OF PROCESSES OCCURRING DURING SOIL COMPACTION

3.1 Introduction

Chapter 2 confirms that crop response is negatively affected as a result of soil compaction (SC). This is because SC alters soil properties causing a decline in soil health. According to Horn (2000), the physical processes occurring in unsaturated soils are complex and become even more difficult to understand or predict when tillage processes and plant growth are also included. The processes that occur in the soil during vehicular traffic depend predominantly on the strength of the soil (otherwise known as pre-compression stress, *SS*). Soil strength in structured unsaturated soils depends on internal soil properties, such as texture, pore water pressure, organic content (OC) and aggregation (Horn, 2000). Soil compaction is a complex feedback process in that it is both affected and affects soil properties. The soil properties such as soil texture (sand / silt / clay contents), water content on a mass basis and organic content have been found to have an impact on the degree of SC (Mitchell and Berry, 2001).

The objective of Chapter 3 is to give an overview and a better understanding of the SC process because in order to model a process it is necessary to understand the process and the factors that affect it. It will also demonstrate the effects of SC on the various soil properties such as structural strength (Lowery and Schuler, 1994; Pagliai *et al.*, 2000; Horn *et al.*, 2003), bulk density (Sands *et al.*, 1979; Greacen and Sands, 1980; Mitchell and Berry, 2001; Horn *et al.*, 2003), soil aeration (Harris, 1971; Koolen and Kuipers, 1983; Pagliai *et al.*, 2000; Mitchell and Berry, 2001; Richard *et al.*, 2001; Tarawally *et al.*, 2004) and various hydraulic properties of the soil (Pagliai *et al.*, 2000; Mitchell and Berry, 2001; Richard *et al.*, 2001; Smith *et al.*, 2001; Horn and Fleige, 2003). The definitions of these soil properties will be described in Section 3.3.

3.2 Determinants of the Severity of Soil Compaction

It has been shown that various physical properties influence the severity of soil compaction (SC). Mitchell and Berry (2001) found that South African soils with a clay content of less than 15% are more susceptible to SC and a particle size analysis could assist in predicting a soil's tendency to be compacted. In general, sandy soils (clay < 30%) were compacted to greater densities at higher water contents than soils with clay contents of greater than 30%. There was a higher degree of compaction when the moisture content was close to field capacity. Koolen and Kuipers (1983) noted that under wet conditions, soils with high OC were more resistant to compaction compared to soils with low OC. The water content in the soil plays an important role in determining the severity of a compaction event.

3.3 Effects of Soil Compaction on Soil Properties (Macro Scale)

Soil compaction is caused by an external load being applied to the surface of the soil. During loading, any change to one property is likely to affect other properties as well. Harris (1971) describes SC as a change in soil volume. This change in volume can affect soil strength (penetration resistance), bulk density, soil aeration and the hydraulic properties of the soil.

3.3.1 Soil strength

Soil strength measurements are used to assess the soil structure following a compaction event (Horn, 2000). These measurements consist of penetration resistance (PR), shear strength, aggregate strength and pre-compression stress. Penetration resistance is defined as the force per unit area on a standard cone (ASABE, 2004) necessary for penetration by the cone (Harris, 1971). It can be deduced that an increase in PR, shear strength and aggregate strength will result in an increase in soil strength. Alakukku (1996) conducted experiments to determine the impacts of SC on PR. It was found that PR was 22% greater in the plots compacted by four passes compared to the control plots. Further experiments confirmed that SC does increase PR (Georges, 1980; Gaultney *et al.*, 1982; Mamman and Ohu, 1997; Jansson and Wasterlund, 1999; Bayhan

et al., 2002; Dauda and Samari, 2002). An increase in soil strength is accompanied by an increase in bulk density.

3.3.2 Dry Bulk density

Dry bulk density is defined as the mass (Mg) per unit volume (m^3) of soil. Authors conducted experiments to determine the effects of vehicle traffic on dry bulk density and their specific results are shown below:

- Voorhees *et al.* (1976) and Fausey and Dylla (1984) found that wheel traffic increased the dry bulk density in the upper 30cm of soil by 15%.
- Johnson *et al.* (1990) noted that 18 Mg axle loads increased the soil dry bulk density by 0.1 to 0.2 Mg.m^{-3} to a depth of 0.5 to 0.6m.
- Abu-Hamdeh and Al-Widyan (2000) showed that SC caused by 5 Mg and 15 Mg axle loads increased dry bulk density by between 1.6 and 6% after a two year period.
- Czyż (2004) found that as a result of increasing tractor passes (1.69 Mg rear axle load and 0.94 Mg front axle load), dry bulk density increased by 2.6 to 6.5% in a loam soil, by 7.9 to 13.2% in a sandy loam soil and by 7.8 to 11% in a sandy soil.
- Flowers and Lal (1998), Meek *et al.* (1988), Jorajuria *et al.* (1997) and Dauda and Samari (2002) also confirmed that SC caused increases in dry bulk density.

3.3.3 Soil aeration

The effects of soil compaction on soil aeration are quantified by porosity, air filled porosity, oxygen diffusion rate, redox potential and air permeability (Lipiec *et al.*, 2003). Porosity is defined as the ratio of the volume of voids in the soil to the total volume of soil (Das, 2002). Figure 3.1 illustrates how porosity changes as a result of SC (Dejong-Hughes *et al.*, 2001).

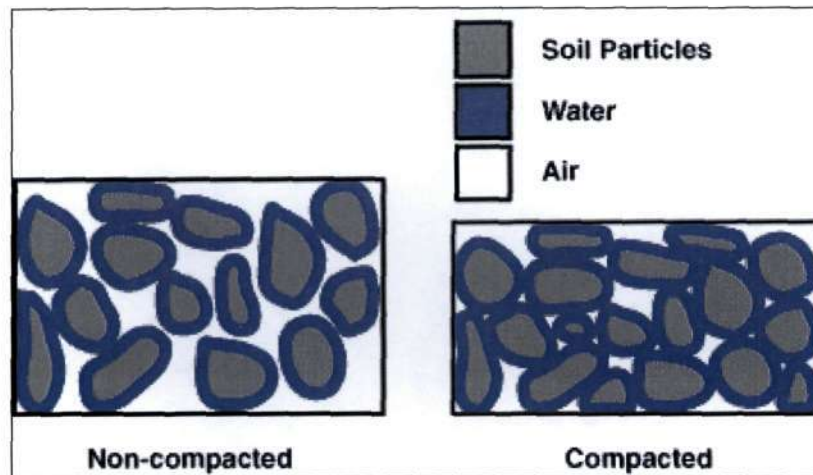


Figure 3.1 The effect of soil particle movement on porosity (Dejong-Hughes *et al.*, 2001)

The non-compacted soil in Figure 3.1 has a large porosity and a low bulk density. Soil compaction treatments were then applied to the non-compacted soil and the resultant is the compacted soil in Figure 3.1. Visually, the reader can see that the SC event has caused a decrease in overall soil volume, it has increased bulk density and has decreased porosity. Porosity can be divided into macroporosity and microporosity. Macroporosity is defined as the porosity which allows great water flow through porous media whilst microporosity is defined as the porosity which allows only capillary water movement through porous media (Alakukku, 1996). Alakukku (1996) found in her specific experiments that SC reduced the macroporosity of a clay subsoil by 70%.

Air filled porosity is defined as the ratio of the volume of air in the soil to the total volume of the soil, and is also very dependant on water content. Air filled porosity is most often used to evaluate soil aeration, and a value of 10 % on a volume basis is regarded as critical for plant growth (Mitchell and Berry, 2001; Lipiec *et al.*, 2003). One of the problems of using air filled porosity to determine the soil aeration status is that at the same air filled porosity, the equivalent pore diameter can be much smaller in a compacted soil than in an uncompacted soil. This may result in different air permeability. Thus, transmission parameters better reflect the aeration status of compacted soils (Lipiec *et al.*, 2003). The response of air permeability to SC is related to soil structure, pore size and pore continuity (ratio of air permeability to air filled porosity). Lipiec (1992) found that at the same level of compactness, air permeability

was greater for coarse structure (4 – 8 mm peds) compared to fine structure (<2 mm peds).

The decrease in soil aeration causes a change in the pore size distribution of the soil. Soil compaction reduces the number of large pores in the soil (Smith *et al.*, 2001). Richard *et al.* (2001) noted that the modification of the pore geometry results from a decrease in structural pores and also from a change in relation between the textural pores and the remaining structural pores. Tarawally *et al.* (2004) showed that SC decreased the number of pores greater than 50 μm and increased the number of pores between 0.5 μm and 50 μm . As a result of a change in pore geometry, the hydraulic properties of the soil are altered.

3.3.4 Hydraulic properties

Soil compaction reduces the rate of water movement through the soil (infiltration) and causes increased contact between soil particles. This affects the water retention characteristic and the hydraulic conductivity of the soil.

Water retention curves

Some studies indicate that an increase in SC results in lower gravimetric water contents at high matric potential range and higher water contents at low matric potentials (Lipiec *et al.*, 2003). These effects are reflected in the flattening of the soil water retention curve (SWRC) which indicates that, as the proportion of large pores decreases, the converse occurs to the number of small pores (Lipiec *et al.*, 2003). Smith *et al.* (2001) conducted experiments to determine the effect of SC on the SWRC in forestry soils in South Africa. Experiments showed that SC flattened the SWRC of all the soils that were tested. The flattening is illustrated in Figure 3.2. In Figure 3.2, Smith *et al.* (2001) showed that as bulk density increases (1.242 to 1.765 Mg.m^{-3}), the volumetric water content decreases (0.5 to 0.37) in the high matric potential range (0 to -7 kPa) and the water content increases (0.15 to 0.25) in the low matric potential range (-7 to -1500 kPa). This confirms the statements made by Lipiec *et al.* (2003). Smith *et al.* (2001) noted that the changes in the SWRC are dependant on the complex relationships between compressive processes, soil properties and pore geometry .

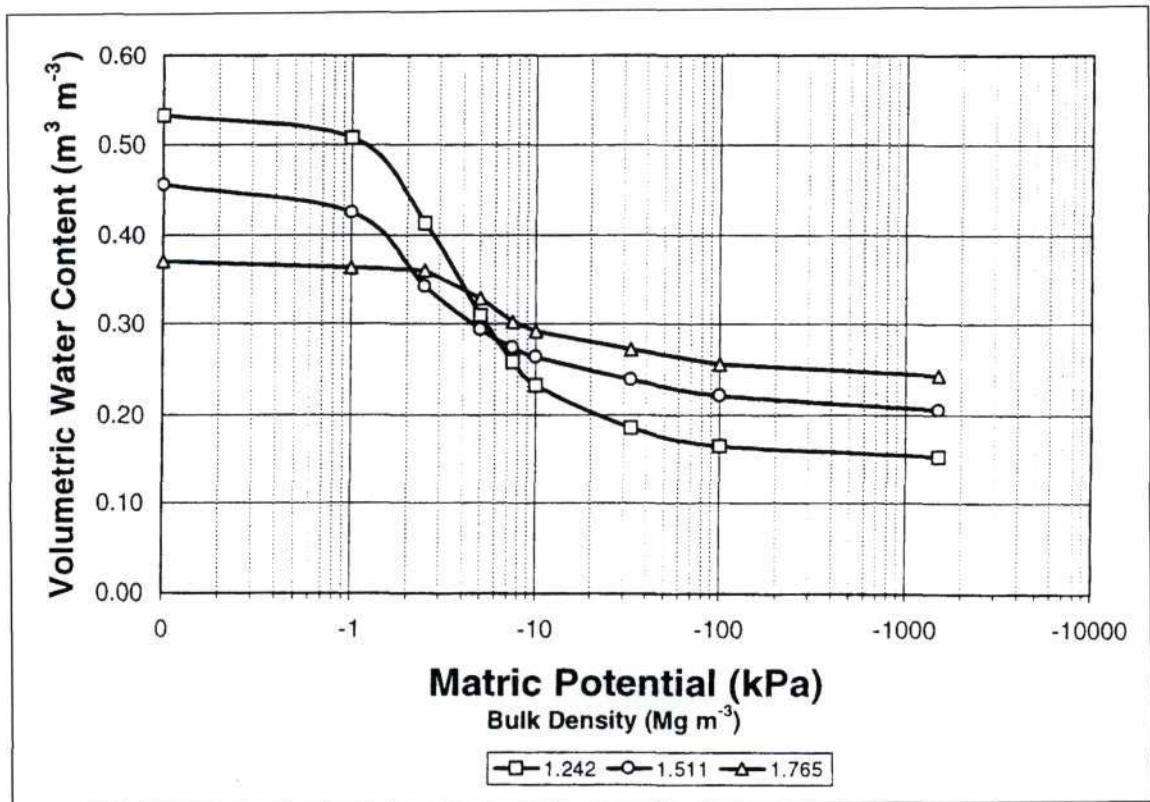


Figure 3.2 Graph showing flattening of soil water retention curves for increasing bulk densities (Smith *et al.*, 2001)

Smith *et al.* (2001) noted that the total available water content (AWC) responded to SC in the three following ways:

- Available water content increased with SC for some sandy and clay soils.
- Available water content was reduced with increasing SC for most soils.
- SC caused AWC to increase up to a point, after which it declined.

Figure 3.3 illustrates some of the findings that were made by Smith *et al.* (2001). It can be seen in Figure 3.3 that the loamy sand and the sandy loam soils undergo increases in AWC, the two sandy clay loam soils undergo decreases in AWC, whilst in the sandy clay and loam soils the AWC increases and then decreases. In all six cases the porosity of the soil decreases with increasing bulk density confirming the statements made in Section 3.3.3.

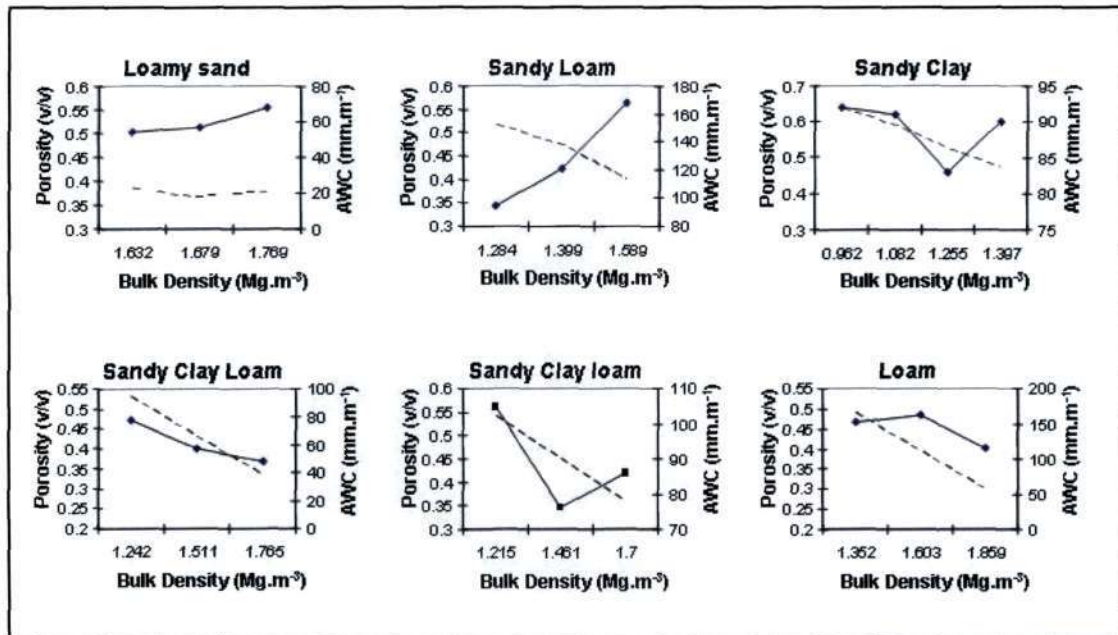


Figure 3.3 Graphs showing the effects of changes in bulk density on porosity (dotted line) and AWC (solid line) (after Smith *et al.*, 2001)

Hydraulic conductivity

Hydraulic conductivity (K) is defined as the rate at which water can move through a permeable medium (Das, 2002). Alakukku (1996) found in specific experiments that saturated hydraulic conductivity (K_{sat}) values were 60 to 98% less in plots with four vehicle passes than in the control plots. Fleige and Horn (2000) pointed out that reduced K_{sat} values increased runoff and consequently soil erosion. It was noted that in highly permeable soils (soils conducive to leaching), lower K_{sat} values improved the soil moisture status of these soils and reduced leaching losses (Lipiec *et al.*, 2003). The effect of SC on saturated water flow is governed by the larger pores, which are reduced by SC. This was shown by Lipiec *et al.* (1998) in their experiments where stained water was used to track water movement through the soil. They found that increasing SC reduced the volume of stained pores (macropores actively contributing to the water flow).

Unsaturated flow largely affects the dynamic processes of water and solute movement in the vadose zone (zone between the water table and the soil surface) (Lipiec *et al.*, 2003). Richard *et al.* (2001) reported that hydraulic conductivity as a function of soil wetness generally decreases with SC, but at some SC range and lower water potentials,

the conductivity is higher in compacted versus un-compacted soils. Section 3.4 provides an overview of the SC process on a micro scale.

3.4 The Soil Compaction Process (Micro Scale)

Harris (1971) produced a basis to define the micro scale soil compaction process specifically applicable to agricultural soils. While this may not be a comprehensive review of soil mechanics, the approach has been found suitable for agricultural applications by Larson *et al.*, (1980), Gaultney *et al.*, (1982) Wood and Wells (1985), McGarry (1989), Jim (1993), Or and Ghezzehei (2002) and Mooney and Nipattasuk (2003). It must be noted that Harris (1971) may differ from more specific engineering textbooks.

When a soil is subjected to an applied load that is sufficient to cause a change in volume, there are four possible factors to which the change in volume of the soil can be attributed (Harris, 1971). These factors are:

- Compression of solid particles.
- Compression of the fluids within the pore spaces.
- Re-arrangement of the soil particles.
- Change in the fluid contents in the pore spaces.

These factors are described in the following sections.

3.4.1 Compression of solid particles

If one considers two partly saturated soil elements that are in close proximity to each other and both are subjected to an external load. When this load is applied, liquid is displaced from between the two soil elements causing the contact area between the two soil elements to increase. The amount the contact area between the particles increases depends on the deformation of solid particles. This deformation, assumed to be elastic, will rebound due to the build up of air pressure in the soil after the applied stress has been released (Harris, 1971). The stress / strain theories are described in Section 3.4.5.

3.4.2 Compression of fluids within pore spaces

In most circumstances, a liquid may be considered as incompressible. However, this is not the case if liquids are subjected to sudden or large changes in pressure. When a unit volume of liquid is subjected to an increase in pressure, say ΔP (kPa), a decrease in volume, say ΔV (m³) occurs. The ratio of the increase in pressure to the decrease in volume is defined as the bulk modulus of elasticity K (kPa.m⁻³), given in Equation 3.1. This component is relatively insignificant, but has been mentioned.

$$K = -\frac{\Delta P}{\Delta V} \quad (3.1)$$

3.4.3 Re-arrangement of soil particles

The state of SC depends on the movement of either the liquid in the soil or the soil particles, or both. This is because these phases are relatively incompressible and do not undergo significant volume change when an external load is applied to the soil (Harris, 1971). The rate at which soil particles rearrange themselves either by sliding or rolling, is a major factor that contributes to the amount of volume change in unsaturated granular soils. For a saturated soil, the controlling factor for a large volume change is the rate at which water moves in and out of the soil (Harris, 1971). Although saturated SC processes can have detrimental impacts on a soil, these processes were omitted from this review since agricultural vehicles should not operate at these moisture levels.

The re-arrangement of soil particles depends on the structural arrangement of the particles and in fine grained soils on the degree of bonding between adjacent particles. The change in state of SC resulting from a rearrangement of particles is as a result of a change in volume of voids. Greacen and Sands (1980) described the change in the state of SC in terms of void ratio rather than bulk density. Equation 3.2 is used to calculate the void ratio of a soil (Das, 2002).

$$e = \frac{V_v}{V_s} \quad (3.2)$$

where e is the void ratio, V_v is the volume of voids (m^3) and V_s is the volume of solids (m^3).

Equation 3.3 was determined from uniaxial compression tests to empirically determine the new void ratio of a soil after an external pressure has been applied to the soil. Equation 3.3 was confirmed by Harris (1971) and Greacen and Sands (1980). Equation 3.3 shows that the relationship between the change in void ratio and the externally applied load is not linear, but logarithmic.

$$e = e_o - I_c \times \ln\left(\frac{P}{P_o}\right) \quad (3.3)$$

where e_o is the void ratio at an arbitrary pressure P_o (kPa), P is the pressure applied by the vehicle (kPa) and I_c is the compression index (see Equation 3.4).

$$I_c = -\frac{de}{d \ln P} \quad (3.4)$$

where I_c is the slope of the virgin compression curve (see Figure 4.4, pg 44), de is the change in void ratio and $d \ln P$ is the change in the log of the applied load.

Harris (1971) and Hadas (1994) found that the particle size distribution of a soil had an effect on the change in void ratio. This was attributed to the rearrangement capacity of soil particles. It was noted that a well graded soil would have more contacts between soil particles compared to a poorly graded soil. Under an applied force, this will cause the resistance to shear motion to increase in a well graded soil and the change in void ratio will therefore be reduced (Harris, 1971).

3.4.4 Change in fluid contents

The fluid contents of a soil are rarely static. Precipitation and irrigation add water to the soil, whilst the soil loses water to evapotranspiration and drainage. As the amount of water in the soil increases, the amount of air in the soil decreases. When water is added

to sandy soils, no volume change occurs. This is unlike clay soils that are normally characterized by volume changes in the form of swelling (Harris, 1971). Soil water is mainly retained by capillary forces and can be forced out between soil particles when a soil is subjected to an applied stress. The quantity of water moved out from in between the soil particles depends on the stress applied, water content of the soil, type of soil particles, and the bonding between the water and the soil particles (Harris, 1971). The next section describes the relationships between applied loads and the resulting SC of the soil.

3.4.5 Relationships between applied loads and resulting compaction

Soil is continually being subjected to forces. The nature of these forces and how the soil reacts to these forces is of particular interest (Horn, 2000). These forces can be divided into stresses and strains. This section describes how these forces interact with the soil and with each other.

Stress

When a load is applied to a solid body, the body changes shape (i.e. becomes distorted). This displacement causes a certain part of the body to be moved with respect to another adjacent part of the body. Due to the displacement, atomic forces of attraction act as restoring forces, which resist this change in shape and return the body to its original state. If these restoring forces act on a area of soil, they can be described as stresses. Since force is vector, the concept of stress can be visualized as the force per unit area acting on an area (Harris, 1971). The stress vector and stress tensor concepts are used to describe the forces acting on a volume element (Harris, 1971). This concept was successfully applied to soil by Terzaghi and Peck (1948) and van den Berg (1962). Figure 3.4 shows the stresses acting on a soil element.

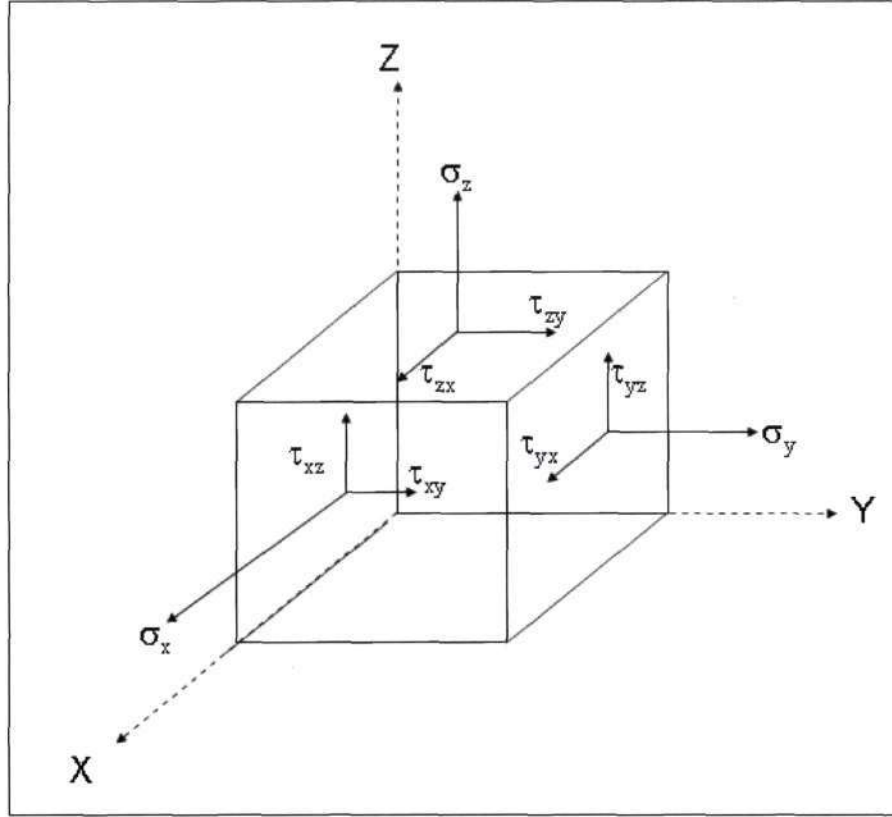


Figure 3.4 Stress components of the stress tensor necessary to completely describe the forces acting on a cubical element of soil, where σ_x , σ_y and σ_z are normal stresses acting on the soil element and τ_{zy} , τ_{zx} , τ_{yz} , τ_{yx} , τ_{xz} and τ_{xy} are shear stresses acting on the soil element (Harris, 1971)

Figure 3.4 shows that there are nine quantities that describe the stress acting on a particular soil element. They are usually written in the matrix form given in Equation 3.5.

$$\text{Stress Tensor} = \begin{pmatrix} \sigma_x & \tau_{xy} & \tau_{xz} \\ \tau_{yx} & \sigma_y & \tau_{yz} \\ \tau_{zx} & \tau_{zy} & \sigma_z \end{pmatrix} \quad (3.5)$$

At equilibrium, it has been shown that $\tau_{xy} = \tau_{yz}$, $\tau_{xz} = \tau_{zx}$ and $\tau_{yz} = \tau_{zy}$. Thus only six of the nine stress components are needed to specify the state of stress of a particular soil element (Harris, 1971). The stress tensor (Equation 3.5) has several points of interest. If the soil element is rotated into such a position so that all the shear forces are zero and only normal stresses are acting on the planes, then these axes are called the principle axes (thus the stresses on these axes become the principle stresses). A more detailed description of the stress tensor is given in Harris (1971) and Horn (2000).

Strain

When soil is subjected to an external load, soil elements may become displaced until a new state of equilibrium is reached between the external and internal forces. When this happens, the soil is in a state of strain (Harris, 1971). Strain can be sub divided into two sections, namely:

- Longitudinal strain – simple extension or contraction of a unit length of a line element (defined as the ratio of the change in length of a element to its original length)
- Shearing strain – is defined as the change in angle between two line elements that were mutually perpendicular.

Strain measurements are the quantitative measures of relative displacement between adjacent parts of the material. The strain tensor is used to describe the strains acting on an element of soil (Harris, 1971). The strain tensor is shown in Equation 3.6. The strain tensor shows that there are nine strains that adequately describe the strains acting on a soil element. Like the stress tensor, at equilibrium conditions, some of the strains are equal to each other ($\epsilon_{xy} = \epsilon_{yx}$, $\epsilon_{xz} = \epsilon_{zx}$ and $\epsilon_{yz} = \epsilon_{zy}$), thus only six strains are required to describe all the strains on the soil element (Harris, 1971; Horn, 2000).

$$\text{Strain Tensor} = \begin{pmatrix} \epsilon_x & \epsilon_{xy} & \epsilon_{xz} \\ \epsilon_{yx} & \epsilon_y & \epsilon_{yz} \\ \epsilon_{zx} & \epsilon_{zy} & \epsilon_z \end{pmatrix} \quad (3.6)$$

The concepts of strain are useful but are slightly complicated as line elements become curves once they are strained (Harris, 1971). Two assumptions have, therefore, been made that result in workable theories, namely:

- The quantities used to describe strain are so small that their squares and products are negligible results in the strain theory (strains $< 0.1\%$).
- All straight lines and all parallel lines remain straight and parallel after straining (implying the state of strain is constant through the material).

Natural strain is defined as the ratio of change in length of a line element to its instantaneous length (Horn, 2000). According to Harris (1971), the most accurate but also the most complicated theory is that of finite strain.

Relationships between stress and strain

Stress strain relationships based on the theories of elasticity and plasticity have been applied to soils with some success (Harris, 1971). Horn (2000) described the relationship between stress and strain in Equation 3.7.

$$\begin{pmatrix} \sigma_x & \sigma_{xy} & \sigma_{xz} \\ \sigma_{yx} & \sigma_y & \sigma_{yz} \\ \sigma_{zx} & \sigma_{zy} & \sigma_z \end{pmatrix} = \frac{E}{(1+\nu)} \begin{pmatrix} \epsilon_x - \epsilon_m & \epsilon_{xy} & \epsilon_{xz} \\ \epsilon_{yx} & \epsilon_y - \epsilon_m & \epsilon_{yz} \\ \epsilon_{zx} & \epsilon_{zy} & \epsilon_z - \epsilon_m \end{pmatrix} + \frac{E}{3(1-2\nu)} \begin{pmatrix} \epsilon_m & 0 & 0 \\ 0 & \epsilon_m & 0 \\ 0 & 0 & \epsilon_m \end{pmatrix} \quad (3.7)$$

where E is Young's Modulus (σ/ϵ) and ν is Poisson's Ratio (-lateral / axial strain). ϵ_m is defined as the mean normal strain acting at a point and is defined in Equation 3.8

$$\epsilon_m = \frac{1}{3}(\epsilon_x + \epsilon_y + \epsilon_z) \quad (3.8)$$

More detailed information on stress – strain relationships are described in Bailey and Johnson (1989), Gupta and Raper (1994) and Upadhyaya *et al.* (2002).

3.5 Conclusion

This chapter provided a detailed description of the macro and micro processes that occur within a soil when an external load is applied to the soil surface causing the soil to be compacted to some degree. This chapter showed that the most important property that determines the degree of SC in unsaturated soils is soil texture. This is because soil texture influences particle rearrangement. In addition, the organic content and water content have an impact on the SC processes primarily in determining the amount of shearing occurring in the soil, the amount of water movement through the soil and the amount of particle re-arrangement that occurs. This chapter also discusses the

relationships between the applied load and the resulting SC. These are of some importance as they will be used in later chapters.

The Chapter met its objectives of giving an overview of the SC processes and it described some of the research that confirms that SC affects soil properties such as structural strength, bulk density, soil aeration and hydraulic properties. The next logical step after understanding the soil dynamics under SC is to attempt to model these processes. Chapter 4 gives a review of the current state of SC modelling. Various models are described and analysed.

4. A REVIEW OF SOIL COMPACTION MODELLING

4.1 Introduction

Modelling is a useful technique to enable people to understand, evaluate and manage a process, such as soil compaction (Defossez and Richard, 2002). The logical development of a soil compaction (SC) model starts by formulating the stress propagation within the soil resulting from a force applied at the soil surface. There after stress – strain behaviour in the soil is modelled, which influences soil structure, *e.g.* increasing bulk density and causing rut formation (Defossez and Richard, 2002).

Defossez and Richard (2002) classified most of the current SC models into two categories, *viz* pseudo-analytical models and finite element models (FEM). These categories are described in Table 4.1. Defossez and Richard (2002) suggest that the structure of SC models be divided into two parts. The first part determines the propagation of the loading forces through the soil resulting from forces exerted by vehicles and acting on a wheel – soil contact (propagation sub-model). The stresses at the wheel – soil interface are described by the contact area and stresses over it (surface-applied force sub-model). The second part deals with modelling the stress – strain behaviour, *i.e.* the relationships between changes in soil volume and the applied stresses (stress – strain behaviour sub-model).

Table 4.1 Classification of soil compaction models (after Defossez and Richard, 2002)

Model	Pseudo – analytical	FEM
Propagation sub-model	Pseudo-analytical calculus of stress distribution	Numerical calculus of the displacement distribution
Surface-applied force sub-model	Inhomogeneous stress distribution over an elliptic contact area	Uniform stress distribution over the contact area
Stress-strain behaviour sub-model	Empirical models	Pseudo-elastic models Cam Clay type models Coupled models

The main difference between the existing models is the procedure used to determine the propagation of loading forces through the soil and the procedure used to model the change in soil volume. These differences are illustrated in Table 4.1. Pseudo-analytical models have been known to simplify tyre action by considering only one invariant

(principle stress σ_1 , kPa), whilst FEM modelling allows for three dimensional problems to be solved (Defosseze and Richard, 2002).

Pseudo-analytical models have been developed by Blackwell and Soane (1981), Gupta and Larson (1982), Smith (1985), Binger and Wells (1992), O'Sullivan *et al.* (1999), and van den Akker (2004), Finite element models have been developed by Raper and Erbach (1990), O'Sullivan and Simota (1995), Raper *et al.* (1995), Upadhyaya *et al.* (2002) and Defosseze and Richard (2002). Some of these models will be discussed later in this section.

The objective of this chapter is to review SC models in the context of the different model types described by Defosseze and Richard (2002) in Table 4.1. The review also includes the SC model SOCOMO (van den Akker, 1999; van den Akker, 2004), which is described in more detail in the second part of this chapter.

4.2 Pseudo-Analytical Models

Pseudo-analytical models consist of three major sections, namely modelling the stress propagation through the soil, modelling the soil – tyre interface and modelling the stress – strain behaviour in the soil (Defosseze and Richard, 2002). Pseudo-analytical models developed by Gupta and Larson (1982) and O'Sullivan *et al.* (1999) will be briefly described in this section whilst the model developed by van den Akker (2004) will be described later.

4.2.1 Modelling the stress propagation through the soil

Pseudo-analytical models developed by Blackwell and Soane (1981), Gupta and Larson (1982), Smith (1985), Binger and Wells (1992), O'Sullivan *et al.* (1999), Arvidsson (2001) and van den Akker (2004) are all based on the work done by Söhne (1958), whereby they all model the distribution of the vertical stress over the contact area (soil – tyre interface) and calculate the propagation of the major principle stress σ_1 (kPa) through the soil. Defosseze and Richard (2002) noted that propagation calculus uses semi-empirical formulas derived by Fröhlich (1934) from Boussinesq's (1885)

analytical solution for a homogeneous, isotropic ideal elastic material. Boussinesq's (1885) solution calculates the propagation of the major principle stress of a vertical loading point acting on a semi-infinite medium of Young's modulus E and Poisson's ratio μ . In 1934, Boussinesq's (1885) solution was applied to soil by Fröhlich (1934). In doing this, Fröhlich (1934) added a concentration factor ξ to Boussinesq's (1885) solution. This is because he noticed that measured soil stresses deviated from the stresses calculated using Boussinesq's solution and that these deviates followed trends according to their location (*i.e.* the soil was non-elastic). Equation 4.1 illustrates Boussinesq's (1885) solution and Equation 4.2 shows the modifications made by Fröhlich (1934).

$$\sigma_1 = \frac{3P}{2\pi r^2} \cos \theta \quad (4.1)$$

$$\sigma_1 = \frac{\xi P}{2\pi r^2} \cos^{\xi-2} \theta \quad (4.2)$$

where σ_1 (kPa) is the major principle stress acting on the soil element, P (kPa) is the applied load, r (m) is the distance under the loading point P , θ is the angle between the radius and the vertical, and ξ is the concentration factor (refer to Figure 4.1). When $\xi = 3$, Equation 4.2 becomes Equation 4.1.

Söhne (1958) suggested that ξ equals values of 4, 5 and 6 for hard, firm and soft soils respectively. The value of ξ depends on empirical combinations of bulk density and the soil water status. The effect of ξ on the principle stress is illustrated in Figure 4.2. The iso-stress lines in Figure 4.2 were calculated using Equation 4.1. Figure 4.2 shows that an increase in ξ leads to a deeper penetration of these iso-stress lines. Harris (1971) and Hadas (1994) later found values of ξ to be 3.5 in a light clay loam, 4.6 in a sandy loam and between 4.5 and 4.8 in a moist, freshly tilled loam soil.

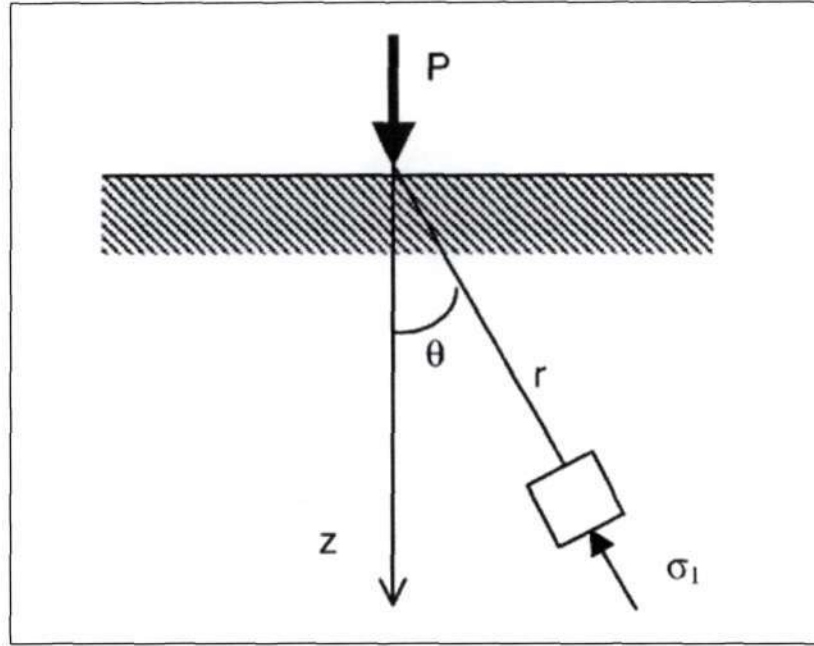


Figure 4.1 Stresses on a volume element caused by a point load P , where P (kPa) is the applied load, r (m) is the distance under the loading point P , θ (radians) is the angle between the radius and the vertical and σ_1 (kPa) is the major principle stress acting on the soil element (Defossez and Richard, 2002)

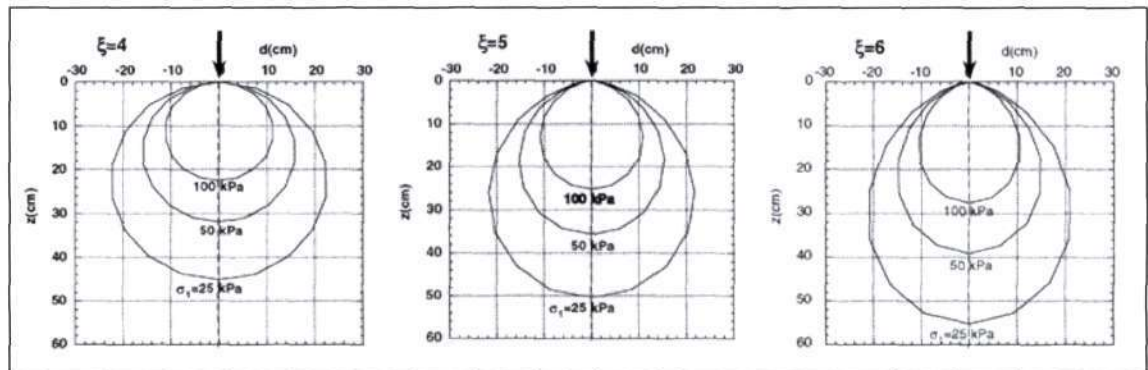


Figure 4.2 Curves of equal pressure under a load point of 8 kN at three concentration factors (after Defossez and Richard, 2002)

Söhne (1958) proposed a method to calculate the stress propagation under a tyre using Boussinesq's (1885) modified formulas. Söhne (1958) modelled the stresses applied by the tyre at the soil – tyre surface. He assumed an elliptical surface area. Söhne (1958) neglected shear stresses due to slip at the soil surface and he described the distribution of the vertical stress at the soil surface by a polynomial of the 16th, 4th and 2nd order for hard ($\xi = 4$), firm ($\xi = 5$) and soft soils ($\xi = 6$), respectively. Figure 4.3 illustrates the distribution of vertical stress at the soil surface for hard, firm and soft soils. Söhne

(1958) calculated the principle stress σ_1 on the load axis and outside the load axis. The minor stresses σ_2 and σ_3 were neglected.

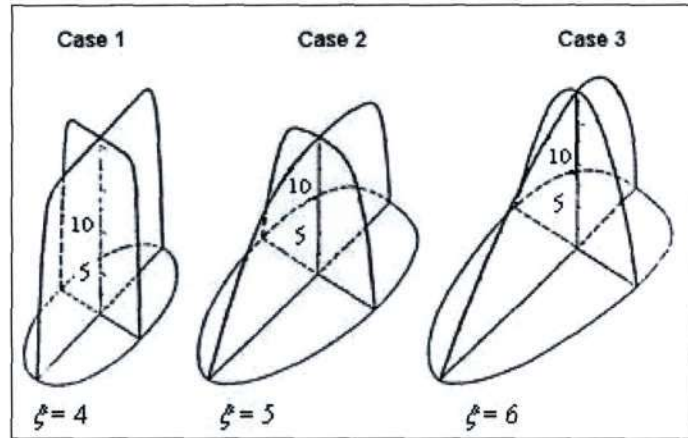


Figure 4.3 Pressure distributions in the contact area between the soil and tyre for different concentration factors Söhne (1958)

The calculus used by Söhne (1958) to calculate the stress propagation through the soil consists of dividing the contact surface into 25 load elements and applying a fraction of the total load to the centre of gravity of each loading element. The applied fraction of the total load depends on the vertical stress distribution (Defosseze and Richard, 2002).

Up until this point, Söhne (1958) had only taken the vertical normal stress into account. van den Akker (1988) and Johnson and Burt (1990) proposed to extend Söhne's (1958) work by considering the effects of shear stress caused by slip. This enabled all three principle stresses (σ_1 , σ_2 and σ_3) to be predicted for any element in the soil. This will be described in greater detail in Section 4.4.1. Once the propagation of stress through the soil has been modelled, the next logical step is to model the stress – strain behaviour in the soil.

4.2.2 Modelling the stress – strain behaviour

There are two methods commonly used to describe the stress – strain behaviour in soils. The first method was developed by Larson *et al.* (1980) after completing uniaxial compression tests on a number of agricultural soils. Larson *et al.* (1980) showed that at given water contents, compression curves (bulk density vs log applied stress)

determined on agricultural soils are linear over the range of stress from 100 to 1000 kPa and that compression curves at different water contents for a given soil are approximately parallel over the range of initial pore water potential from -5 to -70 kPa. The relationship describing the linear portion of the compression curve is shown in Equation 4.3.

$$\rho = [\rho_k + \Delta T(S_1 - S_k)] + Ci \log\left(\frac{\sigma_z}{\sigma_k}\right) \quad (4.3)$$

where ρ_k (kg.m^{-3}) is the bulk density at a known stress, σ_k (kPa) at a known degree of saturation S_k (%). Ci is a compression index and represents the soils sensitivity to SC. ΔT is the slope of ρ_k vs the degree of saturation.

Ci is a function of soil texture and organic matter (Larson *et al.*, 1980). ΔT describes the effect of the degree of saturation on dry bulk density – the higher the water content, the higher the density under a given stress increase (Defosseze and Richard, 2002).

The second method of describing the stress – strain behaviour in soils is based on critical state soil mechanics. The compactness of the soil is expressed as its specific volume (v), which is the ratio of the total volume of the soil to the volume of the solids alone (O'Sullivan *et al.*, 1999). Specific volume is preferred to dry bulk density as it is consistent with critical state soil mechanics. The compactibility of a soil is assessed in terms of its virgin compression line (VCL), which is the maximum specific volume a soil can have at any given value of mean effective stress (Defosseze and Richard, 2002). In other words, the VCL is the result of isotropic compression with no distortion (Figure 4.4). The VCL is characterised by an elastic rebound/recompression parameter κ and a plastic compression parameter λ . The change in slope from reversible to irreversible compression occurs at the maximum past stress p_c , the pre-consolidation pressure (Figure 4.4).

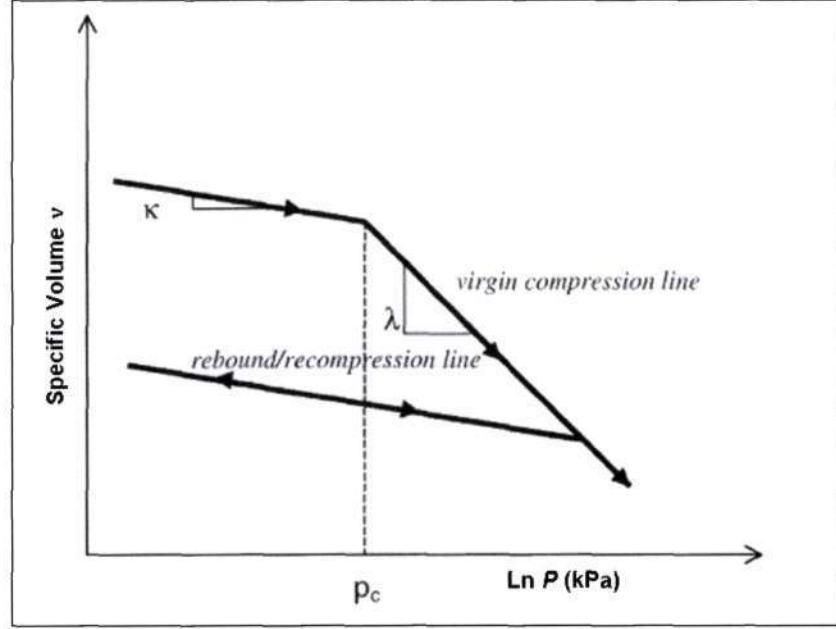


Figure 4.4 Isotropic compression diagram, where κ and λ are compression parameters, v (dimensionless) is the specific volume, P (kPa) is the applied load and p_c (kPa) is the pre-consolidation pressure (Defossez and Richard, 2002)

The VCL gives the specific volume v as a function of the mean normal stress P (Equation 4.4).

$$v = N - \lambda \ln(P) \quad (4.4)$$

where v is specific volume, N is the specific volume at $P = 1\text{kPa}$, λ is the compression index and p is the mean normal stress.

O'Sullivan *et al.* (1999) proposed a method to take the effect of water content on N and λ into account. The intercept of the VCL was modelled as a quadratic function of soil water content (Equation 4.5).

$$N = a_1 - a_2(w - a_3)^2 \quad (4.5)$$

where N is the VCL intercept, w is the soil water content and a_1 , a_2 and a_3 are coefficients for a given soil type.

Values for a_1 , a_2 and a_3 were derived by O'Sullivan *et al.* (1994). The VCL tends to pivot about a point in the v - $\ln P$ space as the water content changes. λ was estimated from N and the coordinates of the pivot point, v_p and p_p (Equation 4.6).

$$\lambda = \frac{N - v_p}{\ln p_p} \quad (4.6)$$

The coordinates of the pivot point varied according to soil type (O'Sullivan *et al.*, 1994). Defossez and Richard (2002) noted that the effect of the water content modelled by O'Sullivan *et al.* (1999) is higher than the effect of saturation described by Equation 4.3 in the model developed by Larson *et al.* (1980).

Now that the theory of most pseudo-analytical models has been described, the next section provides an overview of some of the pseudo-analytical models that have been developed and gives a specific evaluation of two pseudo-analytical models developed by Gupta *et al.* (1985) and O'Sullivan *et al.* (1999).

4.2.3 An overview of some of the pseudo-analytical soil compaction models that have been developed

Table 4.2 summarizes some of the models that have been developed. All of these models use the theory developed by Boussinesq (1885), Fröhlich (1934) and Söhne (1958) to determine the principle stress distribution through the soil. In addition, O'Sullivan *et al.* (1999) used empirical equations to determine minor stresses in the soil.

The SC models developed by Gupta *et al.* (1985) and O'Sullivan *et al.* (1999) were reviewed in a little more detail because they are representative of the two types of pseudo-analytical models and they have been recognised by other people. A cited reference search on the website www.isiknowledge.com showed that the work published by Gupta *et al.* (1985) has been cited 3 times, whilst the work published by O'Sullivan *et al.* (1999) has been cited 14 times (Accessed 5 September 2005).

Table 4.2 Summary of pseudo-analytical soil compaction models

Model Author	Stress – Strain behavioural component	Context
Gupta <i>et al.</i> (1985)	Uses equation developed by Larson <i>et al.</i> (1980)	Compaction in agricultural soils due to traffic
Binger and Wells (1992)	Uses equation developed by Larson <i>et al.</i> (1980)	Effect of surface mining systems on SC
Blackwell and Soane (1981)	Uses critical state theory to describe volume change	Simplified model to predict SC in agriculture
Smith (1985)	Uses critical state theory to describe volume change	Able to compare SC caused by various wheel configurations and arrangements
O'Sullivan <i>et al.</i> (1999)	Uses critical state theory to describe volume change	Simplified Excel based model, that is easy for students to use

Gupta *et al.* (1985) verified their model on three different sites with two types of soil structure (see Table 4.3). They performed the wheeling tests under different water conditions for each site.

Table 4.3 Summary of the tests conducted by Gupta *et al.* (1985) and O'Sullivan *et al.* (1999) (after Defossez and Richard, 2002)

Author	Site	Texture	Structural state	Soil moisture (g.g ⁻¹)	Way of loading	Mean vertical stress (kPa)
Gupta <i>et al.</i> (1985)	Plot 1	Silty loam	Homogeneous 1 m layer	0.27	1 pass	150
	Plot 2	Loam	Homogeneous 1 m layer	0.25	1 pass	130
	Plot 3	Loam	Ploughed 0.5 m layer	0.2 0.17 0.13	1 pass	211 260 320
O'Sullivan <i>et al.</i> (1999)	Plot 1	Silty loam	Homogeneous 0.5m layer	0.24	1 pass	40 80
	Plot 2	Loam	Dense underlying subsoil at 0.35 m	0.21	1 pass	100

The maximum increase in dry density was found to be 0.3 Mg.m⁻³. Each wheeling test was modelled by the calculation of dry density along the load axis and outside the load axis. These calculations take into account the mean soil water content above the plough pan. Gupta *et al.* (1985) calibrated their model using the concentration factor ξ to obtain better agreements between observed and simulated observations. They presented a model sensitivity analysis as a function of ξ . The change in predicted bulk density was shown to be within the error of the field measurements. Figure 4.5 illustrates a

comparison between the simulation and the measured data for the first site for dry density on the central load axis.

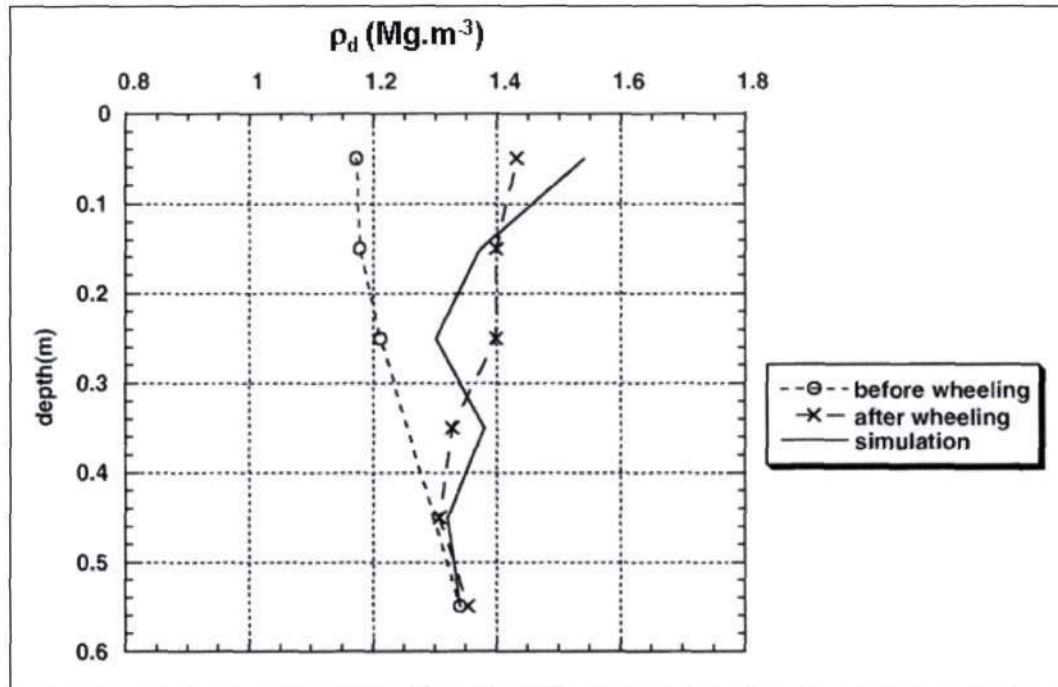


Figure 4.5 Comparison of simulated and measured observations for the model developed by Gupta *et al.* (1985). These results are from Plot 1 (see Table 4.3)

Figure 4.5 shows that the simulated and measured observations follow the same trends. Gupta *et al.* (1985) found that the model did not perform well in the third plot. This was attributed to clods in the soil. Table 4.4 shows the maximum difference between the measured and simulated bulk densities as a function of depth in the three plots. Compaction intensity is defined as the maximum difference observed when comparing the initial and final bulk density profiles as a function of depth. The simulation error ($\Delta\rho_b$) is defined as the maximum difference when comparing the simulated and measured profiles of bulk density against depth (Defosseze and Richard, 2002). Table 4.4 shows that the simulation error was between 0.12 and 0.33 Mg.m⁻³ for the trials run by Gupta *et al.* (1985). The error was found to be higher on the ploughed layer and lower on the artificially homogenous layers.

O'Sullivan *et al.* (1999) tested their model on two soil types and two types of soil structure (see Table 4.3). Their simulations of the dry density profile beneath the centre line of the tyres included the variation of water content through the soil, where as Gupta

et al. (1985) only took into account the mean water content above the plough pan. O'Sullivan *et al.* (1999) tested two tractors in order to range the mean vertical pressure from 40 to 80 kPa. They found that the model accurately predicted the compaction events (see Figure 4.6).

Table 4.4 Evaluation of the models developed by Gupta *et al.* (1985) and O'Sullivan *et al.* (1999) (after Defosseze and Richard, 2002)

Author	Site	Tested model outputs	Compaction intensity	Simulation error
Gupta <i>et al.</i> (1985)	Plot 1	2D profile of dry density $\rho_b(x,z)$	0.3 Mg m ⁻³	$\Delta\rho_b = 0.12 \text{ Mg m}^{-3}$
	Plot 2		0.2 Mg m ⁻³	$\Delta\rho_b = 0.13 \text{ Mg m}^{-3}$
	Plot 3		-	$\Delta\rho_b = 0.33 \text{ Mg m}^{-3}$
O'Sullivan <i>et al.</i> (1999)	Plot 1	1D profile of dry density $\rho_b(z)$	0.24 Mg m ⁻³	$\Delta\rho_b = +0.08 \text{ Mg m}^{-3}$
			0.22 Mg m ⁻³	$\Delta\rho_b = 0.03 \text{ Mg m}^{-3}$
	Plot 2		0.22 Mg m ⁻³	$\Delta\rho_b = 0.2 \text{ Mg m}^{-3}$

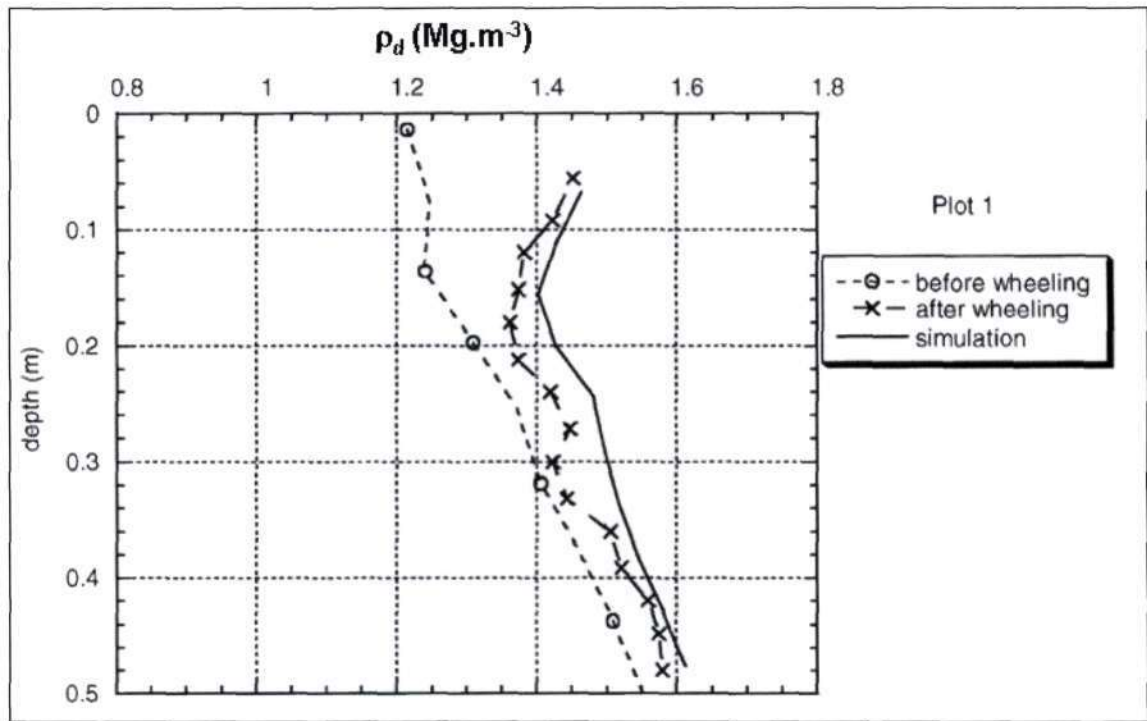


Figure 4.6 Comparison of simulated and measured observations for the model developed by O'Sullivan *et al.* (1999). These results are from Plot 1 (see Table 4.3)

Table 4.4 shows that the SC events caused an increase in dry bulk density of between 0.22 – 0.24 Mg.m⁻³. The differences between the measured and simulated observations were 0.08 and 0.03 Mg.m⁻³ for both experiments. The simulation with the plough pan at a 0.35 m depth yielded larger simulation errors. Table 4.4 confirms that both of these

models performed relatively well. The model developed by O'Sullivan *et al.* (1999) appeared to perform better than the model developed by Gupta *et al.* (1985). One of the pseudo-analytical models not described in this section is the SC model SOCOMO developed by (van den Akker (2004). This model will be described in detail in Section 4.4. The next section in this document gives a brief description of the finite element method (FEM) of modelling SC. It also provides the reader with a few model examples.

4.3 Finite Element Method (FEM) Soil Compaction Models

Finite element method (FEM) soil compaction models consist of two major sections, namely modelling the propagation of displacement through the soil and modelling the stress – strain behaviour in the soil (Defossez and Richard, 2002). The stress – strain behaviour can be modelled using three different techniques, namely with pseudo-elastic models, with Cam Clay type models and with coupled models. Each of these methods will be briefly described in this section. FEM models developed by Raper and Erbach (1990), Kirby (1994), and Gysi *et al.* (2000) will be briefly described in this section.

4.3.1 Modelling the propagation of displacement through the soil

The concept of the FEM is discussed in Upadhyaya *et al.* (2002). The principle of virtual work is used as a basis for the finite element models. The equilibrium condition associated to the principle of virtual work for the static deformation of a soil body is given in Equation 4.7.

$$\int \delta \underline{\varepsilon}^T \underline{\sigma} dV = \int \delta \underline{u}^T \underline{p} dV + \oint \delta \underline{u}^T \underline{t} dS \quad (4.7)$$

where V and S are the volume and the surface of the deformed body, $\underline{\sigma}$ and $\underline{\varepsilon}$ are the stress and strain tensors, $\delta \underline{u}$ is the incremental displacement, \underline{p} and \underline{t} are the body forces and the surface traction (Defossez and Richard, 2002).

The FEM consists of linearizing Equation 4.7 by assuming that the soil continuum is a finite number of elements connected at nodal points (Gupta and Raper, 1994). Numerical calculus is used to calculate the displacements at each nodal point and from

this stress and strain tensors are deduced (Raper *et al.*, 1995). It is important to note that the FEM only allows for small deformations. When a heavy vehicle travels over a soft soil, the soil undergoes a large amount of displacement. This results in a non-linear relationship between strain and displacement. In order to apply the FEM models to agricultural soils, they require specific numerical methods to allow for incremental loading (Upadhyaya *et al.*, 2002). Methods of modelling stress – strain behaviour will be discussed in the next section.

4.3.2 Modelling the stress – strain behaviour

There are currently three methods to model the stress – strain behaviour in FEM models, namely the pseudo-elastic model, the Cam Clay model and the coupled model. Each of these methods will be described in this section.

Pseudo-elastic model

Initially the FEM was developed for isotropic, linear, elastic materials that could be characterised by a Young's modulus E and a Poisson's ratio μ (Defosse and Richard, 2002). Equations 4.8, 4.9 and 4.10 calculate the principle strains for these isotropic materials.

$$\varepsilon_1 = \frac{1}{E} [\sigma_1 - \mu(\sigma_2 + \sigma_3)] \quad (4.8)$$

$$\varepsilon_2 = \frac{1}{E} [\sigma_2 - \mu(\sigma_1 + \sigma_3)] \quad (4.9)$$

$$\varepsilon_3 = \frac{1}{E} [\sigma_3 - \mu(\sigma_1 + \sigma_2)] \quad (4.10)$$

However, tilled soil exhibits a non-linear and irreversible behaviour (Upadhyaya *et al.*, 2002). An approach used to apply the FEM method to soils consists of describing the soil strength by analogy with an isotropic elastic material. This is accomplished by introducing a tangent Young's modulus E_T and a Poisson's ratio μ that can vary with increasing stress values (see Figure 4.7). The expressions for E_T and μ vary from author to author (Raper and Erbach, 1990; Raper *et al.*, 1995). Each nodal element is

characterised by a unique (E_T, μ) couple, which depends on the local stress levels at the previous loading increment (Defossez and Richard, 2002).

Raper and Erbach (1990) compared a pseudo-elastic model with data from soil bin experiments. The model calculates the mean normal stress P from a FEM procedure using E_T and μ . The deviatoric stress values (q) are deduced by multiplying the mean normal stress by an empirical multiplication factor. E_T was derived using Equation 4.11 developed by Bailey *et al.* (1984).

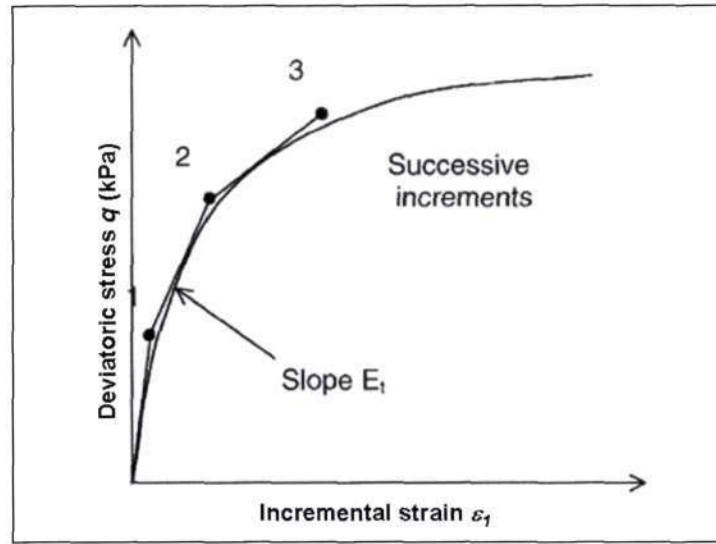


Figure 4.7 Technique used to approximate non-linear stress – strain behaviour used in pseudo-elastic models. The tangent modulus is $E_T = dq / d\epsilon_l$, Poisson's ratio is $\mu = \epsilon_l / \epsilon_v$ and q is the deviator stress (Defossez and Richard, 2002)

$$E_T = [B + e^{-C'p} (A'C' - B' + B'C'p)] \cdot e^{[(A' + B'p)(1 - e^{-C'p})]} \quad (4.11)$$

where p is the mean normal stress, A' , B' , and C' are compatibility co-efficients.

Raper and Erbach (1990) used Equation 4.12 to calculate values of Poisson's ratio μ , which depended on the stress state of the soil.

$$\mu = \frac{\Delta\epsilon_l - \Delta\epsilon_v}{2\epsilon_l} \quad (4.12)$$

where $\Delta\epsilon_v$ is the incremental volumetric strain and $\Delta\epsilon_l$ is the incremental vertical strain.

They integrated the equations for E_T and μ in an FEM procedure to calculate stress values on various nodal points and then compared them to measured values obtained in soil bin experiments. Raper and Erbach (1990) assumed the geometry of the soil to be symmetric and the surface pressure to be uniform.

Cam Clay type models

Cam Clay type models are derived from the critical state soil mechanics theory (Defosse and Richard, 2002). Critical state soil mechanics may be treated as an empirical description that combines different aspects of soil deformation. Soil experiences plastic deformation, elastic deformation and a state at which shear deformation occurs without volume change. Cam Clay models attempt to describe the different physical processes occurring during soil deformation (Berli *et al.*, 2003). The basic modified Cam Clay model was developed by Kirby (1994). The model used by O'Sullivan *et al.* (1999) is an extension of the logarithmic model developed by Kirby (1994) in the deviatoric stress / mean normal stress plane. Figure 4.8 shows that in the P, q plane, the soil deforms elastically in stress states within an elliptical yield surface.

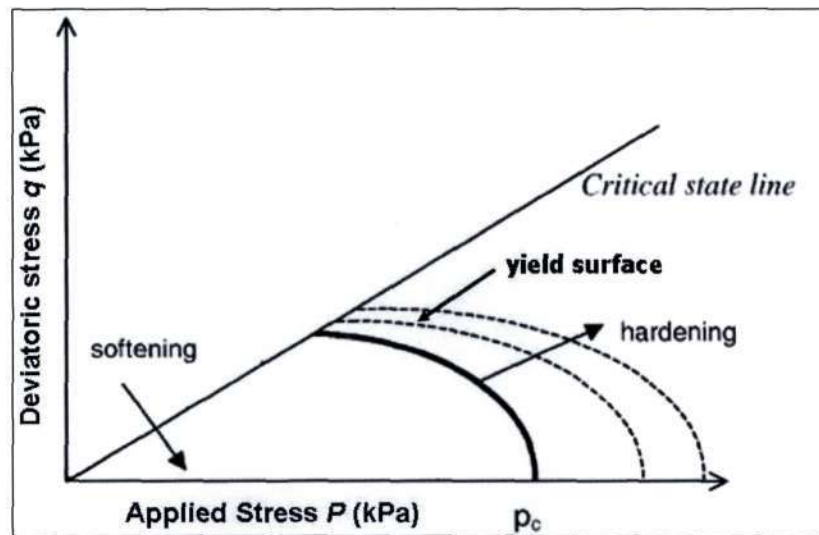


Figure 4.8 Yield surfaces in the modified Cam Clay critical state model (Kirby, 1994)

The intercept on the mean normal stress axis is the pre-consolidated pressure p_c . Once the soil reaches the yield surface it deforms plastically, undergoing irreversible volume change (Defosse and Richard, 2002). Elastic deformation is described by the elastic modulus E and μ and the slope of the recompression / rebound line κ (described in

Section 4.2.2). Plastic deformation depends on the pre-compression stress p_c , the slope of the VCL λ and the internal angle of friction of the soil (described in Section 4.2.2). At higher mean normal stress, the volume decreases during yielding and thus the soil strength increases (hardens). At lower mean normal stress, yielding is accompanied by volume increases and thus the soil strength decreases (softens). The critical state line represents the intermediate normal stress at which shear distortion occurs with no volume change. A detailed description of this model is presented by Kirby (1994).

Coupled models

Early attempts at developing models that couple mechanical and hydraulic processes for unsaturated soils are derived from the effective stress theory (Defosse and Richard, 2002). These models consider interactions between physical processes and fluid flow processes. The one coupling process, models the change in water suction as a result of changes in stress and strain values, whilst the other, models the changes in stress and strain values as a result of changes in water suction (Defosse and Richard, 2002). Gysi *et al.* (2000) used a coupled model to simulate the effect of wheeling on SC. This model fully couples the phases so that any change in soil moisture will affect the soil's mechanical and hydraulic properties. The main features of the model used by Gysi *et al.* (2000) are:

- Pre-consolidation stress increases with soil water suction analogous to the effect of load on pre-consolidation stress.
- Stiffness increases with suction.
- Structural collapse is embedded. The wetting of the soil causes a reduction in porosity.
- Peak strength increases with suction.

A detailed description of the model is presented in Gysi *et al.* (2000). Now that the theory of some of the FEM models has been described, the next section provides an overview of some of the FEM models that have been developed and gives a specific evaluation of FEM models developed by Raper and Erbach (1990), Kirby (1994) and Gysi *et al.* (2000).

4.3.3 An overview of some FEM soil compaction models

Table 4.5 summarizes some of the models that have been developed. All these models use the principle of virtual work described in Section 4.3.1 to model soil deformation.

Table 4.5 Summary of some FEM compaction models (after Defossez and Richard, 2002)

Model Author	Distribution of stress (Contact form)	Stress – Strain behavioural Component
Raper and Erbach (1990)	Constant vertical stress (circular)	Pseudo-elastic model
Kirby (1994)	Constant vertical stress (rectangular)	Cam Clay type model
Raper <i>et al.</i> (1995)	Inhomogeneous distribution of vertical stress, slip (rectangular)	Pseudo-elastic model
Gysi <i>et al.</i> (2000)	Constant vertical stress (rectangular)	Coupled model (18 input parameters)

The SC models developed by Raper and Erbach (1990), Kirby (1994), and Gysi *et al.* (2000) were reviewed in a little more detail because they are representative of the three types of techniques used to model the stress – strain behaviour. They have also been recognised by other authors. A cited reference search on the website www.isiknowledge.com showed that the work published by Raper and Erbach (1990) has been cited 14 times, the work published by Kirby (1994) has been cited 16 times and the work published by Gysi *et al.* (2000) has been cited 7 times (Accessed 5 September 2005).

Raper and Erbach (1990) tested their pseudo-elastic model with compaction data obtained from soil bins (see Table 4.6). Tests were applied on a sandy loam in a 0.54m deep soil bin. Vertical stress was measured by transducers that had been inserted into the soil. The FEM predicted the mean normal stress usually within 95% confidence intervals of the measured values (see Table 4.7).

Kirby (1994) carried out repeated loading experiments on a clay soil in soil bins (see Table 4.6). Kirby (1994) compared the measured values with the Cam Clay type model that he developed (Defossez and Richard, 2002). It was found that repeated loading induced a high increase in dry bulk density (see Table 4.7). Kirby (1994) found that the Cam Clay type model accurately predicted the dry bulk density profile.

Table 4.6 Summary of tests conducted by Raper and Erbach (1990), Kirby (1994) and Gysi *et al.* (2000) (after Defossez and Richard, 2002)

Authors	Site	Texture	Structural state	Soil moisture (g.g ⁻¹)	Way of loading	Mean vertical stress (kPa)
Raper and Erbach (1990)	Bin	Sandy Loam	0.54 m homogeneous layer	0.06	Static load via plate	127
Kirby (1994)	Bin	Clay	0.2 m homogeneous layer	0.16	Repeated loading via plate	105
Gysi <i>et al.</i> (2000)	Plot	Loam	Tilled layer without plough pan	0.28	Single pass	151

Table 4.7 Evaluation of the FEM models at different depths (z) developed by Raper and Erbach (1990), Kirby (1994) and Gysi *et al.* (2000) (after Defossez and Richard, 2002)

Author	Site	Tested model outputs	Compaction intensity	Simulation error
Raper and Erbach (1990)	Bin	2D profile of mean normal stress $p(z)$	-	$\Delta p = -27$ kPa
Kirby (1994)	Bin	1D profile of dry bulk density $\rho_b(z)$	0.4 Mg.m ⁻³	$\Delta \rho_b = + 0.07$ Mg.m ⁻³
Gysi <i>et al.</i> (2000)	Plot	Rut depth d 1D profile of dry bulk density $\rho_b(z)$	0.035 Mg.m ⁻³	$\Delta d = -0.027$ m $\Delta \rho_b =$ inconsistent

Data obtained on a loam soil was tested on a coupled model by Gysi *et al.* (2000). He found that the model accurately predicted rut depth, but the model predicted an inconsistent decrease in dry bulk density after wheeling (Defossez and Richard, 2002). This was attributed to the model that tends to overestimate soil behaviour, pointing out the difficulties in modelling the interaction between water processes and mechanical processes.

It was concluded by Defossez and Richard (2002) that FEM pseudo-elastic and Cam Clay type models are adequate for modelling SC. They have been successfully tested in soil bins and in the field. Coupled models are rather complicated and require large amounts of inputs and evaluation of these models call for improvements of the modelling itself.

Based on the reviews in Sections 4.2 and 4.3, the SC model SOCOMO (van den Akker, 1999; 2004) was selected for further investigation. This was because the model had

sound pseudo-analytical components. The following section gives a detailed description of the pseudo-analytical SC model SOCOMO.

4.4 The Soil Compaction Model (SOCOMO)

This section will describe the theory behind the SOCOMO model, present a sensitivity analysis of the model outputs and give a summary of other authors experiences with the SOCOMO model. The SC model SOCOMO was developed by van den Akker (1988; 1999; 2004) as a research tool for agricultural engineers and scientists to investigate ways of preventing subsoil SC and to enable advisors to make informed recommendations to farmers. The SOCOMO model is a pseudo-analytical model that is able to calculate whether the subsoil will be overstressed by a particular wheel load. This makes it possible to determine the allowable wheel load by taking into account the tyre size, inflation pressure, soil strength, bulk density and moisture conditions (van den Akker, 2004). The model was tested and verified by comparing model results with results from field experiments (van den Akker, 1999). Table 4.8 presents some of the authors that have used SOCOMO.

Table 4.8 Authors that have used SOCOMO with success

Author	Experiment
Vermeulen and Klooster (1992)	Used SOCOMO to investigate the use of low pressure tyres as a possible measure to reduce subsoil compaction.
Hammel (1994)	Used an adapted version of SOCOMO to calculate the soil stress distribution under lugged tyres.
van den Akker (1997)	Used SOCOMO to calculate the carrying capacity of the major soils in The Netherlands. This was the basis for the construction of the wheel-load carrying capacity map.
Arvidsson <i>et al.</i> (2001)	Used SOCOMO to calculate the depth to which plastic deformation occurred under tyres from sugarbeet harvesters in southern Sweden.
Trautner and Arvidsson (2003)	Used SOCOMO to compare measured stresses and deformations caused by high wheel loads on clay loam soils with calculated stresses and calculated deformation depth.

4.4.1 Theoretical basis and description of SOCOMO

The model is based on the theory described in Section 4.2.1. Up until this point, Söhne (1958) had only taken the mean vertical stress into account. This allowed only the major principle stress (σ_I) to be calculated (see Equation 4.2). van den Akker (1988) and

Johnson and Burt (1990) extended the work done by Söhne (1958) to include the effects of shear forces, which are caused by slip. In order to accomplish this, Equation 4.2 was resolved into its vertical and horizontal components (see Equations 4.13 – 4.16). The variables used in these equations are illustrated in Figure 4.9.

$$\sigma_z = \frac{\xi P}{2\pi r^2} \cos^{\xi} \theta \quad (4.13)$$

$$\sigma_h = \frac{\xi P}{2\pi r^2} \cos^{\xi-2} \theta \sin^2 \theta \quad (4.14)$$

$$\sigma_t = 0 \quad (4.15)$$

$$\tau_z = \tau_h = \frac{\xi P}{2\pi r^2} \cos^{\xi-1} \theta \sin \theta \quad (4.16)$$

where σ_z , σ_h , and σ_t are the vertical, horizontal and tangential stresses, respectively, τ_z and τ_h are the vertical and horizontal shear stress, P is the vertical point load, and r and θ are polar co-ordinates.

Since the equations of Boussinesq (1885), Froehlich (1934) and Söhne (1958) are based on a linear elastic material, it is possible to superimpose the stresses on a soil element that are the result of several point loads. Only stresses in the same direction can be summed, which is the case with the vertical stress σ_z . The horizontal and shear stresses must first be resolved into their x and y components. By disaggregating the vertical stress distribution in the soil-tyre interface into separate point loads, it is possible to compute the stress distribution in the soil caused by the vertical wheel load (van den Akker, 2004). In SOCOMO, the stress distribution at the soil-tyre interface is projected onto a horizontal rectangular grid and the stresses are connected to the grid points. The same procedure is followed for the horizontal wheel load in the driving direction. The wheel load input in SOCOMO consists of a matrix that has vertical point loads on the co-ordinates of the grid and a matrix with the same dimensions for the horizontal point loads. This enables erratic stress distributions to be easily converted into point loads on the rectangular grid (Hammel, 1994).

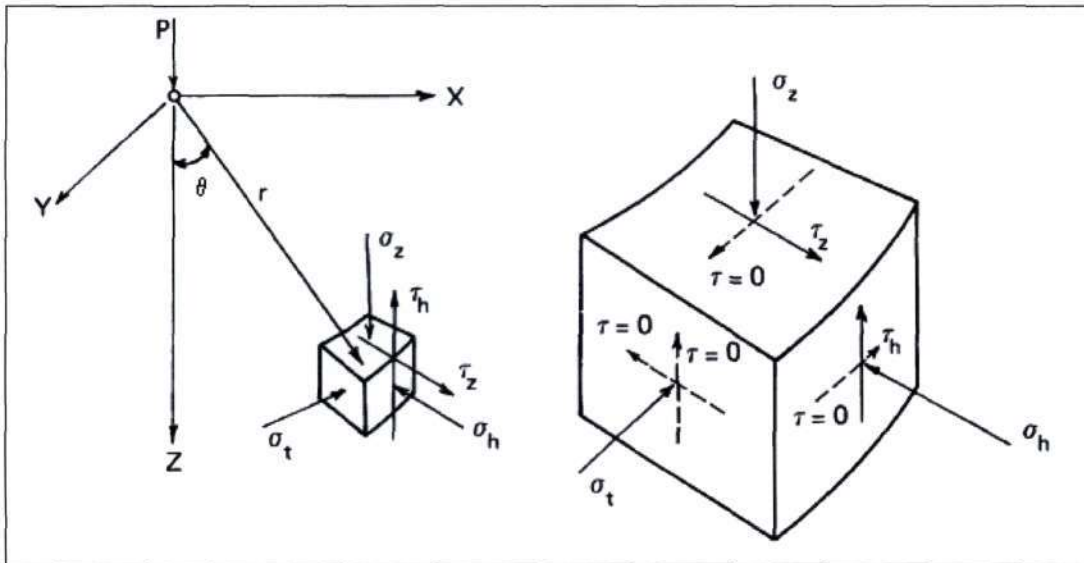


Figure 4.9 Composition of stresses acting on a volume element owing to a point load on a semi-infinite solid where: σ_z , σ_h , and σ_t are the vertical, horizontal and tangential stresses, respectively; τ_z and τ_h are the vertical and horizontal shear stress; P is the vertical point load; r and θ are polar co-ordinates

The principle stresses S_1 , S_2 and S_3 can be derived from the dynamic and static stresses calculated by SOCOMO. The stress at a certain point in the soil is completely represented by these three principle stresses, and as a result SOCOMO can calculate the stress at any point in the soil for any given vertical and horizontal stress distribution (van den Akker, 2004).

Due to the cost of determining stress – volume relationships, it was decided by van den Akker (2004), that the main goal of the project was to use SOCOMO to prevent SC and not to calculate to what extent the subsoil would be compacted by a certain wheel load. The main part of SC occurs during plastic deformation, thus SC can be prevented by making sure that the stresses exerted on the subsoil by the wheel load do not exceed the strength of the subsoil. In other words, no plastic deformation should occur. Two failure mechanisms were considered by van den Akker (2004):

- The structural strength is exceeded by the soil stresses so that the soil aggregates are crushed, resulting in a collapse of the inter-aggregate pore systems. Under these conditions, the inter-aggregate pore systems would affect plant growth and crop yield.
- The soil shear strength represented by the Mohr-Coulomb failure line is exceeded and shear strength failure occurs. Inter-aggregate and intra-aggregate

pore systems would be destroyed and the structure dependant pore system would deform and become a texture dependant one.

The stresses in the soil were measured using pressure cells, whilst deformations and SC were measured by photographing a vertical point grid positioned in the soil profile, perpendicular to the direction of travel. van den Akker (1999) concluded that the results of SOCOMO agreed well with infield measurements. A more detailed description of the model theory along with the model validation is provided by van den Akker (1999; 2004). The input parameters for SOCOMO are wheel load, tyre width, soil bulk density, soil moisture, concentration factor ξ (see section 4.2.1) and various soil strength parameters, such as the internal angle of friction, the cohesion, and the pre-consolidation stress of the soil.

4.4.2 Model sensitivity

A sensitivity analysis was done to determine the sensitivity of some of the model outputs to model inputs. Figure 4.10 shows the area of soil that is affected by plastic deformation (■), structural failure (■) and combined failure (■), which is both plastic deformation and structural failure after a vehicle has passed over the soil. Two scenarios were run to evaluate the relative sensitivity of the model to its soil inputs.

Scenario 1:

Constants: Cohesion (10 kPa), angle of internal friction (10°), the vertical wheel load, the soil bulk density (0.99 Mg.m^{-3}) and the grid dimensions.

Variables: The concentration factor was varied from $\xi = 4$ to $\xi = 6$, whilst the pre-consolidation stress was varied from 50 to 150 kPa.

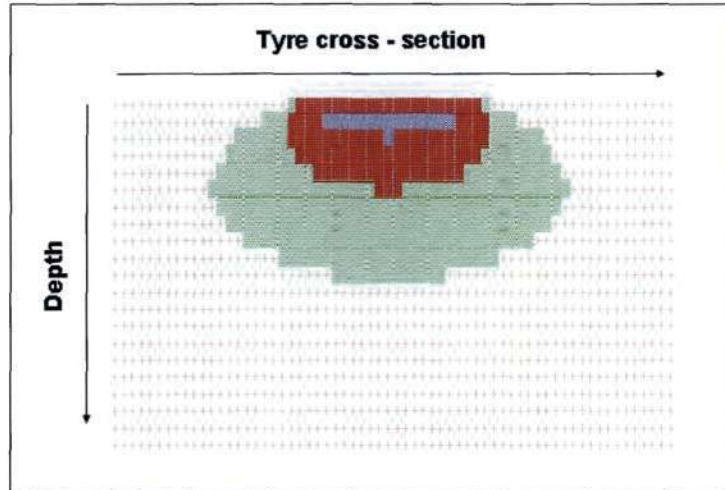


Figure 4.10 Area of soil under the tyre affected by plastic deformation (■), structural failure (■) and combined failure (■) as a result of a vehicle passing over the soil

Figure 4.11 illustrates the results of the first sensitivity analysis. The diagram shows that as the pre-consolidation stress increases, the area affected by the combined failure decreases. As ξ increases, the depth of penetration of the plastic deformation and the combined failure increases. Another observation is that as ξ increases the area affected by the combined failure becomes narrower.

Scenario 2:

Constants: Concentration factor ($\xi = 4$), pre-consolidated stress (100kPa), the vertical wheel load (parabolic distribution), the soil bulk density (0.99 Mg.m^{-3}) and the grid dimensions.

Variables: The internal angle of friction was varied from $\phi = 0$ to $\phi = 30^\circ$ and the cohesion was varied from $C = 0$ to $C = 30 \text{ kPa}$.

Figure 4.12 summarizes the results from the second sensitivity analysis. In general, the diagram shows that as cohesion and the internal angle of friction increase, the area affected by plastic deformation decreases. Figure 4.12 shows that under these specific conditions, soils with high internal angle of friction and cohesion values do not undergo as much plastic deformation.

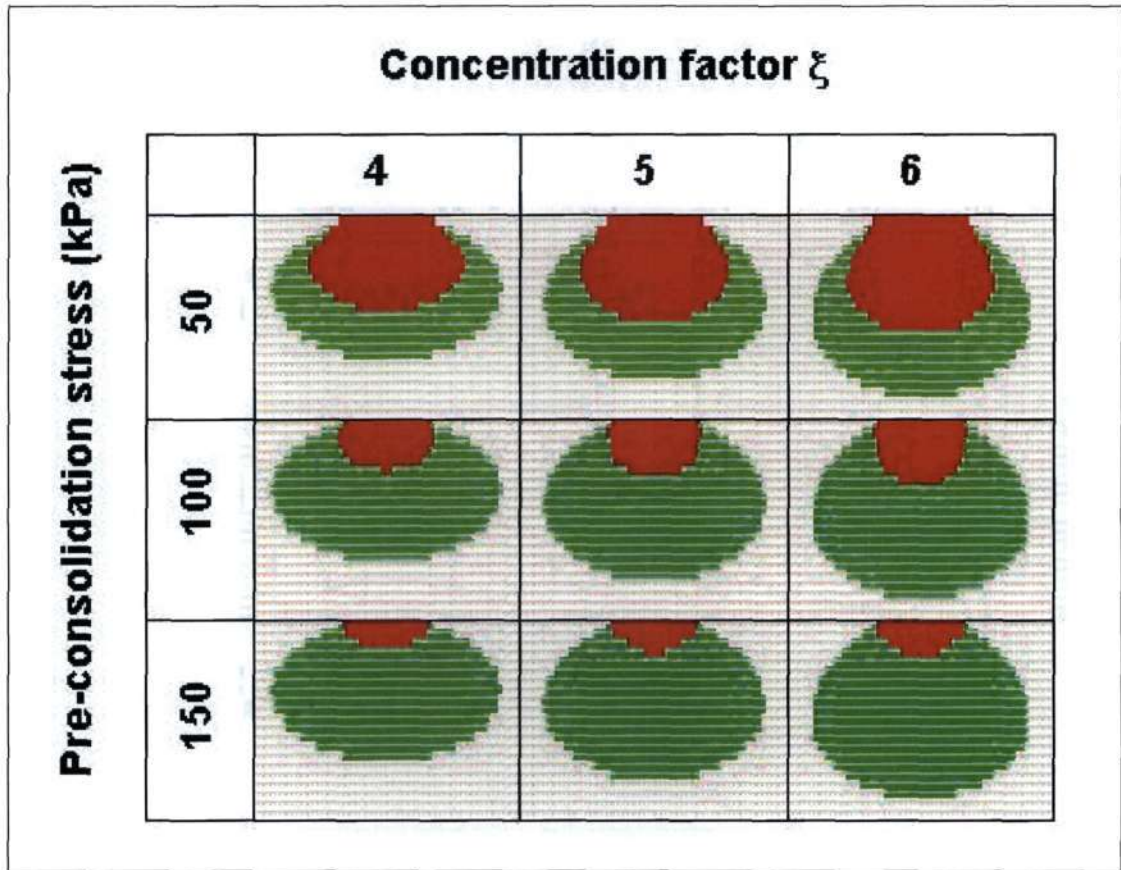


Figure 4.11 Scenario one sensitivity analysis: Area of soil under the tyre affected by plastic deformation (■), structural failure (■) and combined failure (■) as a result of a vehicle passing over the soil

In general, the sensitivity analysis showed that the area subjected to structural failure depends mainly on the pre-consolidated stress and the concentration factor, whilst the area subjected to plastic deformation depends on the concentration factor, the cohesion and the internal angle of friction of the soil. In a separate sensitivity analysis, variations in the principle stresses were found to depend predominately on the concentration factor ξ and the pre-consolidated stress.

The outputs from the SOCOMO model include the three principle stresses acting on a soil element (S_1 , S_2 and S_3), the vertical and horizontal forces acting on a soil element (σ_z , σ_y and σ_x), the shear stresses acting on a soil element (τ_{xz} , τ_{xy} , τ_{yz}), the minimum cohesion to prevent plastic deformation and the figures to show where plastic deformation and structural failure occur.

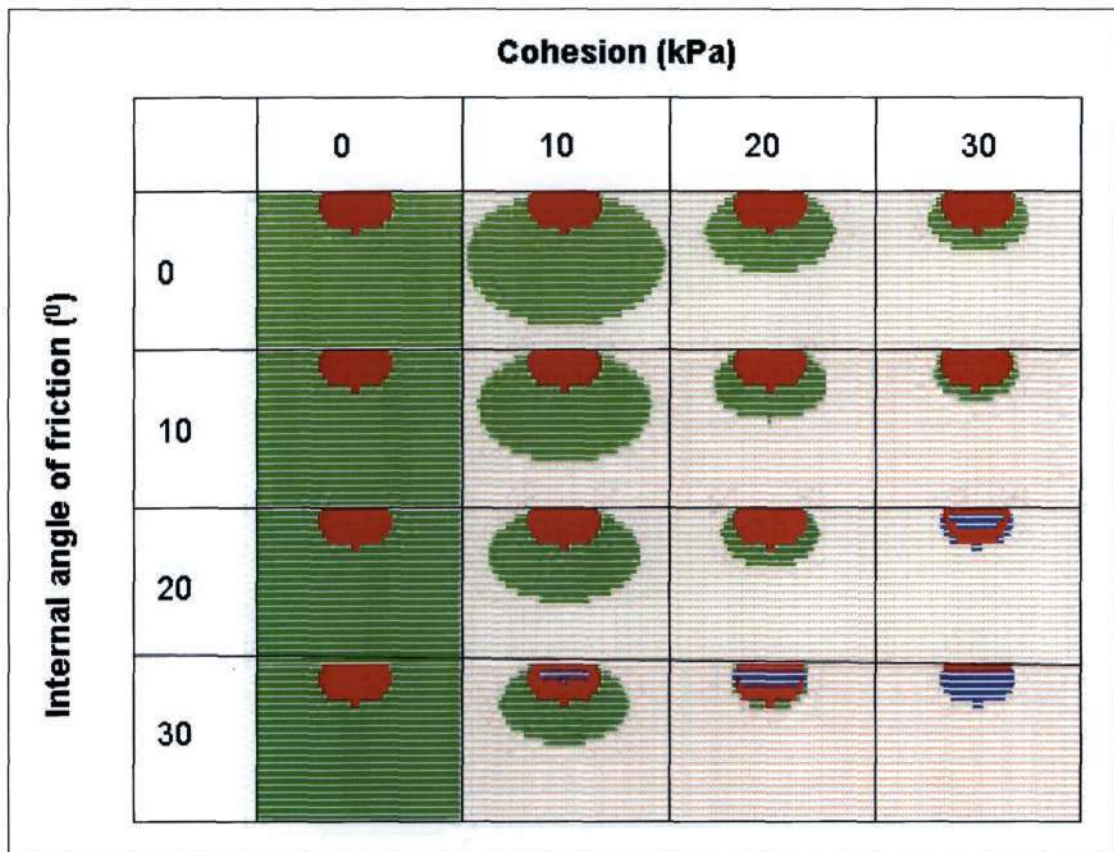


Figure 4.12 Scenario two sensitivity analysis: Area of soil under the tyre affected by plastic deformation (■), structural failure (■) and combined failure (■) as a result of a vehicle passing over the soil

4.4.3 Experiences of other users with SOCOMO

van den Akker (1992) used SOCOMO to determine whether terra tyres and tandem and dual wheel configurations could be used to prevent subsoil SC. The stresses and the minimum required strength to prevent plastic deformations were computed for these different alternatives. The results from this experiment are described by van den Akker (1992; 2004). van den Akker (1992) found that the major principle stresses were significantly higher under the normal tyres compared to the low pressure tyres. The vertical pressure distribution had a noticeable effect on the major principle stress and the soil strength. Replacing the terra tyre with two smaller tyres resulted in slightly higher stresses and soil strength in the topsoil, and lower stresses in the subsoil (van den Akker, 1992).

Hammel (1994) used an adapted version of SOCOMO to calculate the stress distribution under lugged tyres at a depth of 0.25 m. The calculated stresses were compared with the measured stresses and it was found that the measured stresses were well described by SOCOMO. Hammel (1994) concluded that SOCOMO was a capable tool to analyse stress distributions to shallow depths.

van den Akker (1997) used the SOCOMO model to construct a load bearing capacity map of The Netherlands. SOCOMO was used to calculate the area where the stresses exceeded the structural and shear strength. The bearing capacities of the soils were limited by the shear failure criterion and the structural failure criterions. He found that the thickness of the top soil played an important role in determining the bearing capacity of the soil. van den Akker (1997) found that the calculated bearing capacities were too low. This could have been caused by using conservative values for the strength properties.

Arvidsson *et al.* (2001) used SOCOMO to calculate the depth to which plastic deformation occurred under the tyres of sugarbeet harvesters in Sweden. They found that there was good agreement between the estimated depth of SC and the depth to which displacement was measured in the soil. Arvidsson *et al.* (2001) noted some model advantages and limitations. The model was simple to use. It was based on well recognised principles of stress distribution and some inputs were readily available. Limitations were that the model did not include the magnitude of SC and some of the soil inputs, such as soil strength, cohesion and internal angle of friction, are difficult to obtain.

Trautner and Arvidsson (2003) used SOCOMO to compare measured stresses and deformations caused by wheel loads of up to 70 kN with calculated stresses and calculated deformation depth. In this case, the results were less satisfactory. Vertical soil stresses were measured at 0.3, 0.5 and 0.7m. At the 0.3 m depth, the vertical stresses calculated by SOCOMO were significantly lower than the measured values. Meanwhile at the 0.5 and 0.7 m depths, the calculated values were reasonable in moist soils, but too low in dry soils. The authors noted that the difference in the measured and calculated values was due to cracks and clods in the soil that formed as the soil dried out. They concluded that SOCOMO should not be used in soils with high shrink – swell

characteristics as the theory of the model was based on an isotropic homogeneous medium.

4.5 Discussion and Conclusion

The concept of modelling SC is an old concept that has been in use for many decades. Soil compaction models that have received a lot of interest over the years can be split into two categories, namely pseudo-analytical models and finite element models (FEM).

Pseudo-analytical models use recognised theories developed by Boussinesq's (1885), Fröhlich (1934) and Söhne (1958) to determine stress propagation through the soil and critical state soil mechanics and equations developed by Larson *et al.* (1980) to determine volume change in the soil. Examples of pseudo-analytical models include those developed by Blackwell and Soane (1981), Gupta and Larson (1982), Smith (1985), Binger and Wells (1992), O'Sullivan *et al.* (1999) and van den Akker (2004). One of the advantages of using pseudo-analytical models is that they are simple and most of the inputs are relatively available. Some limitations of these models were that they do not include the magnitude of the SC event and there is a lack of pedotransfer functions that determine soil strength.

Finite element models use the principle of virtual work to describe the deformation of the soil and pseudo-elastic, Cam Clay and coupled models to describe the change in soil volume as a result of the SC event. Pseudo-elastic models were developed for isotropic linear elastic media with Young's modulus E and Poisson's ratio μ . Cam Clay type models are based on critical state soil mechanics, whilst coupled models attempt to model the effects of SC on mechanical and hydraulic properties. This is based on the effective stress theories. Examples of FEM models include those who have been developed by Raper and Erbach (1990), Kirby (1994), O'Sullivan and Simota (1995), Raper *et al.* (1995), Gysi *et al.* (2000) and Upadhyaya *et al.* (2002). The main limitation of these models is that they are complex and require large quantities of data.

The SC model SOCOMO was described in detail in this Chapter. SOCOMO is a pseudo-analytical model, and it was decided that this model would be used for the

remainder of this research study. One of the major problems with this model is that it requires information that is difficult to obtain. Chapter 5 provides a method used to derive some of these inputs, such as cohesion, internal angle of friction and pre-consolidated soil strength.

5. DERIVATION OF DEFAULT GEOTECHNICAL SOIL INPUT VALUES FOR THE SOCOMO MODEL

5.1 Introduction

The soil compaction (SC) model SOCOMO uses complex geotechnical soil properties, such as cohesion (C in kPa), internal angle of friction (θ in degrees) and the pre-consolidated soil strength (SS in kPa), as input parameters for the model. The internal angle of friction and the cohesion of the soil can be determined by conducting drained and undrained triaxial tests and shear box tests. The pre-consolidated soil strength can be determined by conducting consolidation tests. These tests are expensive and time consuming. One undrained triaxial test takes approximately half an hour, a drained triaxial test takes three days and the consolidation test takes a week. Another issue is that, in order to obtain significant test results, three tests have to be done for each sample. To avoid conducting all these tests, an alternative method based on results by Francis (1988) to estimate the geotechnical properties of any soil in KwaZulu-Natal was developed. Previous research (Mitchell and Berry, 2001) has suggested that a particle size distribution could assist in predicting a soil's tendency to be compacted.

van den Akker (1997) used soil information derived by Lebert and Horn (1991) to compile Table 5.1. This table shows the above mentioned geotechnical strength properties for soils in the Netherlands. Table 5.1 shows that clay soils in the Netherlands have unusually high internal angle of friction values, compared to sandy soils.

Table 5.1 Angle of internal friction (θ), cohesion (C) and structural strength (SS) of the major subsoils in the Netherlands (after van den Akker, 1999)

Soil Type	Clay content (%)	C (kPa)	θ (degrees)	SS (kPa)
Sandy soils	< 8	12	28	198
Coarse sand	< 8	10	32	240
Sandy loam	< 8	10	32	122
Clay loam	18 - 25	14	31	79
Light clay	25 - 35	26	36	118
Medium clay	35 - 50	26	36	96
Heavy clay	> 50	34	38	114
Sandy silt	< 18	15	39	82
Silt loam (loess)	< 18	26	37	110

The objective of this chapter is to derive a table similar to that of van den Akker (1999, see Table 5.1) that has default geotechnical inputs for typical soils in the sugar and timber industries of KwaZulu-Natal. This would provide default C , θ and SS values for SOCOMO model simulations without the necessity of conducting triaxial tests.

5.2 Methodology

Francis (1988) conducted experiments to determine the relationship between the formation of soil catenas and their engineering properties in the Durban municipal area (KwaZulu-Natal). Drained and undrained tri-axial tests, shear box and consolidation tests were performed on 33 different soils. The main soil catenas tested were Natal granite, Natal sandstone, Dwyka tillite, Eccca group, Karoo dolerite, Berea formation and Quaternary. Soil samples were taken on the crests, mid and lower slopes, footslopes, and in gullies of these soil cantenas. Table 5.2 summarises results from the shear box tests done by Francis (1988). In order to achieve the objectives of this chapter the data from Francis (1988) was analysed as follows:

- The consolidation test results were used to determine the pre-consolidated soil strength (SS) of each soil using the graphical technique developed by Casagrande (1936) (see Section 5.2.1).
- Each soil was classified according to its texture and statistical analyses were performed to establish the mean geotechnical inputs for each soil texture (see Section 5.2.2).
- The geotechnical inputs were then corrected with respect to bulk density (see Section 5.2.3).

5.2.1 Determination of pre-consolidated soil strength (SS)

The pre-consolidated soil stress (SS) for each soil was determined by plotting a curve of void ratio (y -axis) against the log of the applied pressure (kPa). This data was obtained from the consolidation tests completed for the 33 soils by Francis (1988). Casagrande (1936)'s graphical technique was then applied to the graphs to determine SS .

Table 5.2 A summary of soils and their properties obtained from Francis (1988). Properties include texture (see Table 5.3), dry density (DD), internal angle of friction (θ) and cohesion (C)

NO	DD (Mg. m ⁻³)	Sand (%)	Silt (%)	Clay (%)	θ (deg)	C (kPa)	Texture
1	1810	67	16	17	35	0	SLM
2	1793	71	12	18	40	8	SLM
3	1753	56	19	25	29	15	SCLM
4	1039	47	14	41	32	7	SCL
5	1149	42	23	35	34	0	CLLM
6	1551	82	12	8	32	4	LMS
7	1368	76	14	11	16	24	SLM
8	1788	69	10	24	34	5	SCLM
9	1499	37	21	43	28	16	CL
10	1404	79	7	15	29	0	SLM
11	1564	60	12	28	29	9	SCLM
12	1454	45	32	15	35	7	LM
13	1604	39	26	19	36	28	LM
14	1611	42	22	33	34	11	CLLM
15	1614	42	32	33	21	20	CLLM
16	1723	80	11	10	34	3	SLM
17	1696	49	17	32	35	21	CLLM
18	1282	25	31	38	29	6	CL
19	1476	31	31	40	29	23	CLLM
20	1410	23	24	52	25	16	CL
21	1676	38	35	29	18	43	CLLM
22	1574	33	27	40	21	39	CL
23	1298	25	38	35	33	16	CLLM
24	1295	39	44	17	26	12	LM
25	1480	43	23	32	26	27	CLLM
26	1279	45	33	25	33	6	LM
27	1601	73	8	22	31	4	SCLM
28	1629	86	7	7	32	2	LMS
29	1501	88	4	4	32	2	S
30	1568	80	7	9	32	3	LMS
31	1755	94	2	5	37	1	S
32	1575	44	23	31	20	30	CLLM
33	1136	36	38	29	26	10	CLLM
33	1136	36	38	29	9	46	CLLM
32	1575	44	23	31	20	30	SCLM
22	1574	33	27	40	21	39	CLLM

The technique used by Casagrande (1936) as described by Das (2002) is given below. Figure 5.1 supports this description.

- By visual observation, establish a point a , at which the curve has a minimum radius of curvature.
- Draw a horizontal line ab .

- Draw the line ac tangent at a .
- Draw the line ad , which is the bisector of the angle $b\hat{a}c$.
- Project the straight-line portion gh of the curve back to the intersect line ad at f . The abscissa of the point f is the pre-consolidation stress (SS).

This procedure was repeated for all 33 soils. All the results are summarized in Table 5.4. Soil numbers 12, 26, 29 and 31 had insufficient data to determine point a according to Casagrande (1936)'s technique.

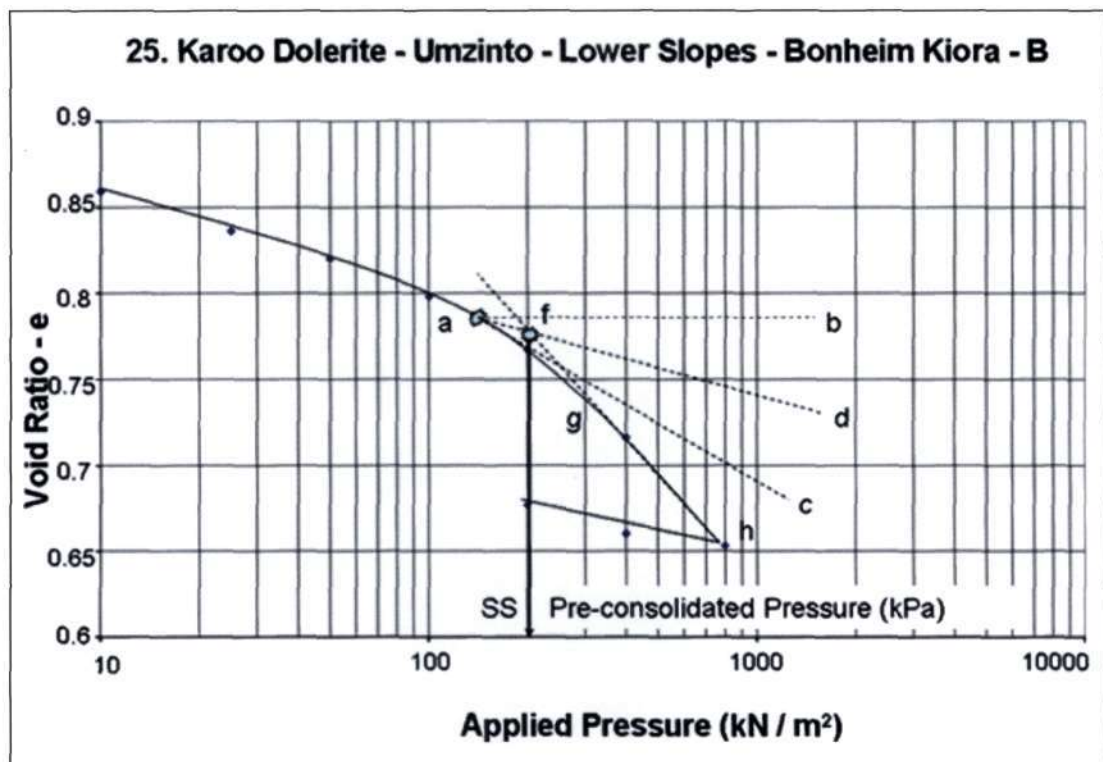


Figure 5.1 Technique of Casagrande (1936) being applied to a Karoo dolerite (from Francis, 1988)

5.2.2 Establishing mean / median geotechnical inputs for each soil texture

Each soil was then positioned according to its texture (see Tables 5.2 and 5.3) on a soil triangle (Figure 5.2). Mean and median geotechnical inputs for each soil texture were statistically determined. The results are summarised in Table 5.4. From Figure 5.2 it is evident that no soil samples for silty clay, silty clay loam, silty loam and silt textures were available. This is mainly attributed to the fact that the study by Francis (1988) focussed on soils suitable for building and civil engineering applications. Whilst this is

incomplete, the available soil types represent most soils in the SA sugar industry and to a slightly lesser extent soils in forestry (Meyer, 2004; Smith, 2004). The soil textures are described in Table 5.3.

Table 5.3 Description of soil textures

Code	Texture
SLM	Sandy loam
SCLM	Sandy clay loam
SCL	Sandy clay
CLLM	Clay loam
LMS	Loamy sand
CL	Clay
LM	Loam
S	Sand

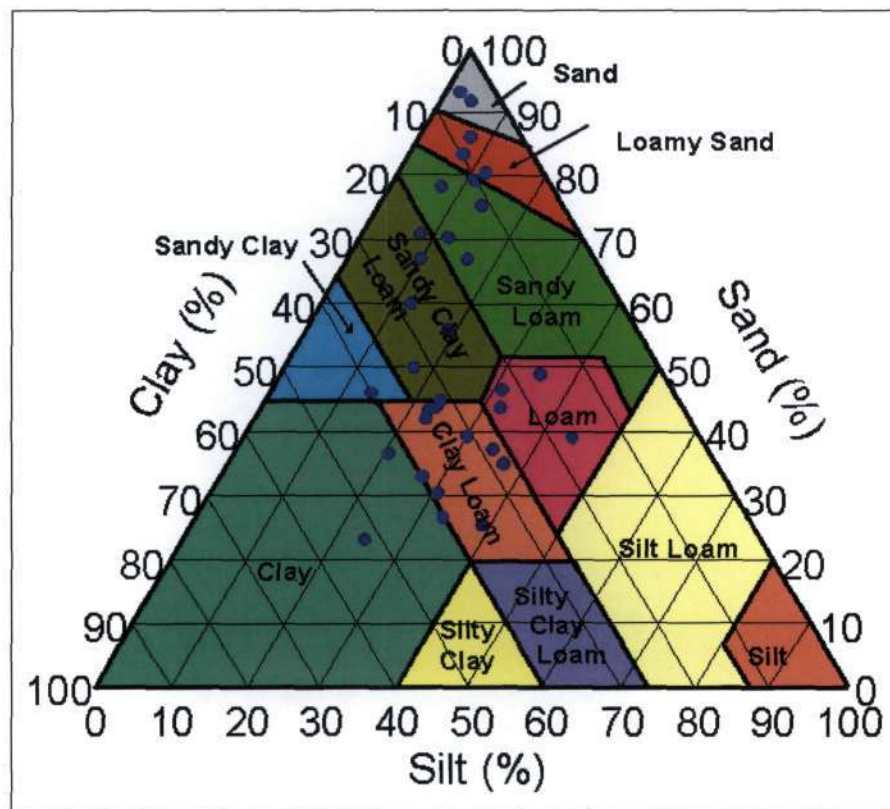


Figure 5.2 A soil triangle plot showing the texture distribution of the soils used by Francis (1988)

5.2.3 Correcting geotechnical inputs with respect to bulk density

The median values of θ and C were calculated for each soil category. The soils in each category were regressed with respect to dry density. The median C and θ values were deducted from the intercepts of the regression lines. This resulted in indicating an estimated change to C and θ values under different dry density scenarios (see Figure 5.3).

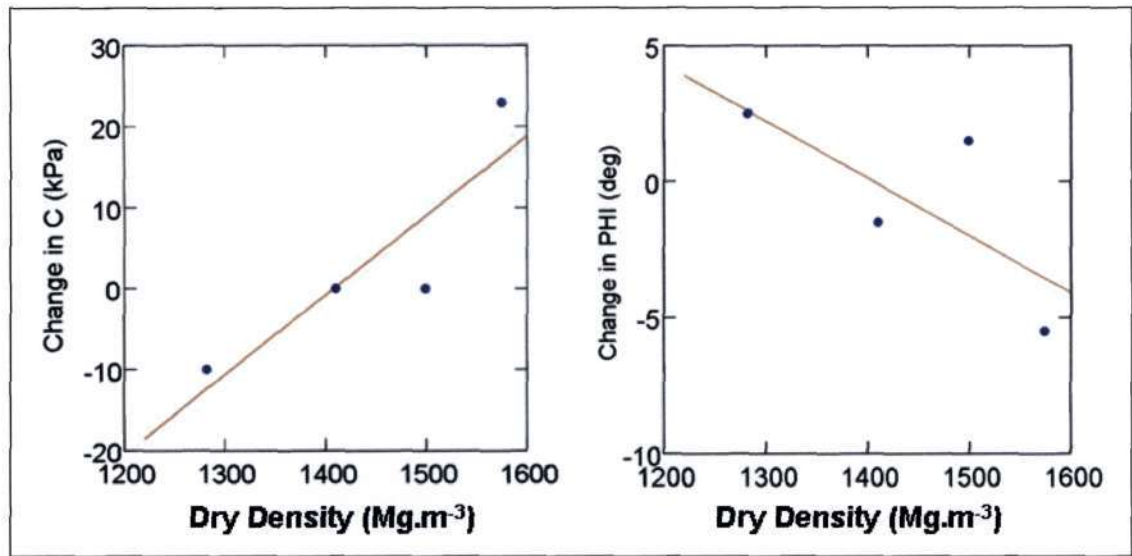


Figure 5.3 Graphs illustrating how C and θ vary with dry density

The slopes and intercepts were determined from these graphs and C and θ were hence corrected for dry density using Equations 5.1 and 5.2.

$$C' = C_{med} + \chi_c + \zeta_c \cdot \rho_k \quad (5.1)$$

$$\theta' = \theta_{med} + \chi_\theta + \zeta_\theta \cdot \rho_k \quad (5.2)$$

where C' and θ' are C and θ corrected for dry density, C_{med} and θ_{med} are the median C and θ values before the correction, χ_c and χ_θ are the intercepts of the regression line after the median values were subtracted (see Figure 5.3), ζ_c and ζ_θ are the slopes of the plots (see Figure 5.3) and ρ_k is the dry density. The results showing all the slopes and intercepts are summarized in Table 5.5

5.3 Results and Discussion

Table 5.4 summarises the default geotechnical information obtained for the selected soil textures. The results show that the mean and median values in all the textural classes are close. It was decided that the median values of θ , C and SS were to be used as the default model inputs.

Table 5.4 Summary of the default geotechnical properties assigned to soil texture. N/A denotes insufficient data

Soil texture	Soil Number	SS (kPa)	θ (deg)	C (kPa)	Med SS (kPa)	Mean SS (kPa)	Med θ (deg)	Mean θ (deg)	Med C (kPa)	Mean C (kPa)
SLM	1	145	35	0	145.0	137.0	34.0	30.8	3.0	7.0
	2	90	40	8						
	7	200	16	24						
	10	70	29	0						
	16	183	34	3						
SCLM	3	174	29	15	176.0	173.2	30.0	29.8	12.0	14.0
	8	180	34	5						
	11	207	29	9						
	17	135	35	21						
	27	165	31	4						
	32	178	20	30						
SCL	4	50	32	7	50.0	50.0	32.0	32.0	7.0	7.0
CLLM	5	148	34	0	165.0	164.6	26.0	24.6	23.0	24.1
	14	195	34	11						
	15	140	21	20						
	19	165	29	23						
	21	139	18	43						
	22	169	21	39						
	23	266	33	16						
	25	195	26	27						
	32	178	20	30						
	33	108	26	10						
LMS	33	108	9	46						
	6	50	32	4	150.0	189.3	32.0	32.0	3.0	3.0
	28	150	32	2						
CL	30	368	32	3						
	9	170	28	16	171.0	171.8	26.5	25.8	16.0	19.3
	18	172	29	6						
	20	176	25	16						
	22	169	21	39						
LM	12	N/A	35	7	210.0	210.0	34.0	32.5	9.5	13.3
	13	140	36	28						
	24	280	26	12						
	26	N/A	33	6						
S	29	N/A	32	2	N/A	N/A	34.5	34.5	1.5	1.5
	31	N/A	37	1						

Table 5.4 can be summarized in the box and whisker plots illustrated in Figures 5.4 and 5.5. These figures illustrate the means and the medians of θ and C , as well as the ranges of the properties within each soil texture.

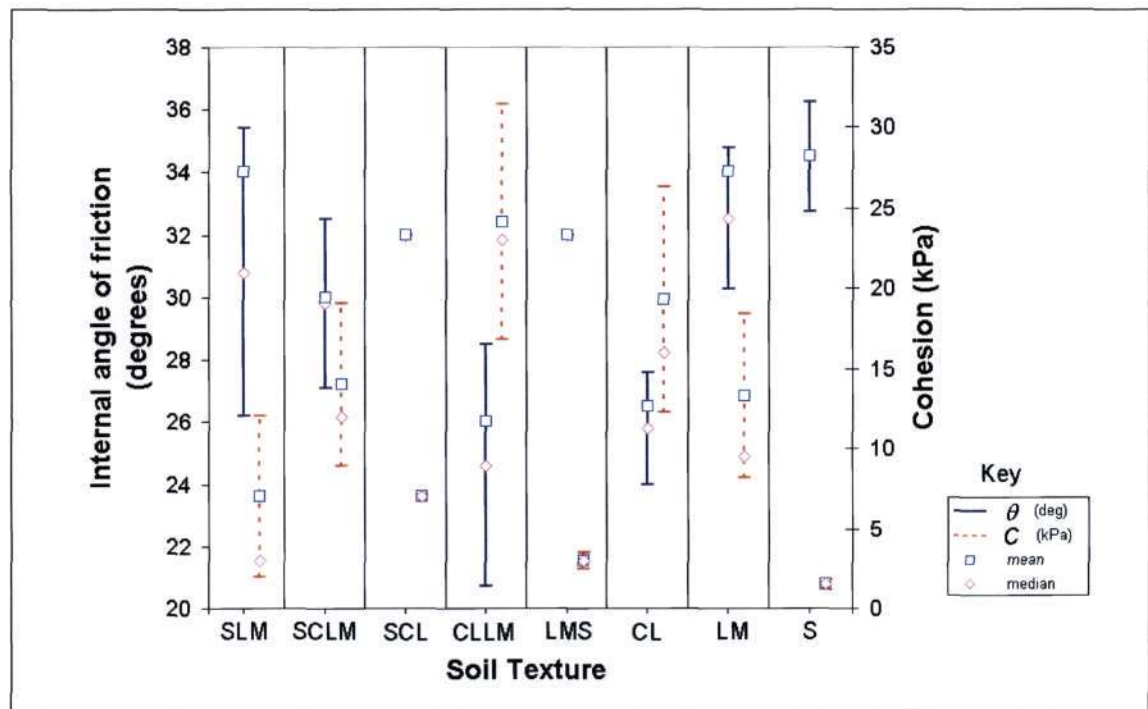


Figure 5.4 Box and whisker plots for θ and C

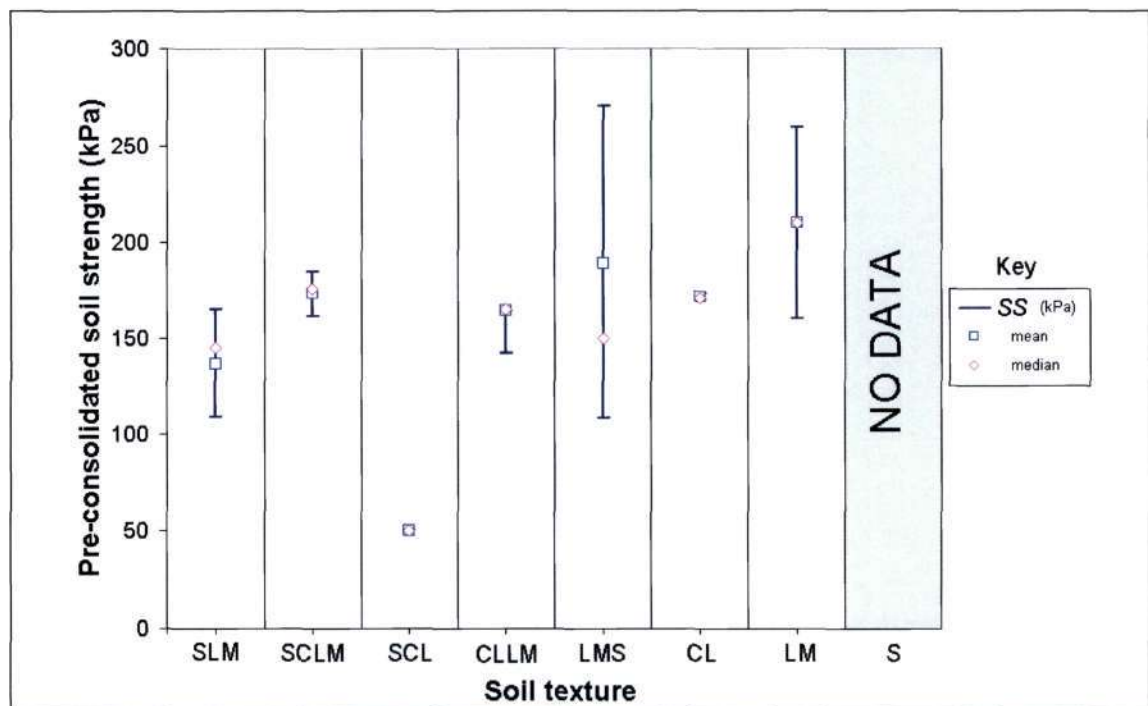


Figure 5.5 Box and whisker plots for SS

The box and whisker plots for C confirm assumptions that soils with high clay fractions have high cohesion values and that soils with high sand fractions have low cohesions. This is particularly evident for sand, loamy sand and sandy loam textures where the cohesions were found to be less than 10 kPa. θ appears to be larger in soils with higher sand fractions and smaller in soils with high clay fractions. These observations were confirmed by Das (2002), who noted that typical values of C and θ are 0 kPa and 30 to 45° for sands and 10 to 20 kPa and 8 to 28° for overconsolidated clays, respectively. The box and whisker plots for SS are inconclusive as no trends could be seen. SS is known to be affected by the previous stress history of the soil.

Table 5.5 summarizes the slopes and intercepts obtained when the dry densities of the soil were regressed against of θ and C . Only one soil sample existed for the SCL soil texture and hence no dry density correction could be made. All the slopes (ζ) summarized in Table 5.5 are statistically insignificant ($P < 0.05$). Although these trends will be assumed for the remainder of this study, caution is raised and future research will have to be conducted to verify these results.

Table 5.5 The slopes (ζ) and intercepts (χ) used to correct θ and C for changing dry densities

Soil Texture	χ_{θ}	ζ_{θ}	χ_c	ζ_c
SLM	-62.484	0.037	41.638	-0.023
SCLM	2.100	-0.002	-31.737	0.023
SCL	N / A	N / A	N / A	N / A
CLLM	-54.018	0.032	41.481	-0.024
LMS	0	0	36.690	-0.023
CL	29.564	-0.021	-138.324	0.098
LM	-31.113	0.021	-70.332	0.053
S	-32.047	0.020	6.409	-0.004

Table 5.5 shows that χ varies from -62.5 to 29.5 for θ and from -138.3 to 41.6 for C , respectively. ζ varies from -0.021 to 0.037 for θ and from -0.024 to 0.098 for C , respectively. It must be noted that negative values of ζ are highly dubious. Further research needs to be done to validate these values. The geotechnical properties of clay

loam and clay soil textures were most susceptible to changes as a result of changing dry density.

5.4 Conclusion

This is the first time, to the author's knowledge, where the estimation of geotechnical soil properties was based on soil texture and bulk density information. van den Akker (1999) used pedotransfer functions developed by (Lebert and Horn (1991) and Horn and Fleige (2003) to determine SS . These functions had inputs such as θ , C , ρ_k , air capacity, available water capacity, non-available water capacity, saturated hydraulic conductivity and organic matter content. The outcomes of this chapter need verification, but can potentially be related to a wide range of civil engineering and other related soil physics disciplines.

Several multi-regressional attempts were made to link values of θ , C and SS to sand, silt and clay contents. These attempts yielded insignificant results and valuable results were only obtained once soil samples were grouped into their different texture classes.

The estimation of default θ , C and SS values from soil texture information opens a wide range of SC modelling opportunities. Given that the necessary verifications have been done, these models could be applied over large areas where geotechnical soil information is not available. This may have large benefits to areas under agriculture and thus needs further investigation. Chapter 6 provides a description of the decision support system that was developed to evaluate the SOCOMO model in South African forestry. θ , C and SS default values determined in Chapter 5 were added into the decision support system.

6. A DESCRIPTION OF THE SOCOMO DECISION SUPPORT SYSTEM (DSS)

6.1 Introduction

The purpose of a decision support system (DSS) is, *inter alia*, to simplify a complex application and make it user friendly. For the purpose of this project, this involves simplifying the inputs for the SOCOMO model (van den Akker, 2004), running the model quickly and effectively, obtaining model outputs and adequately displaying these outputs. An add-on advantage of the DSS is that it would enable the user to conduct stochastic simulations.

The SOCOMO model runs in MS DOS[®]. One of the main problems with the software was that, keyboard inputs needed to be entered into the model. Figure 5.1 shows a flow diagram of the model and the keyboard inputs required from the user. This would be a major stumbling block if stochastic simulations were to be performed. To address this problem, the model source code was adjusted to allow automatic inputs via a pre-written input file.

The next step was to construct an interactive MS Excel[®] based spreadsheet that would be able to:

1. Create input files for the model.
2. Execute the model.
3. Obtain and display outputs from the model.

The spreadsheet was enhanced using the embedded VBA programming language. All model inputs were determined and stored in the MS Excel[®] spreadsheet. This is further explained in Sections 6.3 - 6.4. The spreadsheet was also configured to calculate the bulk density after SC. This was done using the bulk density equations developed by Larson *et al.*, (1980) and applied by Smith (1995) under South African conditions.

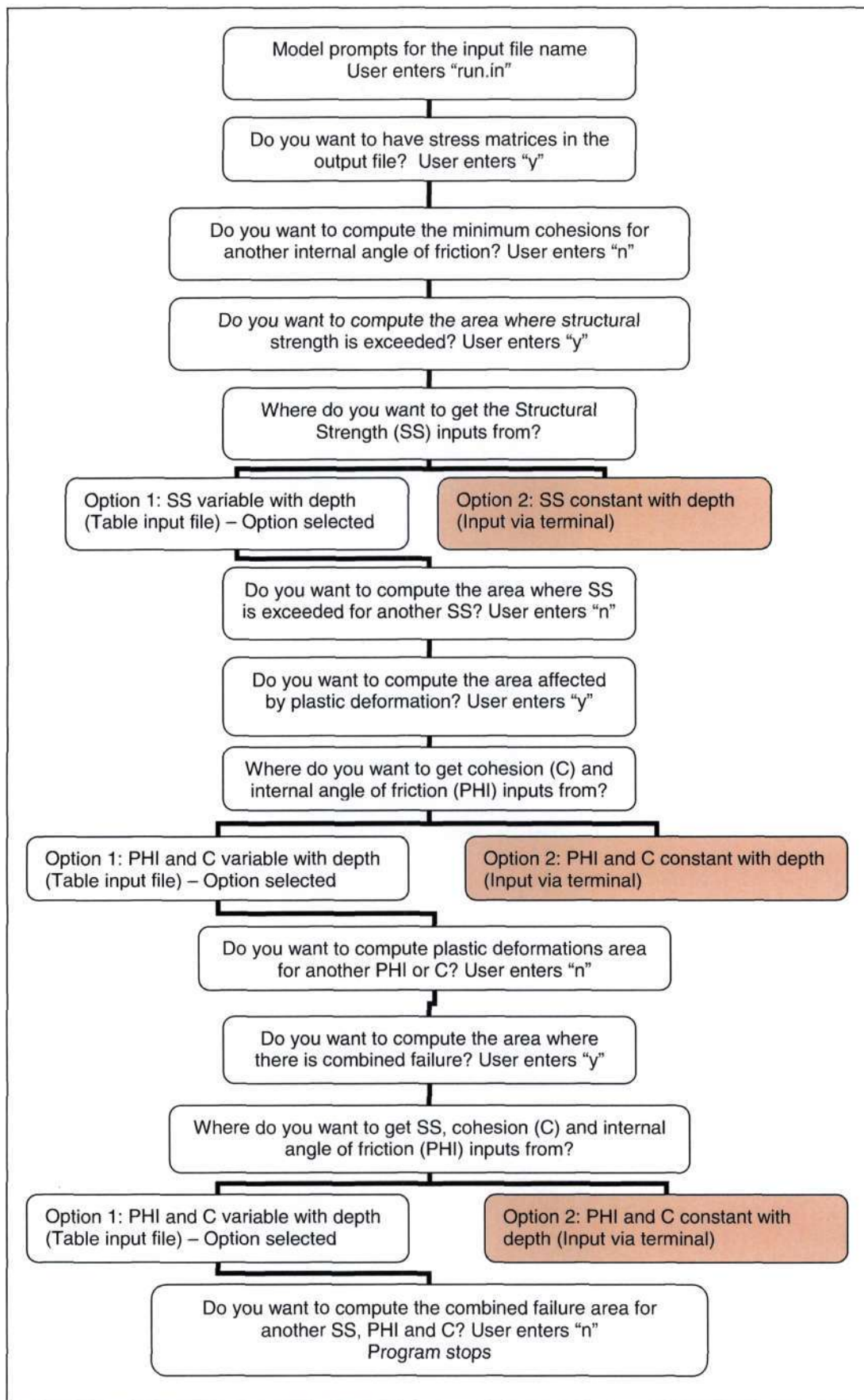


Figure 6.1 Flow chart showing some keyboard inputs required by the SOCOMO model

The inputs of the SOCOMO model consist of vehicle inputs (wheel load and tyre width) and soil inputs (bulk density, moisture content and soil strength parameters). The objective of this chapter is to describe how these inputs are incorporated into the SOCOMO DSS and to demonstrate the functionality of the DSS.

6.2 The DSS User – Interface

Figure 6.2 illustrates the user interface of the SOCOMO DSS. Typically the user would execute the following steps in order to successfully use the DSS.

Step 1: Select the soil type and moisture content (further explained in Section 6.3).

Step 2: Select the tyre used to compact the soil (further explained in Section 6.4.1).

Step 3: Choose the contact area scenario (further explained in Section 6.4.2).

Step 4: Choose the loading distribution (further explained in Section 6.4.3).

Step 5: Run the model and obtain outputs (further explained in Section 6.5)

The screenshot displays the SOCOMO DSS user interface. At the top, there are logos for SASRI, a green square icon, ICFR, the University of KwaZulu-Natal, and a circular logo celebrating 10 years of prosperity from 1994 to 2004. The interface is divided into several sections:

- Select Tyre:** A dropdown menu showing 'Richmond Tyre'.
- Radial Tyre?** A checked checkbox.
- O'Sullivan Contact Area:** An unchecked checkbox.
- Wheel Load (kg):** A text input field with the value '2148'.
- Uniform Load?:** A checked checkbox.
- Koolen Contact Area:** An unchecked checkbox.
- Tyre Type:** A dropdown menu showing 'Richmond Tyre'.
- Width(mm):** A text input field with the value '280'.
- Diameter (mm):** A text input field with the value '1000'.
- Inflation Pressure (kPa):** A text input field with the value '425'.
- RUN MODEL:** A large grey button.
- Select Soil:** A dropdown menu showing 'Sandy Loam'.
- Water Content %:** A text input field with the value '44.1'.
- Advanced Inputs:** A section with several input fields and checkboxes:
 - Over-ride these values?:** A checked checkbox.
 - Internal Friction Angle (deg):** A text input field with the value '21'.
 - Cohesion (kPa):** A text input field with the value '10'.
 - Pre-consolidation stress (kPa):** A text input field with the value '150'.
 - Over-ride DRY Density?:** A checked checkbox.
 - DRY Density (Mg m⁻³):** A text input field with the value '796'.
- Select Soil Moisture:** A dropdown menu showing 'Wet Soil'.
- Water Content (%):** A text input field with the value '44.1'.
- Wet Soil:** A text input field with the value '5'.

Below the 'Select Soil' dropdown, there is a table of soil properties for 'Sandy Loam':

Soil Type	Sandy Loam
Internal Friction Angle (deg)	21
Cohesion (kPa)	10
Pre-consolidation stress (kPa)	150
Clay Content (%)	3
Sand Content (%)	65
Silt Content (%)	26
Dry density (Mg m ⁻³)	796

Figure 6.2 The user – interface of the SOCOMO DSS

6.3 Soil Inputs

Soil information can be obtained in the DSS using one of two methods. The first method involves choosing the soil texture from a drop down menu in the Excel® spreadsheet. Each soil texture is assigned default geotechnical properties that were derived in Chapter 5. The initial dry density of the soil is calculated using Equation 6.1 developed by Larson *et al.* (1980).

$$\rho_K = 1.544 - 5.560 \times 10^{-3}(Cl) - 3.468 \times 10^{-5}(Cl)^2 \quad (6.1)$$

where ρ_K is the initial bulk density (kg.m^{-3}) of the soil at a reference degree of saturation of 50% and Cl is the percentage clay.

The soil moisture can also be selected from a drop down menu in the MS Excel® spreadsheet. This is done in order to select the most appropriate concentration factor (ξ), which varies with moisture content. The concentration factor has a significant effect on the loading distribution (see Section 6.6). Four default values for ξ were entered from the work completed by Soehne (1958). They are as follows:

- $\xi = 3$ for an elastic body.
- $\xi = 4$ for a dry soil (matric potential between -300 and -1500 kPa).
- $\xi = 5$ for a moist soil (matric potential between -50 and -300 kPa).
- $\xi = 6$ for a wet soil (matric potential between 0 and -50 kPa).

Field capacity is on average between -10 kPa and -30 kPa (Hillel, 1982). The soil water content must be entered into the space provided. In the event that the dry density and the geotechnical properties of the soil are known, they can be overridden in the DSS and used in the simulations.

6.4 Vehicle Inputs

These inputs include tyre selection, choosing the method of estimating the contact area and choosing the loading distribution. These inputs will be discussed in subsequent subsections.

6.4.1 Tyre selection

A list of the most common tyres and their particular inputs used in the South African sugar industry (Meyer, 2005) was inserted within a menu in the DSS. The DSS user could therefore select a pre-configured standard wheel specification or enter his own wheel specifications. The user has to specify if the tyre is radial or cross ply to account for tyre characteristics. This is further explained in the next section.

6.4.2 Contact area scenarios

The contact area of the tyre was estimated in the DSS using one of two methods according to the user's preference. The first method involved an assumption made by Koolen and Kuipers (1983), while the second method was based on the equation developed by O'Sullivan *et al.* (1999). These two methods are described below.

Koolen and Kuipers (1983) deduced a “rule of thumb” that the mean normal stress in the soil-tyre interface is equal to 1.2 times the inflation pressure of the tyre. This assumption is valid when the tyre side wall deflects by about 20 %. This principle was applied to the DSS as follows.

- The inflation pressure was multiplied by 1.2 to estimate the mean stress on the soil-tyre interface.
- The load on the tyre was obtained in Newtons.
- By re-arranging the equation $\text{Pressure} = \text{Force} / \text{Area}$, the contact area can be calculated.
- This area is used to determine the size of the loading matrix as described in Section 6.4.3.

The equation developed by O'Sullivan *et al.* (1999) intended to demonstrate the influence of vehicle characteristics on SC. Two equations were developed, one to estimate the contact area on a rigid surface and another for soft soil. The following variables were found to influence contact area:

- Tyre width.
- Tyre diameter.
- Tyre load.
- Inflation pressure.

Equation 6.2 shows the relationship between these variables and the contact area (A in m^2).

$$A = s_1 b d + s_2 L + s_3 L / p_i \quad (6.2)$$

where A is the contact area (m^2), L is the tyre load (kN), b is the tyre section width (m), d is the tyre diameter, p_i is the inflation pressure (kPa) and s_1 , s_2 and s_3 are empirical coefficients. It was noted by the author that Equation 6.2 is empirical, and units are not dimensionally consistent.

The coefficients for the rigid surface were derived from unpublished data by O'Sullivan *et al.* (1999) and from data published by Blackwell and Soane (1981). The coefficients for the soft soils were collected by O'Sullivan *et al.* (1999) during SC experiments. The values of the coefficients s_1 , s_2 and s_3 for both surfaces are summarized in Table 6.1.

Table 6.1 Coefficients for Equation 6.1 for estimating contact area from tyre width, diameter, inflation pressure and load for rigid and soft surfaces (after O'Sullivan *et al.*, 1999)

Constant	Rigid surface (non deformable)	Soft surface (deformable)
s_1	0.041	0.31000
s_2	0.000	0.00263
s_3	0.613	0.23900

The rigid surface coefficients are used if the soil bulk density is 1.8 Mg.m^{-3} or greater and the soft soil parameters if the soil bulk density is 1.0 Mg.m^{-3} or less. For the intermediate densities the values are linearly interpolated between the rigid surface and soft soil values.

The O'Sullivan *et al.* (1999) equation applies predominantly to cross ply tyres. This is because there was more available data for cross ply tyres than for radial tyres. Radial tyres deform differently to cross ply tyres. Experiments showed that the contact area of a radial tyre is between 20 to 50 % greater compared to the equivalent cross ply tyre (O'Sullivan *et al.*, 1999). In order to account for this, the contact area for radial tyres in the DSS was increased by a conservative value of 20%.

6.4.3 Loading scenarios

Axle load (kg) is entered into the DSS in the space provided. The load was then distributed over the contact area by either a uniform loading pattern or a parabolic loading pattern according to the users preference. The input of wheel load in SOCOMO consists of a matrix with vertical point loads (kg) on it. A horizontal grid was superimposed on the contact area. A grid size of 11×11 was assumed, thus giving 121 nodal points. This resolution was regarded as fine enough to capture any non-uniformities in load distribution under the wheel. The dimensions of the grid varied according to the size of the contact area, therefore allowing a relatively large gridded surface area when a wheel has a large contact area. The load was then distributed over the gridded area.

Only vertical loading was considered in the DSS. Although horizontal loading can be accommodated in SOCOMO, their effects were not considered in this study. This was because horizontal forces only become an issue in high draft applications. A vertical pressure distribution along the length of the tyre footprint was assumed using a modification of the formulas of Johnson and Burt (1990). These formulae are given in Equations 6.3 - 6.5.

$$p_i = \left[A + (B - A) \left(\frac{y}{y_{\max}} \right)^n \right] \left[1 - \left(\frac{x}{x_{\max}} \right)^m \right] \quad (6.3)$$

where p_i is the grid point based pressure (kPa), A is the maximum vertical pressure at tyre print centre (kPa), B the maximum vertical pressure at the tyre print sides (kPa), x and y are the x and y co-ordinates of point i (m), x in the direction of travel, x_{\max} and y_{\max}

is half the footprint length and width (m), and m and n are the powers for the parabolas in the x and y direction.

$$B = rA \quad (6.4)$$

where r is the ratio of B to A .

$$A = \frac{p_m (n+1)(m+1)}{[m(n+r)]} \quad (6.5)$$

where p_m is the mean vertical pressure over the tyre print (kPa).

In the DSS, p_i for each individual grid point was divided by the area of a single grid point to convert the load from kPa into kg. This enabled the parabolic distributions to be applied to the loading matrix. Values for n and r were set at 3 and 0.8, respectively, while m varied according to the soil moisture according to van den Akker (1999). These differences are illustrated in Figures 6.3, 6.4 and 6.5.

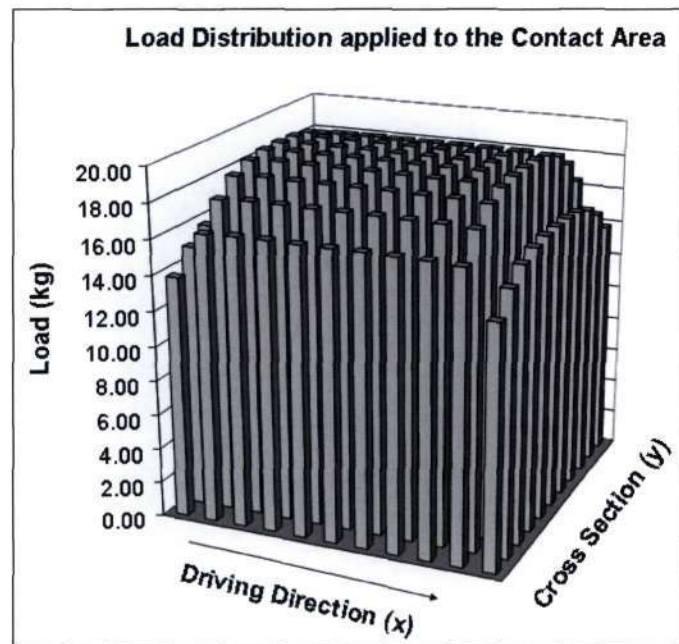


Figure 6.3 Graph illustrating the load distribution over the soil surface ($r = 0.8$, $n = 3$ and $m = 16$). This distribution represents a dry soil

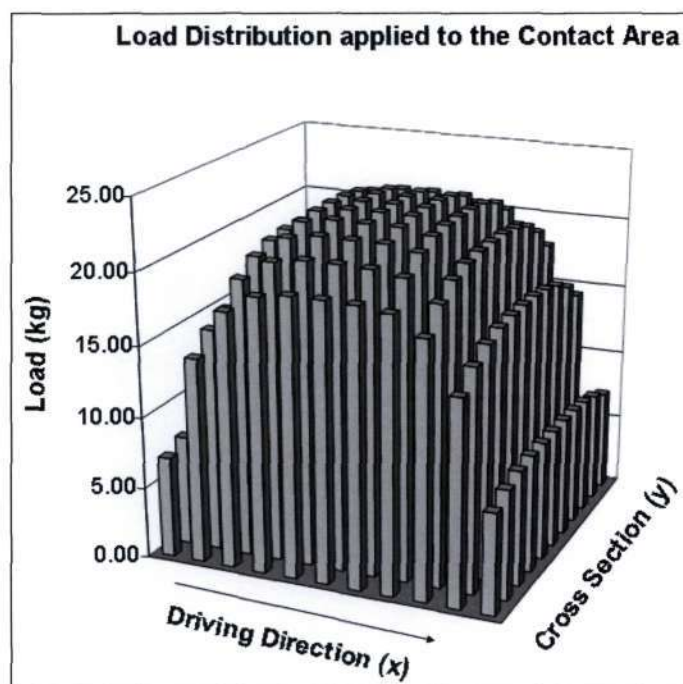


Figure 6.4 Graph illustrating the load distribution over the soil surface ($r = 0.8$, $n = 3$ and $m = 4$). This distribution represents a medium wet soil

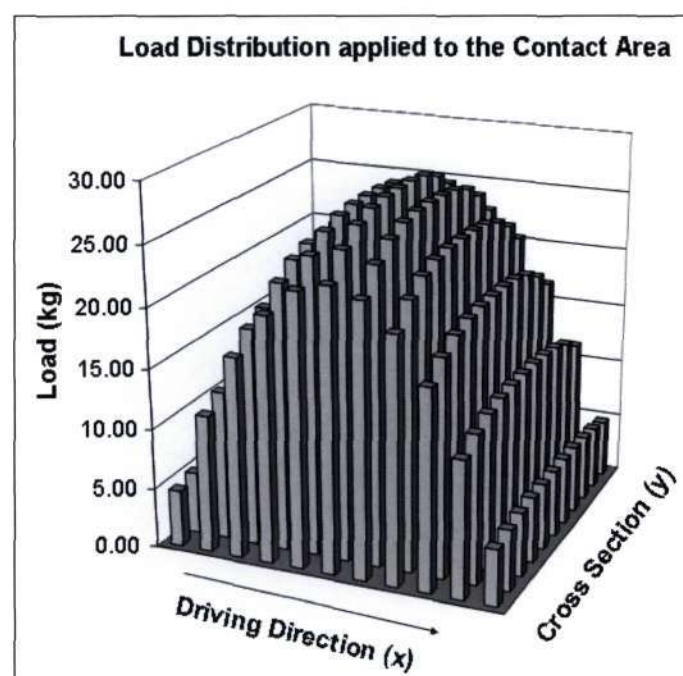


Figure 6.5 Graph illustrating the load distribution over the soil surface ($r = 0.8$, $n = 3$ and $m = 2$). This distribution represents a wet soil

6.5 DSS Outputs

The outputs from the SOCOMO model are stored in an output file. The variables shown in the output file include:

- Major and minor principle stresses (S_1 , S_2 and S_3).
- Stresses acting on each soil element (σ_z , σ_x and σ_y).
- Shear forces acting on each soil element (τ_y , τ_x and τ_{yx}).

The DSS splits the outputs into two categories, viz the resultant pressure distribution and the compacted dry density. The following subsections elaborate on these.

6.5.1 Pressure distribution

The stress vectors acting on each soil element were extracted from the output file and summed (see Equation 6.6) to obtain the resultant stress (σ_a in kPa) acting on each soil element. Typical outputs of pressure distribution from the DSS are illustrated in Figure 6.6

$$\sigma_a = \sqrt{(\sigma_z^2 + \sigma_x^2 + \sigma_y^2)} \quad (6.6)$$

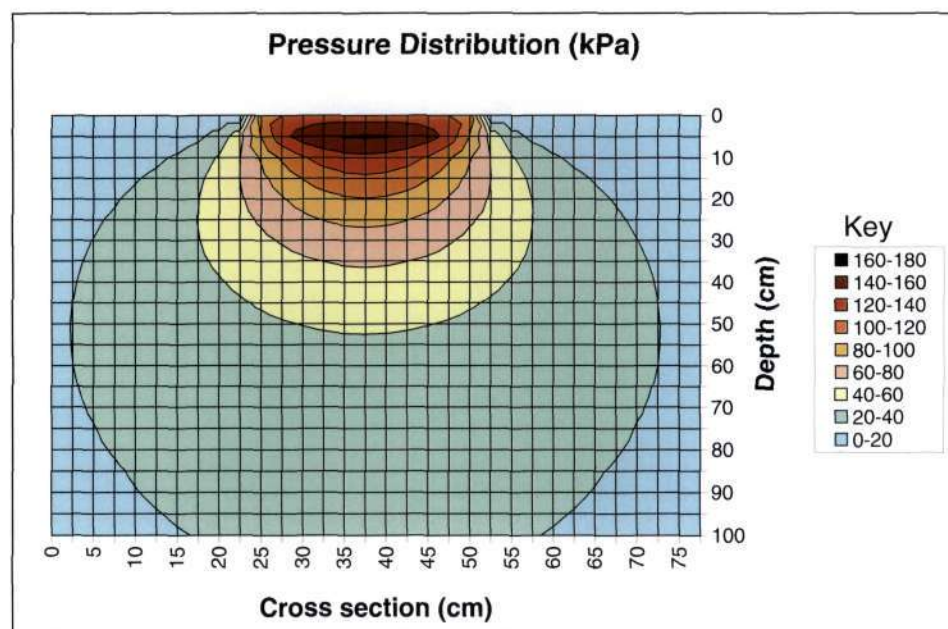


Figure 6.6 Typical DSS outputs of pressure distribution obtained from SOCOMO

6.5.2 Compacted dry density

The compacted dry density was calculated using Equation 6.7 developed by Larson *et al.* (1980). A value for σ_z is extracted from the output file and used as an input by the DSS for Equation 6.7. The other inputs for Equation 6.7 are described below.

$$\rho = [\rho_k + \Delta T(S_1 - S_k)] + Ci \log\left(\frac{\sigma_z}{\sigma_k}\right) \quad (6.7)$$

The compression index (Ci) is calculated using Equations 6.8 and 6.9. Equation 6.8 is used to calculate Ci for a soil in a temperate region with expanding type clays, whilst Equation 6.9 is used to calculate Ci for soils in tropical and semi-tropical regions with non expanding clays (Larson *et al.*, 1980). Gupta and Larson (1982) showed that the compression index Ci increases up to a clay content of 33 % and then levels off.

$$Ci = 2.033 \times 10^{-1} + 1.423 \times 10^{-2}(Cl) - 1.447 \times 10^{-4}(Cl)^2 \quad (6.8)$$

$$Ci = 1.845 \times 10^{-1} + 1.205 \times 10^{-2}(Cl) - 1.108 \times 10^{-4}(Cl)^2 \quad (6.9)$$

In this DSS, the soils were expected to be in a temperate region with expanding clay types, thus Equation 6.7 was used. The slope of the dry density to water saturation curve (Δ_T) was estimated using expressions developed by Larson *et al.* (1980). Two relationships were developed, one for fine textured soils (Equation 6.10) and one for coarsely textured soils (Equation 6.11).

$$\Delta_T = 3.461 \times 10^{-3} + 1.742 \times 10^{-4}(Si) - 2.980 \times 10^{-6}(Si)^2 \quad (6.10)$$

$$\Delta_T = 3.217 \times 10^{-3} + 3.254 \times 10^{-4}(Cl) - 5.385 \times 10^{-6}(Cl)^2 \quad (6.11)$$

where Si is the silt percentage.

In the DSS Equations 6.10 and 6.11 are applied for clay contents higher and lower than 45%, respectively. Typical outputs of compacted dry density from the DSS are illustrated in Figure 6.7.

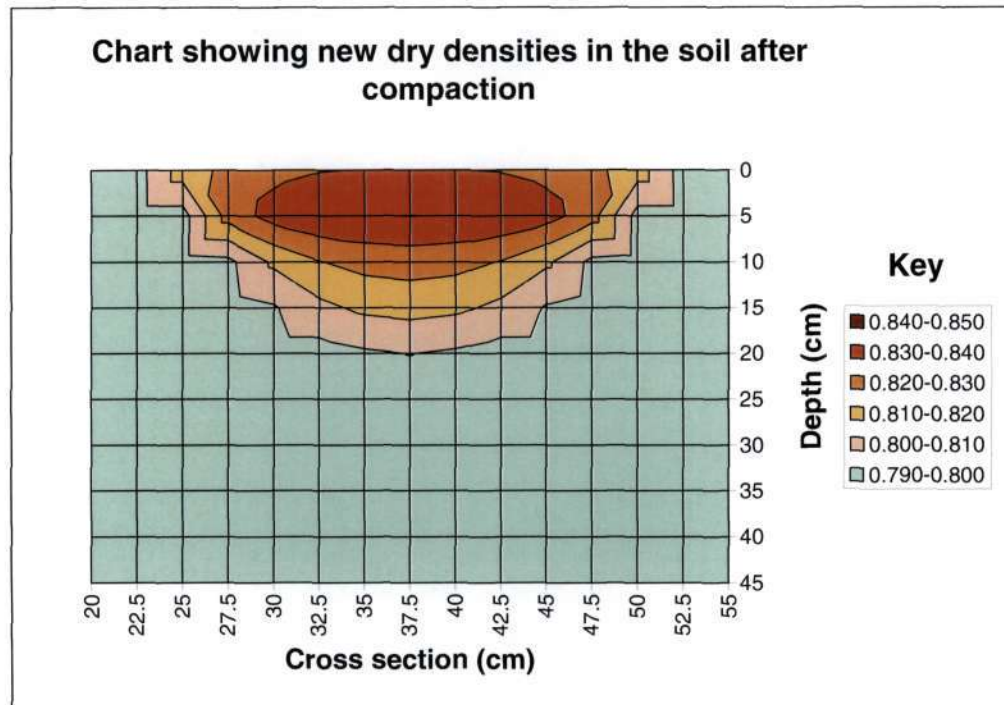


Figure 6.7 Typical DSS outputs of compacted dry density calculated using Larson *et al.* (1980)

6.6 Conclusions

This chapter describes the development of a DSS for the SOCOMO model. Several other research outcomes, such as tyre pressure and dimensions (Koolen and Kuipers, 1983; O'Sullivan *et al.*, 1999), default geotechnical properties for soil texture (Francis, 1988) and the calculation of compacted dry density (Larson *et al.*, 1980) were integrated into an MS Excel[®] spreadsheet. The DSS creates the opportunity for a wide range of scientists, managers and consultants to utilise and integrate valuable existing scientific information. Providing that verification has been completed, the DSS can be used in future research to make operational, tactical and strategic decisions on a micro, medium and macro scale. Prior to the distribution and utilization of this DSS it was necessary to verify the models outcomes. Chapter 7 describes a verification exercise that was undertaken.

7. EVALUATION OF THE SOCOMO DECISION SUPPORT SYSTEM

7.1 Introduction

In Chapter 6 a user friendly decision support system (DSS) for the SOCOMO soil compaction (SC) model (van den Akker, 2004) was developed. Many of the assumptions made in Chapter 6 have not been verified and it is hence necessary to evaluate the DSS. The purpose of this chapter is to give an evaluation of the SOCOMO based DSS by verifying model outcomes against independent data. Eweg (2005) conducted an experimental trial on a sandy loam soil at a forestry site in Richmond, KwaZulu-Natal, South Africa. Eweg (2005) developed and tested a pressure sensor to measure changing pressures in the soil during a SC event. The data obtained from this experiment were used to evaluate the SOCOMO based decision support system.

7.2 Methods

The following subsection describes the trial site, the vehicle description, how the soil pressure measurements were obtained and a description of the simulations run using the DSS.

7.2.1 Site description

Field testing took place on a forestry site near Richmond in KwaZulu-Natal, South Africa (29° 51' S; 30° 12' E; 1075 m above sea level). The site was on a slope of 11% with recently harvested 15-year old *Eucalyptus Smithii*. The soil properties for this site are presented in Table 7.1.

Soil samples were analysed by the South African Sugar Research Institute (SASRI) to determine soil texture and organic matter. Core samples were taken to determine the dry bulk density of the soil before and after the SC event.

Table 7.1 Description of Richmond soil properties

Texture: Sandy Loam		Soil moisture content (%)	44.1
Clay (%)	19	Internal angle of friction (θ in $^{\circ}$)	21
Silt (%)	14	Cohesion (C in kPa)	10
Sand (%)	67	Preconsolidated soil strength (SS in kPa)	150
Organic matter (%)	6.42	Dry Density (ρ in kg.m^{-3})	796

Three undrained triaxial tests were performed on three undisturbed soil samples of height 75 mm and diameter 38 mm, taken from the upper 0.3 m of the soil. At the time, the average moisture content of the soil was 44.1%. The range of dry densities was between 725 - 991 kg.m^{-3} . The deformation rate used in the triaxial tests was 1.25 mm.min^{-1} . This would give failure for the simple test at 20% strain in about 20 minutes. The cell pressures used were 25, 44 and 60 kPa. The pre-consolidated strength (SS) of this soil is known to be much higher than the shear strength and was therefore not considered (Smith, 2004).

7.2.2 Vehicle description

The timber was placed in bundles of approximately 4 tons and then loaded onto a self-loading trailer. The trailer was hitched to an agricultural tractor. Figure 7.1 illustrates the tractor and trailer combination, note the smooth tyre on the trailer, which was used to apply the SC. A smooth tyre was selected to reduce any possible effects lugged tyres may have. The tyre was a Firestone 10.5/16/ZS. It was a 14 ply radial, had a diameter of approximately 1 m, a contact width of approximately 280 mm and was slightly over-inflated to 424 kPa and therefore would not deflect the required 20%. The weight on the wheel was measured as 2148 kg.



Figure 7.1 Self-loading trailer used to apply the compaction

7.2.3 Soil pressure measurements

Fluid filled soil pressure sensors were designed and developed by Eweg (2005). One of the objectives of the work completed by Eweg (2005) was to develop a simple and cheap sensor that could be inserted into the soil without changing its structure significantly. Figures 7.2 and 7.3 illustrate the components of the sensor. The sensor is made up of a latex bulb attached to a hydraulic tube. A “T” piece is attached at the other end of the tube which allows two ports, one to which a Motorola MPX 5700DP pressure transducer was attached, while the other port had a tap to allow the user to bleed and pre-pressurise the bulb.



Figure 7.2 Diagram of the fluid filled pressure sensor made out of latex (Eweg, 2005)

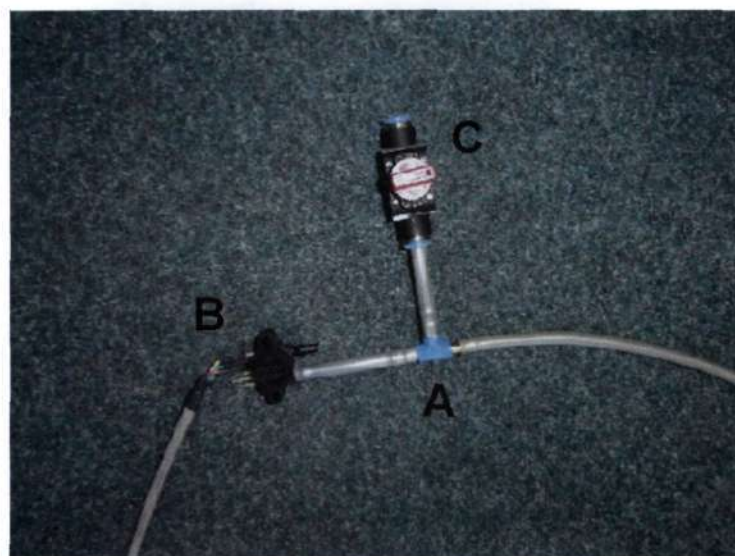


Figure 7.3 Diagram illustrating (A) the “T” piece, (B) the Motorola MPX 5700DP pressure transducer and (C) the tap used to pre-pressurise the bulb (from Eweg, 2005)

The fluid filled sensors were inserted into the soil using the insertion technique and frame described by Eweg (2005). Sixteen sensors were placed in a nest in the soil perpendicular to the direction of travel. Figure 7.4 illustrates the orientation of Sensors 1 to 16 in the nest.

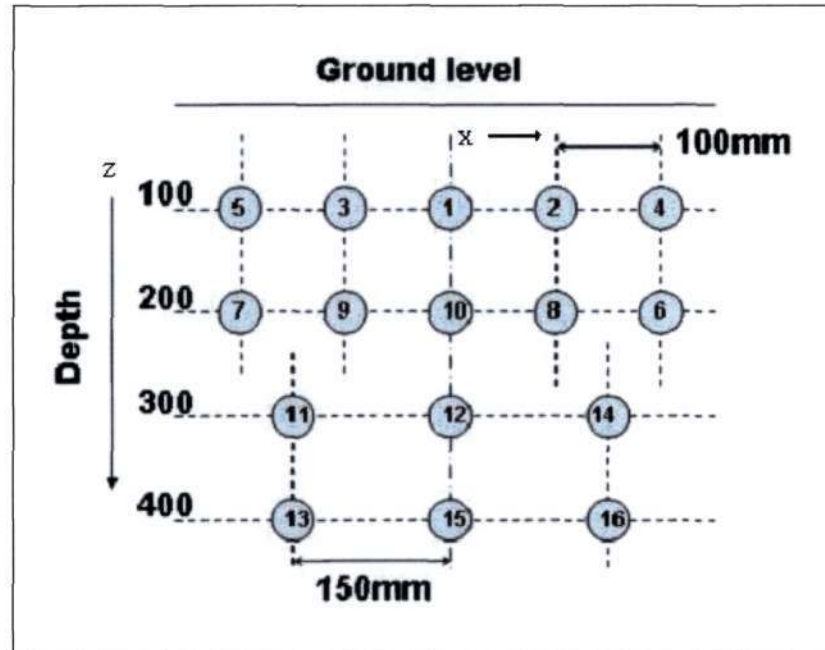


Figure 7.4 Diagram showing sensor orientation in the soil.

Once the sensors were inserted into the soil, the trailer was reversed over the nest of sensors causing the SC. The pressure changes in the sensors as a result of the event were logged by a computer and a data acquisition cord. These results are shown in Section 7.3.

7.2.4 SOCOMO DSS simulation runs

SOCOMO Simulations were carried out to evaluate and verify the DSS. The simulations involved trying various options that were available in the DSS, for example geotechnical inputs *vs.* easy inputs, the two contact area scenarios and the two loading scenarios (see Sections 6.3 and 6.4). Descriptions of the simulations are summarised in Table 7.2.

The results from the simulations were displayed graphically and compared to the pressure values and the measured bulk density values obtained in Section 7.3. Plots of

residuals (simulated minus observed) were drawn to illustrate the accuracy of the model. Linear trend lines were fitted through the data, and the slope and R^2 of these lines was also compared. The root mean square error (RMSE), the mean error (ME), the maximum error (MAXE) was used to compare measured and simulated data.

Table 7.2 Description of the SOCOMO simulations carried out for the Richmond trial. The different references and concepts are explained in Section 6.3 and 6.4

Code	Soil input	Contact area equation	Loading pattern
A I 1	Measured geotechnical inputs	O'Sullivan <i>et al.</i> (1999)	Uniform pressure distribution
A I 2	Measured geotechnical inputs	O'Sullivan <i>et al.</i> (1999)	Parabolic loading based on Johnson and Burt (1990)
A II 1	Measured geotechnical inputs	Koolen and Kuipers (1983)	Uniform pressure distribution
A II 2	Measured geotechnical inputs	Koolen and Kuipers (1983)	Parabolic loading based on Johnson and Burt (1990)
B I 1	"Easy " input based on soil texture	O'Sullivan <i>et al.</i> (1999)	Uniform pressure distribution
B I 2	"Easy " input based on soil texture	O'Sullivan <i>et al.</i> (1999)	Parabolic loading based on Johnson and Burt (1990)
B II 1	"Easy " input based on soil texture	Koolen and Kuipers (1983)	Uniform pressure distribution
B II 2	"Easy " input based on soil texture	Koolen and Kuipers (1983)	Parabolic loading based on Johnson and Burt (1990)

7.3 Results and Discussion

7.3.1 Observed data

Table 7.3 shows the peak pressures in the sensors during the SC event. The table shows that the pressures are high close to the soil surface, and decrease with depth. Figure 7.7 illustrates these values on graphs drawn in SYSTAT (Statistical package). The dry bulk density readings before and after the SC event are shown in Table 7.4. The soil density increases with depth. Figure 7.5 gives a graphical representation of the dry density before and after the SC event.

The peak pressure at 100 mm beneath the centre of the tyre was measured at 128 kPa. This is significantly less than the inflation pressure of the tyre (425 kPa). The peak pressure at 400 mm below the centre of the tyre was measured at 5.2 kPa (see Table 7.3), which is very small.

Table 7.3 Peak pressures recorded in each soil pressure sensor (from Eweg, 2005)

Sensor	Z (mm)	X (mm)	Pressure (kPa)
1	100	0	128.3
2	100	100	38
3	100	-100	7.32
4	100	200	8.9
5	100	-200	7.1
6	200	200	7.3
7	200	-200	13.4
8	200	100	17.8
9	200	-100	22.5
10	200	0	61.8
11	300	-150	2.8
12	300	0	16.2
13	400	-150	3.2
14	300	150	3.9
15	400	0	5.2
16	400	150	3.4

Table 7.4 Dry bulk densities (kg.m^{-3}) before and after the compaction event

Depth (mm)	<i>Before</i> X Position (mm)					<i>After</i> X Position (mm)				
	-200	-100	0	100	200	-200	-100	0	100	200
50 - 100	825	820	810	790	783	968	976	992	914	871
150 - 200	805	799	726	772	835	888	908	897	894	843

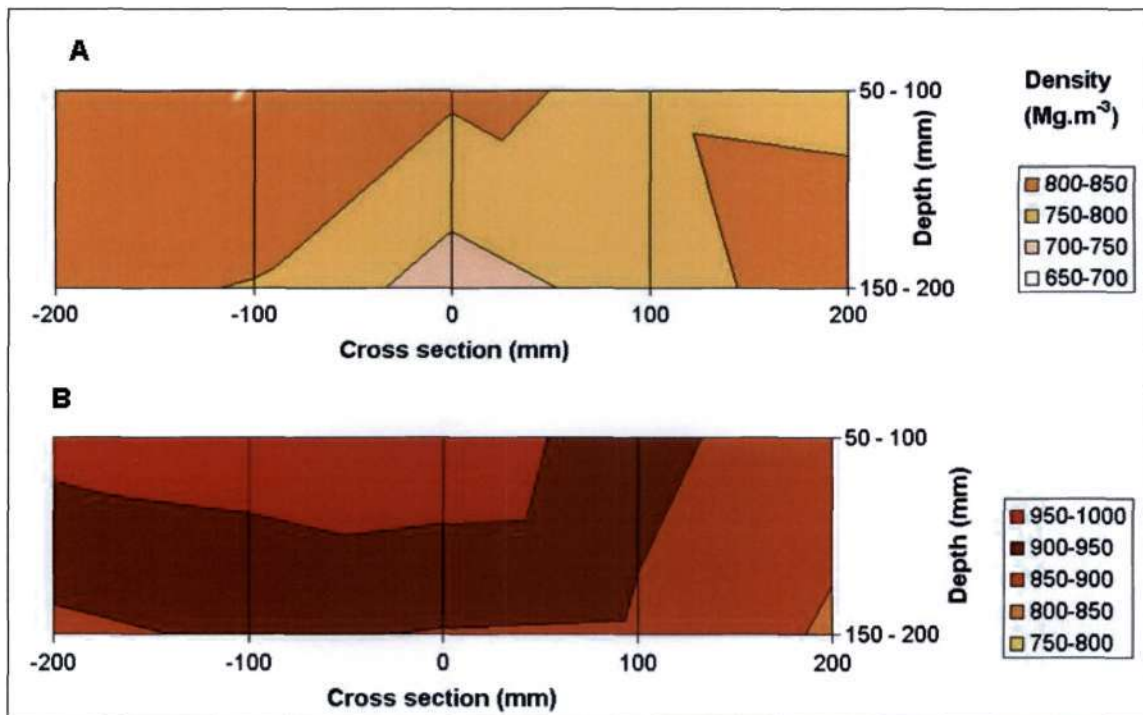


Figure 7.5 Graphs illustrating dry density (A) before the compaction event and (B) after the compaction event

After consultation with various tyre manufactures, it was found that the tyre used in this trial was over inflated. This would have an effect on the rule of thumb by Koolen and Kuipers (1983). The vehicle caused an average increase in dry density from 796 to 914 kg.m^{-3} over the profile that was tested (see Table 7.4). The measured rut depth as a result of the SC event was approximately 35 mm.

7.3.2 Model evaluation

Table 7.5 summarises the test statistics after comparing the simulated values to the measured values. When it comes to simulating the pressure distribution, with respect to RMSE, test BI1 performed the best (RMSE 47.9 kPa). This was extremely close to test AI1, which had a RMSE of 48 kPa. The RMSE ranged from 48 to 195 kPa over the simulations and in all cases the pressure was overestimated (ME>0).

Table 7.5 Test statistics comparing the SOCOMO DSS against measured data. The best situation is highlighted for each test statistic

Pressure Distribution					
Test	RMSE (kPa)	ME (kPa)	MAXE (kPa)	Slope	r ²
AI1	48.0	42.1	79.0	0.684	0.518
AI2	67.9	61.4	130.8	1.090	0.583
AII1	168.2	138.7	378.7	2.905	0.604
AII2	194.6	155.5	452.0	3.548	0.629
BI1	47.9	42.2	79.8	0.695	0.528
BI2	68.3	62.0	130.3	1.092	0.590
BII1	168.7	139.8	378.7	2.929	0.616
BII2	195.0	156.1	452.0	3.541	0.628
Bulk Density					
Test	RMSE (kg.m^{-3})	ME (kg.m^{-3})	MAXE (kg.m^{-3})	Slope	r ²
AI1	122.2	-115.1	171.7	0.117	0.499
AI2	100.6	-93.9	171.9	0.351	0.387
AII1	71.1	-47.3	171.9	0.765	0.312
AII2	69.9	-37.7	171.3	0.902	0.332
BI1	98.1	90.4	151.1	0.208	0.410
BI2	115.5	109.6	151.1	0.386	0.336
BII1	165.8	156.0	230.9	0.803	0.305
BII2	176.3	165.0	250.9	0.943	0.327

Test AII2 most accurately predicted the new dry density of the soil after the compaction event with a RMSE of 70 kg.m^{-3} . Test BII2 performed the worst in both the pressure distribution and bulk density.

Figure 7.6 illustrates the differences between the pressure bulb derived in SYSTAT from the data measured by Eweg (2005) against the best SOCOMO simulation BI1 (RMSE = 47.9 kPa). Figure 7.7 presents the residual (error) plot. The residual plot shows that at shallow depths directly under the tyre the simulated values and the measured values were reasonably similar (errors of 0 to 25 kPa). These errors increase with depth and towards the right. Possible reasons for the increase in error could be due to the fact that organic matter is not taken into account in the model. Organic matter is known to help soils to rebound and thereby reduce stress propagation. The residual plot also shows that to the right of the centre line there is a sharp increase in the residual to 75kPa. This is probably due to the fact that during the field experiment, the vehicle did not travel over the centre of the sensors, but slightly to the side (40mm).

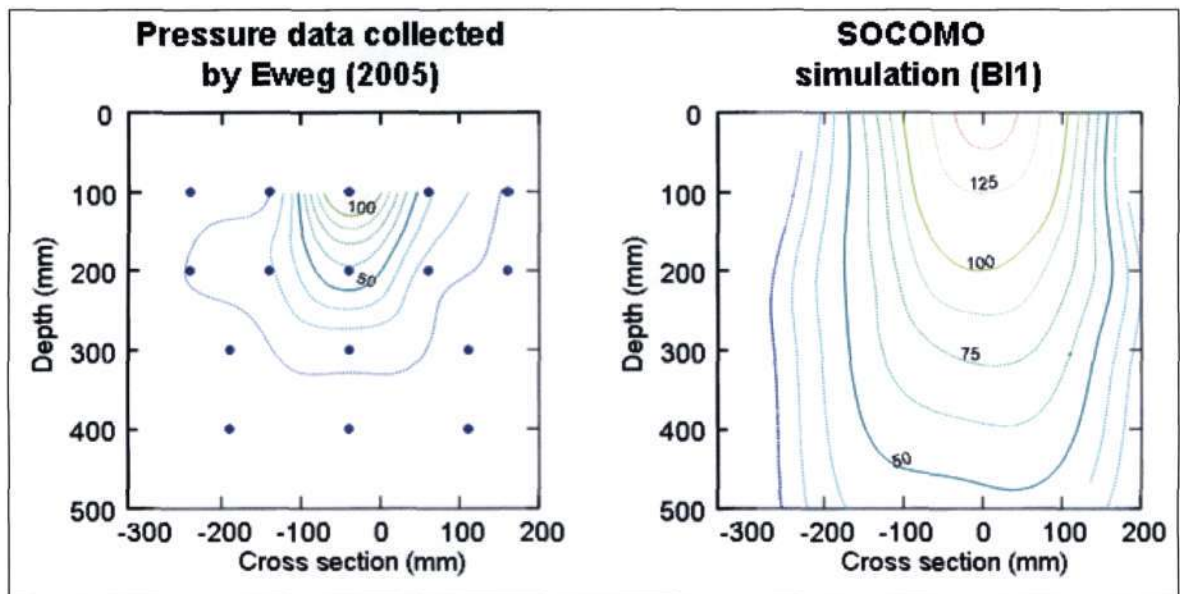


Figure 7.6 Graphs illustrating the difference between the pressure (kPa) data collected by Eweg (2005) and a SOCOMO simulation

Figure 7.8 shows a scatter plot of measured vs. simulated values for the pressure distribution simulated in test BI1. The graph shows that, in this case the SOCOMO model overestimates the stresses occurring at deep depth, whilst it is more accurately predicting the stresses at the shallow depths directly under the centre of the tyre.

Table 7.5 shows that where the Koolen and Kuipers (1983) rule of thumb was used to determine the contact area, there was always a high RMSE (>168kPa). These high errors could be because the Koolen and Kuipers (1983) rule of thumb (mean normal

stress at the soil-tyre interface is 1.2 times the inflation pressure) is invalid for tyres that are over inflated. Manufactures recommend that tyres should be allowed to deform by 20%.

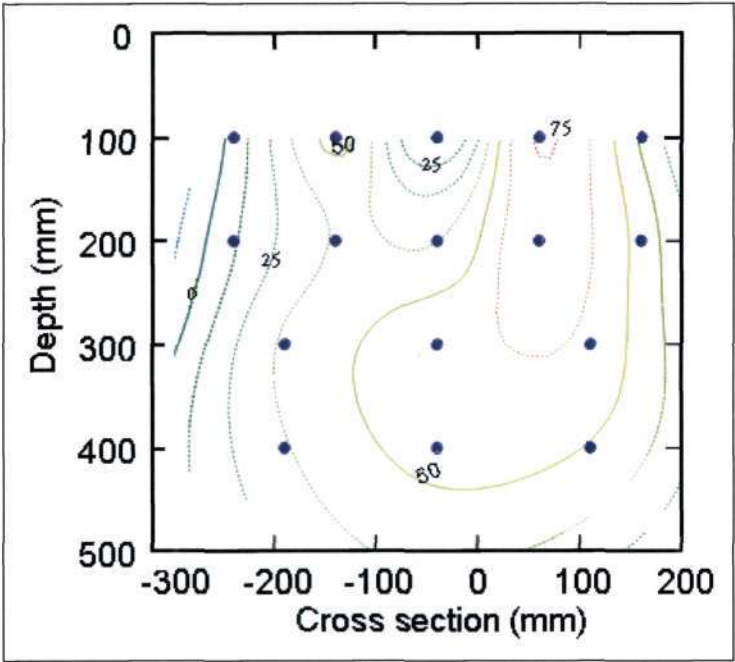


Figure 7.7 Residual plot comparing the measured pressures (kPa) against simulated pressures (BI1)

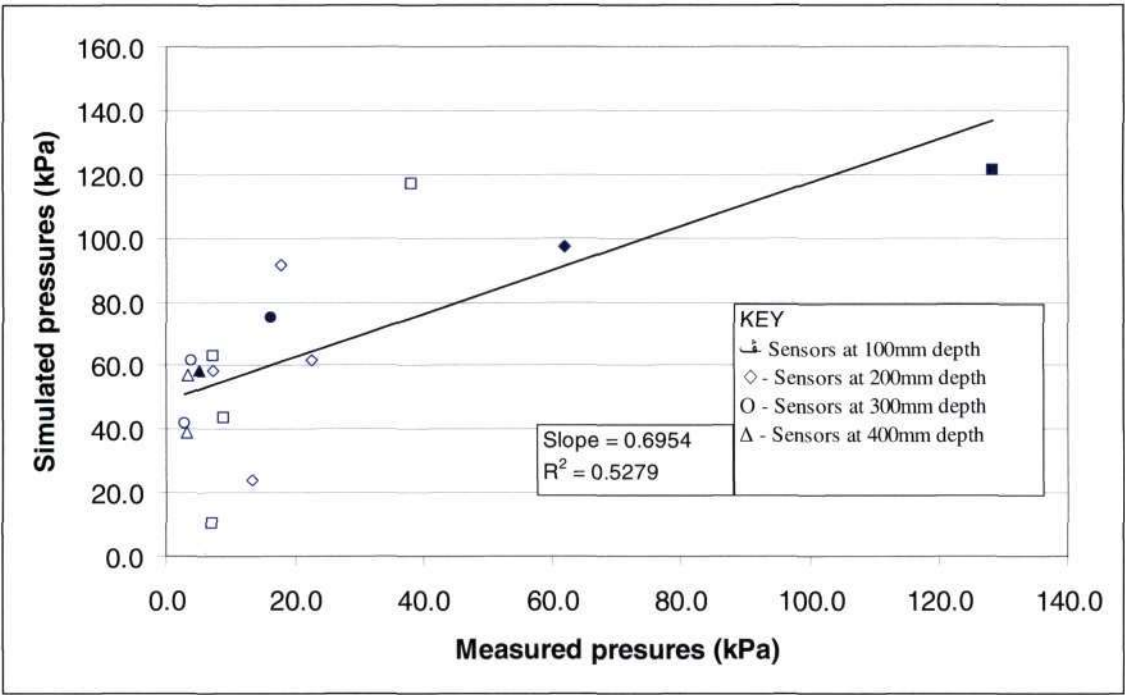


Table 7.5 suggests that the best simulations of pressure distribution do not necessarily result in the best results in simulated changes to bulk density. This could be due to the organic matter in the soil and due to model insensitivity. The Larson *et al.* (1980) bulk density equation does not take organic matter into account and it is an empirical equation that was calibrated for specific soils.

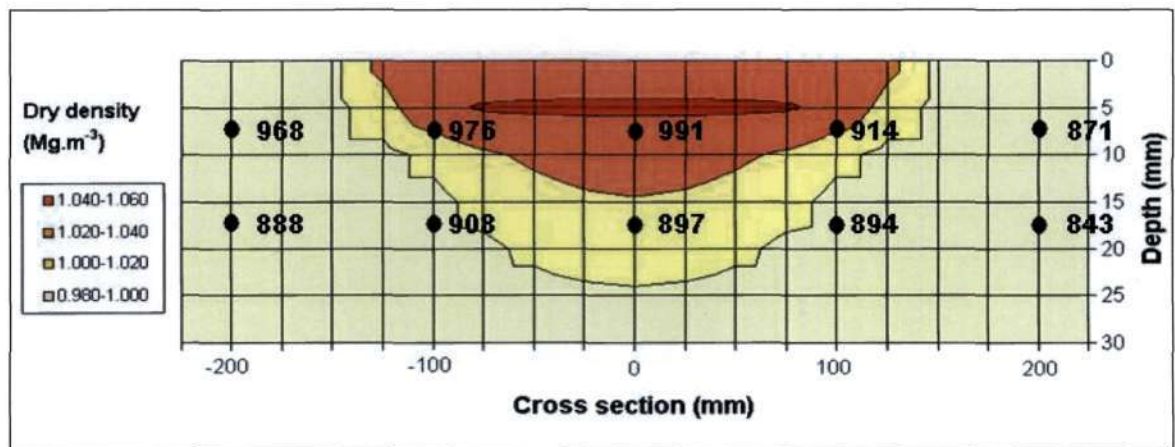


Figure 7.9 Graph illustrating the simulated dry densities for Test B11 (colour shadings) against the measured dry densities in the soil profile (labelled dots in Mg.m^{-3})

Figure 7.9 illustrates the difference between the measured changes in dry density and the simulated values for the best pressure distribution (B11). Figure 7.9 shows that the Larson *et al.* (1980) bulk density equation generally over estimates the bulk density. This could be because the model does not take organic matter into account. Table 7.5 shows that for all the “A” scenarios, the mean errors were all negative ($\text{ME} < 0$) and for all the “B” scenarios, the mean errors are positive ($\text{ME} > 0$). This is because of the way the initial dry density is calculated in these scenarios. In the geotechnical soil input scenarios, the dry density was measured (core samples), whilst in the easy input scenarios, the dry density was calculated using Equation 6.1. The two methods of determining the initial dry density give different results, and thus the final outcome.

7.4 Conclusions

The SOCOMO DSS simulated pressure distributions with RMSE values of between 47.9 kPa and 195 kPa. These values are relatively low compared to the pressures exerted at shallow depths by vehicles. In addition, the largest component of the error

was due to over estimating deep pressures, which are not as critical compared to the shallow high pressures. With the exception of the rule of thumb by Koolen and Kuipers (1983), easy inputs performed reasonably well. It is suggested that Koolen and Kuipers (1983) rule of thumb would have performed well if tyres were not over inflated. The simulated pressure distributions always overestimated the measured values ($ME > 0$)

The SOCOMO DSS simulated changes in dry density using equations developed by Larson *et al.* (1980). The RMSE for the dry density simulations varied from 69 kg.m^{-3} to 176 kg.m^{-3} . In the geotechnical soil input scenarios, the DSS under estimated the simulated dry density ($ME < 0$), whilst in the easy soil input scenarios the DSS over estimated the simulated dry density ($ME > 0$). This was because of the way the initial dry density was calculated for these simulations.

Overall, the DSS performed satisfactory. However, there is a need to test the DSS under more tyre configurations, more soils and more other conditions. This will greatly enhance user confidence and model applicability.

8. DISCUSSION, CONCLUSIONS AND RECOMMENDATIONS

8.1 Discussion and Conclusions

Soil compaction (SC) is evidently a problem of worldwide concern in agriculture. Compaction not only affects crop production, it has been seen to increase soil erosion, decrease soil infiltration rates, decrease general soil health, affect nutrient and water uptake by plants and affect several soil properties. A review in this study confirms that SC, caused by agricultural traffic, affects soil properties such as structural strength, bulk density, soil aeration and hydraulic soil properties. The review shows how changes in these soil properties causes a decrease in plant height, root elongation, leaf appearance rates, dry root weights and most importantly, yields of many crops that were subjected to a SC event. The study concluded that the most important property that determines the degree of SC in unsaturated soils is soil texture. A detailed description of the SC process as well as the relationships between applied load and the resulting SC were presented. These relationships are based on well known stress and strain theories.

The concept of modelling SC is an old concept that has been in use for many decades. Several SC models have been developed in the past. These models can be sub divided into two categories, *viz.* pseudo-analytical and finite element models. Psuedo-analytical models are simpler and easier to use compared to finite element models. These models, however, do have some limitations. Generally pseudo-analytical models are limited by a lack of pedotransfer functions, whilst finite element models are limited by a lack of input data. These models have been used successfully by various authors. One prominent pseudo-analytical model is SOCOMO. This model was successfully used by a number of authors and based on this and the model's availability, the model was chosen for further analysis.

Often a limitation for SC modelling is the necessity for detailed input variables such as geotechnical soil properties. There is a relatively large amount of spatial variability within these variables, thus obtaining representative variables for large areas is extremely difficult.

A significant outcome of this study is the estimation of geotechnical soil properties from soil texture and bulk density. This type of relationship, to the author's knowledge, has not been attempted before. Given the necessary verifications have been done, the SOCOMO model could potentially be applied with relative ease over large areas where geotechnical soil information is not available. The outcomes could be related to a wide range of civil engineering and other relevant fields.

The SOCOMO DSS simulated pressure distributions with RMSE values of between 47.9 kPa and 195 kPa. These values are relatively low compared to the pressures exerted at shallow depths by vehicles. In addition, the largest component of the error was due to over estimating deep pressures, which are not as critical compared to the shallow high pressures. With the exception of the rule of thumb by Koolen and Kuipers (1983), easy inputs performed reasonably well. It is suspected that the rule of thumb of Koolen and Kuipers (1983) will perform well if tyres are not over inflated. Simulated pressure distributions always overestimated measured pressures ($ME > 0$ kPa).

The SOCOMO DSS simulated changes in dry density using equations developed by Larson *et al.* (1980). The RMSE for the dry density simulations varied from 69 to 176 kg.m^{-3} . In the geotechnical soil input scenarios, the DSS under estimated the simulated dry density ($ME < 0 \text{ Mg.m}^{-3}$), whilst in the easy soil input scenarios the DSS over estimated the simulated dry density ($ME > 0 \text{ Mg.m}^{-3}$). This was because of the way the initial dry density was calculated for these scenarios. The bulk density equation developed by Larson *et al.* (1980) did not perform satisfactory. This is an area where more work needs to be done to increase user confidence in the DSS.

This study successfully produced a DSS that has the potential to be of great benefit to scientists, managers and consultants in the South African timber and sugar industries. Although this is probably one of the first simple and easy to use DSS's for SC management in these industries, caution is raised with respect to the model's validity. Further verification is needed to increase confidence in the outcomes.

8.2 Future Recommendations

From this study, a number of aspects were identified where future research may greatly enhance this research. They are listed below:

Modelling:

1. The SOCOMO model does not take organic matter into account. This study has shown that organic matter may affect stress propagation into the soil.
2. The SOCOMO model is able to calculate the stress at any point in the soil for any given vertical and horizontal stress distribution in the soil-tyre interface. In this study, only the vertical stress distribution was considered. The effects of wheel slip were neglected (*i.e.* the horizontal stress distribution is equal to zero). Research has shown that the magnitude of the horizontal stress is 0.5 times the vertical stress (van den Akker, 2004). Future simulations containing the horizontal stress component may increase user confidence in the DSS.
3. The bulk density model developed by Smith (1995) could be added to the DSS.
4. Peotransfer functions developed by Nhantumbo (1999) could be added to the DSS.
5. Need to establish links between soil compaction and crop production.

Model Inputs:

1. Higher confidence in the use of texture and dry density to determine geotechnical soil inputs is required. The results from Chapter 5 therefore need to be verified and expanded. This can be achieved by collecting more soil samples and applying a similar methodology to them. The soils used in Chapter 5 also do not include any silty soils.
2. A better database of tyre information needs to be collected.
3. The equation by O'Sullivan *et al.* (1999) to estimate the contact area of the tyre-soil interface (see Equation 6.2) is mainly applicable to crossply tyres. A similar equation needs to be developed for radial tyres.

Decision Support System:

1. The DSS needs to be verified for a larger number of soils, wheel configurations and moisture conditions. This will greatly increase user confidence.

2. At the moment the DSS only utilizes the three major stresses acting on each soil element (σ_z , σ_x , and σ_y). SOCOMO has various other outputs. One of the most interesting outputs not mentioned in this document are graphs which give an estimation of how much plastic deformation and structural failure occurs beneath the soil as a result of a SC event. These graphs give an indication of the percentage area that is affected by SC. These graphs may be used innovatively in future research.

Applications of the DSS:

1. The DSS could be used to construct a load bearing capacity map like that constructed by van den Akker (1997) for South African soils and conditions. The map could be used to show farmers and consultants under what conditions it is possible to enter the field with heavy vehicle without causing irreparable damage to the soil.
2. The DSS could be run stochastically to obtain a range of outputs for a range of inputs. This will increase representivity of variable soil profiles.
3. The DSS could be used to make operational, tactical and strategic decisions on a micro, medium and macro scale. For example, the DSS could be used to determine:
 - a. The effects of entering a particular field when it is too wet (micro scale).
 - b. How much money could be saved if high floatation tyres were bought for all the transport vehicles of an estate (medium scale).
 - c. What are the consequences (in terms of yield and income) of using radial compared to high floatation tyres in a mill area (regional scale)

9. REFERENCES

- Abu-Hamdeh, NH. 2003. Compaction and subsoiling effects on corn growth and soil bulk density. *Soil Science of America Journal* 67: 1213-1219.
- Abu-Hamdeh, NH and Al-Widyan, MI. 2000. Effect of axle load, tyre inflation pressure, and tillage system on soil physical properties and crop yield of a Jordanian soil. *Transactions of the ASAE* 43 (1): 13-21.
- Akinci, I, Cakir, E, Topakci, M, Canakci, M and Inan, O. 2004. The effect of subsoiling on soil resistance and cotton yield. *Soil and Tillage Research* 77 (2): 203-210.
- Alakukku, L. 1996. Persistence of soil compaction due to high axle load traffic. II Long-term effects on the properties of fine textured and organic soils. *Soil and Tillage Research* 37: 223-238.
- Alblas, J, Wanink, F, van den Akker, JJH and van der Werf, HMG. 1994. Impact of traffic-induced compaction of sandy soils on the yield of silage maize in the Netherlands. *Soil and Tillage Research* 29: 157-165.
- Arvidsson, J. 2001. Subsoil compaction caused by heavy sugarbeet harvesters in southern Sweden I. Soil physical properties and crop yield in six field experiments. *Soil and Tillage Research* 60: 67-78.
- Arvidsson, J, Trautner, A, van den Akker, JJH and Schjonning, P. 2001. Subsoil compaction caused by heavy sugarbeet harvesters in southern Sweden II. Soil displacement during wheeling and model computations of compaction. *Soil and Tillage Research* 60: 79-89.
- ASABE. 2004. Soil Cone Penetrometer - ASAE Standard S313.3 February 2004. [Internet]. American Society of Agricultural and Biological Engineers, St. Joseph, Michigan, USA. Available from: www.asabe.org. [Accessed: 4 October 2005].
- Bailey, AC and Johnson, CE. 1989. A soil compaction model for cylindrical stress states. *Transactions of the ASAE* 32 (3): 822-825.
- Bailey, AC, Johnson, CE and Schafer, RL. 1984. Hydrostatic compaction of agricultural soils. *Transactions of the ASAE* 27 (4): 952-955.
- Bayhan, Y, Kayisoglu, B and Gonulol, E. 2002. Effect of soil compaction on sunflower growth. *Soil and Tillage Research* 68: 31-38.
- Berli, M, Kirby, JM, Springman, SM and Schulin, R. 2003. Modelling compaction of agricultural soils by tracked heavy construction machinery under various moisture conditions in Switzerland. *Soil and Tillage Research* 73: 57-66.
- Bezuidenhout, CN. 2005. Personal communication. University of KwaZulu-Natal, Pietermaritzburg, South Africa, 20 September 2005.
- Binger, RL and Wells, LG. 1992. COMPACT-A reclamation soil compaction model part I. Model development. *Transactions of the ASAE* 35 (2): 405-413.

- Blackwell, PS and Soane, BD. 1981. A method of predicting bulk density changes in field soils resulting from compaction by agricultural traffic. *Journal of Soil Science* 32: 51-65.
- Boussinesq, J. 1885. *Application des Poteneiels a l'Etude de l'Equilibre et du Mouvement des Solides Elastiques*. Gauthier-Villas, Paris, France.
- Brais, S. 2001. Persistence of soil compaction and effects on seedling growth in Northwestern Quebec. *Soil Science of America Journal* 65: 1263-1271.
- Casagrande, A. 1936. Determination of the preconsolidation load and its practical significance. In: *Proceedings of the 1st International Conference on Soil Mechanics and Foundation Engineering*, pp.60-64. ICSMFE, Cambridge, Massachusetts, USA.
- Clemente, EP, Schaefer, CEGR, Novais, RF, Viana, JH and Barros, NF. 2005. Soil compaction around Eucalyptus grandis roots: a micromorphological study. *Australian Journal of Soil Research* 43 (2): 139-146.
- Czyz, EA. 2004. Effects of traffic on soil aeration, bulk density and growth of spring barley. *Soil and Tillage Research* 79: 153-166.
- Das, BM. 2002. *Principles of Geotechnical Engineering*. Brooks/Cole, Pacific Grove, USA.
- Dauda, A and Samari, A. 2002. Cowpea response to soil compaction under tractor traffic on a sandy loam soil in the semi arid region of northern Nigeria. *Soil and Tillage Research* 68: 17-22.
- Defossez, P and Richard, G. 2002. Models of soil compaction due to traffic and their evaluation. *Soil and Tillage Research* 67: 41-64.
- Dejong-Hughes, J, Moncrief, J and Voorhees, W. 2001. Soil Compaction - Causes and Consequences. [Internet]. University of Minnesota Extension Service, Minnesota, USA. Available from: <http://www.extension.umn.edu/distribution/cropsystems/components/3115s01.html>. [Accessed: 22 June 2004].
- Douglas, JT and Crawford, CE. 1991. Wheel induced soil compaction effects on ryegrass production and nitrogen uptake. *Grass and Forage Science* 46: 405-416.
- Eweg, JL. 2005. The design and testing of soil pressure sensors for in-field agricultural and forestry traffic. Unpublished MSc Eng Dissertation. School of Bioresources Engineering and Environmental Hydrology, University of KwaZulu-Natal, Pietermaritzburg, South Africa.
- Fausey, NR and Dylla, AS. 1984. Effects of wheel traffic along one side of corn and soyabean rows. *Soil and Tillage Research* 4: 147-154.
- Fleige, H and Horn, R. 2000. Field experiments on the effect of soil compaction on crop properties, runoff, interflow and erosion. In: eds. Arvidsson, J, *Subsoil*

Compaction, Distribution, Processes and Consequences: Advances in GeoEcology, Ch. 3, 258-268. CANTENA VERLAG GMBH, Reiskirchen, Germany.

- Flowers, MD and Lal, R. 1998. Axle load and tillage effects on soil physical properties and soybean grain yield on a mollic ochraqualf in northwest Ohio. *Soil and Tillage Research* 48: 21-35.
- Francis, TE. 1988. The relationship between the formation of soil catenas and their engineering properties, with reference to urban development. Unpublished Ph.D Thesis. Department of Geology, University of Natal, Durban, South Africa.
- Froehlick, HA. 1979. Soil compaction cfrom logging equipment. Effects on growth of young ponderosa pine. *Journal of Soil Water Conservation* 34: 276-278.
- Fröhlich, OK. 1934. *Drukverteilung in Baugrunde*. Verlag von Julius Springer, Wein, Germany.
- FSC. 2003. Forestry Stewardship Council - Because forests matter. [Internet]. Forest Stewardship Council A.C., Bonn, Germany. Available from: www.fsc.org/en/. [Accessed: 21 August 2005].
- Gaultney, L, Krutz, GW, Steinhardt, GC and Liljedahl, JB. 1982. Effects of subsoil compaction on corn yields. *Transactions of the ASAE* 25: 563-569,575.
- Georges, JEW. 1980. Effects of harvest traffic and soil water content on soil compaction and regrowth of sugarcane. In: *Proceedings of the XVII ISSCT Congress*, pp.1078-1088. Executive committee of the ISSCT, Manila, Philippines.
- Gomez, A, Powers, RF, Singer, MJ and Horwath, WR. 2002a. N uptake and N status in ponderosa pine as affected by soil compaction and forest floor removal. *Plant and Soil* 242 (2): 263-275.
- Gomez, A, Powers, RF, Singer, MJ and Horwath, WR. 2002b. Soil compaction effects on growth on young ponderosa pine following litter removal in California's Sierra Nevada. *Soil Science of America Journal* 66: 1334-1343.
- Greacen, EL and Sands, R. 1980. Compaction of Forest Soils. A Review. *Austrailian Journal of Soil Research* 18: 163-189.
- Grigal, DF. 2000. Effects of extensive forestry management on soil productivity. *Forest Ecology and Management* 138 (1-3): 167-185.
- Gupta, SC, Hadas, A, Voorhees, W, Wolfe, DW, Larson, WE and Schneider, EC. 1985. Field testing of a soil compaction model. In: *Proceedings of the international conference of soil dynamics*, pp.979-994. ICSD, Auburn, USA.
- Gupta, SC and Larson, WE. 1982. Modeling soil mechanical behavior during tillage. In: Van Doren Jr, DM, *Predicting tillage effects on soil physical properties and processes.*, pp.515-578. American Agronomy Society, Madison, USA.

- Gupta, SC and Raper, RL. 1994. Prediction of Compaction. In: eds. van Ouwerkerk, C, *Soil Compaction in Crop Production*, Ch. 4, 71-91. Elsevier, Amsterdam, Netherlands.
- Gysi, M, Klubeertanz, G and Vulliet, L. 2000. Compaction of an Eutric Cambisol under heavy vehicle traffic in Switzerland - field data and modelling. *Soil and Tillage Research* (56): 117-129.
- Hadas, A. 1994. Soil compaction caused by high axle loads- review of concepts and experimental data. *Soil and Tillage Research* 29: 253-276.
- Hammel, K. 1994. Soil stress distribution under lugged tyres. *Soil and Tillage Research* 32: 163-181.
- Harris, WL. 1971. The soil compaction process. In: eds. van den Berg, GE, *Compaction of agricultural soils*, Ch. 1, 9-47. ASAE, St Joseph, Michigan, USA.
- Hillel, D. 1982. *Introduction to Soil Physics*. Academic Press, INC, London, UK.
- Horn, R. 2000. Subsoil compaction processes - State of knowledge. In: *4th International conference on Soil Dynamics*, pp.1-13. ICSD-IV, Adelaide, Australia.
- Horn, R and Fleige, H. 2003. A method for assessing the impact of load on mechanical stability and on physical properties of soils. *Soil and Tillage Research* 73: 89-99.
- Horn, R, Way, T and Rostek, J. 2003. Effect of repeated tractor wheeling on stress/strain properties and consequences on physical properties in structured arable soils. *Soil and Tillage Research* 73: 101-106.
- Ishaq, M, Hassan, M, Saeed, A, Ibrahim, M and Lal, R. 2001a. Subsoil compaction effects on crops in Punjab, Pakistan: I. Soil physical properties and crop yield. *Soil and Tillage Research* 59 (1-2): 57-65.
- Ishaq, M, Ibrahim, M, Hassan, M, Saeed, A and Lal, R. 2001b. Subsoil compaction effects on crops in Punjab, Pakistan: II. Root growth and uptake of wheat and sorghum. *Soil and Tillage Research* 60 (3-4): 153-161.
- Ishaq, M, Ibrahim, M and Lal, R. 2003. Persistence of subsoil compaction effects on soil properties and growth of wheat and cotton in Pakistan. *Experimental Agriculture* 39 (4): 341-348.
- Jansson, KJ and Wasterlund, I. 1999. Effect of traffic by lightweight forest machinery on the growth of young Picea abies trees. *Scandinavian Journal of Forest Research* 14 (6): 581-588.
- Jim, CY. 1993. Soil compaction as a constraint to tree growth in tropical and subtropical urban habitats. *Environmental Conservation* 20 (1): 35-49.
- Johnson, CE and Burt, EC. 1990. A method of predicting soil stress state under tyres. *Transactions of the ASAE* 33 (3): 713-717.

- Johnson, CE, Voorhees, WB, Nelson, WW and Randall, GW. 1990. Soyabean growth and yield as affected by surface and subsoil compaction. *Agronomy Journal* 82: 973-979.
- Jorajuria, D, Draghi, L and Aragon, A. 1997. The effect of vehicle weight on the distribution of compaction with depth and the yield of *Lolium* / *Trifolium* grassland. *Soil and Tillage Research* 41: 1-12.
- Kirby, JM. 1994. Simulating soil deformation using a critical-state model: 1. Laboratory tests. *European Journal of Soil Science* 45: 239-248.
- Koolen, AJ and Kuipers, H. 1983. *Agricultural Soil Mechanics*. Springer - Verlag, Berlin, Germany.
- Lal, R. 1996. Axle load and tillage effects on crop yields on a mollic ochraqualf in northwest Ohio. *Soil and Tillage Research* 37: 143-160.
- Lal, R and Ahmadi, M. 2000. Axle load and tillage effects on crop yield for two soils in central Ohio. *Soil and Tillage Research* 54: 111-119.
- Larson, WE, Gupta, SC and Useche, RA. 1980. Compression of agricultural soils from eight soil orders. *Soil Science of America Journal* 44: 450-457.
- Lebert, M and Horn, R. 1991. A method to predict the mechanical strength of agricultural soils. *Soil and Tillage Research* 19: 275-286.
- Lipiec, J. 1992. Soil physical properties and crop growth in relation to soil compaction. *Japanese Journal of Soil Science and Plant Nutrition* 93: 21-30.
- Lipiec, J, Arvidsson, J and Murer, E. 2003. Review of modelling crop growth, movement of water and chemicals in relation to topsoil and subsoil compaction. *Soil and Tillage Research* 73: 15-29.
- Lipiec, J, Hatano, R and Slowinska-Jurkiewicz, A. 1998. The fractal dimension of pore distribution patterns in variously-compacted soils. *Soil and Tillage Research* 47: 61-66.
- Lowery, B and Schuler, RT. 1991. Temporal effects of subsoil compaction on soil strength and plant growth. *Soil Science of America Journal* 55: 216-223.
- Lowery, B and Schuler, RT. 1994. Duration and effects of compaction on soil and plant growth in Wisconsin. *Soil and Tillage Research* 29: 205-210.
- Mamman, E and Ohu, JO. 1997. Millet yield as affected by tractor traffic in a sandy loam soil in Borno State, Nigeria. *Soil and Tillage Research* 42 (1-2): 133-140.
- McGarry, D. 1989. The effect of wet cultivation on the structure and fabric of a vertisol. *Journal of Soil Science* 40 (1): 199-207.

- Meek, BD, Rechel, EA, Carter, LM and DeTar, WR. 1988. Soil compaction and its effect on alfalfa in zone production systems. *Soil Science of America Journal* 52: 232-236.
- Meyer, E. 2005. Personal communication. South African Sugarcane Research Institute, Durban, South Africa, 14th February 2005.
- Meyer, J. 2004. Personal communication. South African Sugarcane Research Institute, Durban, South Africa, 14th September 2004.
- Mitchell, FJ and Berry, WAJ. 2001. The effects and management of compaction in agricultural soils. In: *Proceedings of the South African Sugar Technologists Association Annual Congress*, pp.115-121. SASTA, Durban, South Africa.
- Mooney, SJ and Nipattasuk, W. 2003. Quantification of the effects of soil compaction on water flow using dye tracers and image analysis. *Soil Use and Management* 19 (4): 356-363.
- Nevens, F and Reheul, D. 2003. The consequences of wheel-induced compaction and subsoiling for silage maize on a sandy loam soil in Belgium. *Soil and Tillage Research* 70: 175-184.
- Nhantumbo. 1999. The compaction susceptibility of soils in the Free State. Unpublished MSc Thesis. University of the Free State, Bloemfontein, South Africa.
- Onofiok, OE. 1989. Effect of soil compaction and irrigation interval on the growth and yield of cowpea on a Nigerian ultisol. *Soil and Tillage Research* 13 (1): 47-55.
- Or, D and Ghezzehei, TA. 2002. Modelling post-tillage soil structural dynamics: a review. *Soil and Tillage Research* 64 (1): 41-59.
- O'Sullivan, MF, Campbell, DJ and Hettiatatchi, DRP. 1994. Critical state parameters derived from constant cell volume triaxial tests. *European Journal of Soil Science* 45: 249-256.
- O'Sullivan, MF, Henshall, JK and Dickson, JW. 1999. A simplified model for estimating soil compaction. *Soil and Tillage Research* 49: 325.
- O'Sullivan, MF and Simota, C. 1995. Modelling the environmental impacts of soil compaction: a review. *Soil and Tillage Research* 35: 69-84.
- Pagliai, M, Pellegrini, S, Vignozzi, N, Rousseva, S and Grasseli, O. 2000. The quantification of the effect of subsoil compaction on soil porosity and related physical properties under conventional and reduced management practices. In: eds. Arvidsson, J, *Subsoil Compaction - Distribution, Processes and Consequences*, Ch. 3, 305-313. CANTENA VERLAG GMBH, Reiskirchen, Germany.
- Phillips, RE and Kirkham, D. 1962. Soil compaction in field and corn growth. *Agronomy Journal* 54: 29-34.

- Radford, BJ, Bridge, BJ, Davis, RJ, McGarry, D, Pillai, UP, Rickman, JF, Walsh, PA and Yule, DF. 2000. Changes in properties of a vertisol and responses of wheat after compaction with harvester traffic. *Soil and Tillage Research* 54: 155-170.
- Radford, BJ, Yule, DF, McGarry, D and Playford, C. 2001. Crop responses to applied soil compaction and to compaction repair treatments. *Soil and Tillage Research* 61: 157-166.
- Raper, RL and Erbach, DC. 1990. Prediction of soil stresses using the Finite Element Method. *Transactions of the ASAE* 33 (3): 725-730.
- Raper, RL, Johnson, CE, Bailey, AC, Burt, EC and Block, WA. 1995. Prediction of soil stresses beneath a rigid wheel. *Journal of Agricultural Engineering Research* 61: 57-62.
- Richard, G, Cousin, I, Sillon, JF, Bruand, A and Guerif, J. 2001. Effect of compaction on the porosity of a silty soil: influence on unsaturated hydraulic properties. *European Journal of Soil Science* 52: 49-58.
- Sands, R and Bowen, GD. 1978. Compaction of sandy soils in radiata pine forests.II. Effects of compaction on root configuration and growth of radiata pine seedlings. *Australian Forestry Research* 8: 163-170.
- Sands, R, Greacen, EL and Gerard, CJ. 1979. Compaction of sandy soils in radiata pine forests. 1. A penetrometer study. *Australian Journal of Soil Research* 17: 101-113.
- Smith, CW. 1995. Assessing the compaction susceptibility of South African forestry soils. Unpublished Ph.D Thesis. Department of Agronomy, University of Natal, Pietermaritzburg, South Africa.
- Smith, CW. 2004. Personal communication. Institute for Commercial Forestry Research, Pietermaritzburg, South Africa, 14th September 2004.
- Smith, CW and Johnston, MA. 2001. Managing soil compaction to ensure long-term site productivity in South African forest plantations. In: *Proceedings of the South African Sugar Technologists Association Annual Congress*, pp.126-130. SASTA, Durban, South Africa.
- Smith, CW, Johnston, MA and Lorentz, S. 1997. Assessing the compaction susceptibility of South African forestry soils. II. Soil properties affecting compactibility and compressibility. *Soil and Tillage Research* 43: 335-354.
- Smith, CW, Johnston, MA and Lorentz, S. 2001. The effect of soil compaction on the water retention characteristics of soils in forest plantations. *South African Journal of Plant Soil* 18 (3): 87-97.
- Smith, DLO. 1985. Compaction by wheels: a numerical model for agricultural soils. *Journal of Soil Science* 36: 621-632.

- Soane, BD and van Ouwerkerk, C. 1994. Soil compaction problems in world agriculture. In: eds. van Ouwerkerk, C, *Soil Compaction in Crop Production*, Ch. 1, 1-22. Elsevier, Amsterdam, Netherlands.
- Söhne, W. 1958. Fundamentals of pressure distribution and soil compaction under tractor tyres. *Agricultural Engineering* 39: 276-281,290.
- Swinford, JM and Boevey, TMC. 1984. The effects of soil compaction due to infield transport on ratoon cane yields and soil physical characteristics. In: *Proceedings of the South African Sugar Technologists Association Annual Congress*, pp.198-203. SASTA, Durban, South Africa.
- Tarawally, MA, Medina, H, Frometa, ME and Itza, CA. 2004. Field compaction at different soil-water status: effects on pore size distribution and soil water characteristics of a Rhodic Ferralsol in Western Cuba. *Soil and Tillage Research* 76: 95-103.
- Terzaghi, K and Peck, RB. 1948. *Soil Mechanics in Engineering Practice*. John Wiley and Sons, New York, USA.
- Torres, JS and Rodriguez, LA. 1995. Soil compaction management for sugarcane. In: Kumar, V, *Proceedings of the XXII ISSCT Congress*, pp.222-229. Executive committee of the ISSCT, Cartagena, Columbia.
- Torres, JS, Yang, SJ and Villegas, F. 1990. Soil compaction and sugarcane stool damage to semi mechanised harvesting in the wet season. *Sugar Cane* 5: 12-16.
- Trautner, A and Arvidsson, J. 2003. Subsoil compaction caused by machinery traffic on a Swedish Eutric Cambisol at different water contents. *Soil and Tillage Research* 73: 107-118.
- Tubeileh, A, Groleau-Renaud, V, Plantureux, S and Guckert, A. 2003. Effect of soil compaction on photosynthesis and carbon partitioning within a maize-soil system. *Soil and Tillage Research* 71: 151-161.
- Upadhyaya, SK, Rosa, UA and Wulfsohn, D. 2002. Application of the finite element method in agricultural soil mechanics. In: eds. Chancellor, WJ, *Advances in Soil Dynamics Volume 2*, Ch. 2, 117-153. ASAE, Michigan, USA.
- van den Akker, JJH. 1988. Model computations of subsoil stress distribution and compaction due to field traffic. In: *Proceedings of the 11th international conference of ISTRO*, pp.403-408. ISTRO, Edinbrough, UK.
- van den Akker, JJH. 1992. Stresses and required soil strength under terra tyres and tandem and dual wheel configurations. In: *Proceedings of the international conference on soil compaction and soil management*, pp.23-26. ICCMSM, Tallinn, Estonia.
- van den Akker, JJH. 1997. Construction of a wheel-load bearing capacity map of the Netherlands. In: *Proc. 14th ISTRO conference*, pp.15-18. Bibliotheca Fragmenta Agnomica, Pulawy, Poland.

- van den Akker, JJH. 1999. Development, verification and use of the subsoil compaction model SOCOMO. In: *Proceedings of the concerted action " Experiences with the impact of subsoil compaction on soil, crop growth and environment and ways to prevent subsoil compaction"*, pp.321-336. DLO Winand Staring Centre, Wageningen, The Netherlands.
- van den Akker, JJH. 2004. SOCOMO: a soil compaction model to calculate soil stresses and the subsoil carrying capacity. *Soil and Tillage Research* 79: 113-127.
- van den Berg, GE. 1962. Requirements for Soil Mechanics. *Transactions of the ASAE* 9: 460-463,367.
- Vermeulen, GD and Klooster, JJ. 1992. The potential of a low ground pressure traffic system to reduce soil compaction on a clayey loam soil. *Soil and Tillage Research* 24: 337-358.
- Voorhees, WB, Carlson, VA and Senst, CG. 1976. Soyabean nodulation as affected by wheel traffic. *Agronomy Journal* 68: 976-979.
- Voorhees, WB, Johnson, JF, Randall, GW and Nelson, WW. 1989. Corn growth and yield as affected by surface and subsoil compaction. *Agronomy Journal* 81: 294-303.
- Warkotsch, PW, van Huyssteen, L and Olsen, GJ. 1994. Identification and quantification of soil compaction due to harvesting methods - A case study. *South African Forestry Journal* 170: 7-15.
- Wolfe, DW, Topoleski, DT, Gundersheim, NA and Ingall, BA. 1995. Growth and yield sensitivity of 4 vegetable crops to soil compaction. *Journal of the American Society for Horticultural Science* 120 (6): 956-963.
- Woods, RK and Wells, LG. 1985. Characterizing soil deformation by direct measurement within the profile. *Transactions of the ASAE* 28 (6): 1754-1758.
- Woodward, CL. 1996. Soil compaction and topsoil removal effects on soil properties and seedling growth in Amazonian Ecuador. *Forest Ecology and Management* 82 (1-3): 197-203.
- Wronski, EB and Murphy, G. 1994. Responses of Forest Crops to Soil Compaction. In: eds. van Ouwerkerk, C, *Soil Compaction in Crop Production*, Ch. 14, 317-342. Elsevier, Amsterdam, Netherlands.